PTPIP51 and its regulation in tumour cells

Meike Katinka Petri

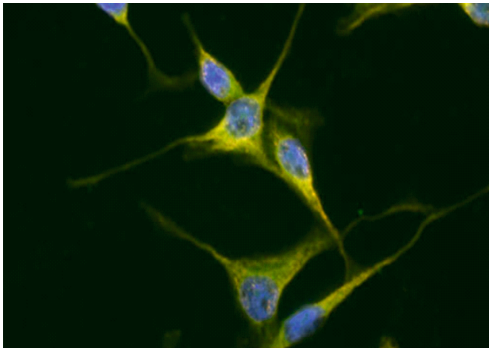

INAUGURAL-DISSERTATION
(Cumulative Thesis) for the Doctoral degree
of the Faculty of Medicine
of the Justus-Liebig-University Giessen

edition scientifique
VVB LAUFERSWEILER VERLAG

1. Auflage 2017

1st Edition 2017

édition linguistique
VVB LAUFERSWEILER VERLAG

STAUFENBERGRING 15, D-35396 GIESSEN
Tel: 0641-5599888 Fax: 0641-5599890
email: redaktion@doktorverlag.de

www.doktorverlag.de

PTPIP51 and its regulation in tumour cells

INAUGURAL-DISSERTATION
(Cumulative Thesis)
for the Doctoral degree
of the Faculty of Medicine
of the Justus-Liebig-University Giessen

by

Meike Katinka Petri
of Lippstadt

Giessen 2013

From the Institute of Anatomy and Cell Biology
Managing Director: Prof. Dr. med. W. Kummer
Faculty of Medicine, Justus-Liebig-University Giessen

1. Reviewer: Prof. Dr. med. Till Acker

2. Reviewer: Prof. Dr. rer. nat. Monika Wimmer

Chairman: Prof. Dr. med. Christian Hamm

Member of the commission: Prof. Dr. med. Hakan Akintürk

Day of doctoral defense: 21.03.2016

Declarations

"I declare that I have completed this dissertation single-handedly without the unauthorized help of second party and only with the assistance acknowledged therein. I have appropriately acknowledged and referenced all text passages that are derived literally from or based on the content of published or unpublished work of others, and all information that relates to verbal communications. I have abided by the principles of good scientific conduct laid down in the character of the Justus-Liebig-University of Giessen in carrying out the investigations described in the dissertation."

Hiermit erkläre ich:
Ich habe die vorgelegte Dissertation selbständig und ohne fremde Hilfe und nur mit den Hilfen angefertigt, die ich in der Dissertation angegeben habe. Alle Textstellen, die wörtlich oder sinngemäß aus veröffentlichten oder nicht veröffentlichten Schriften entnommen sind, und alle Angaben, die auf mündlichen Auskünften beruhen, sind als solche kenntlich gemacht. Bei den von mir durchgeführten und in der Dissertation erwähnten Untersuchungen habe ich die Grundsätze guter wissenschaftlicher Praxis, wie sie in der „Satzung der Justus-Liebig-Universität Gießen zur Sicherung guter wissenschaftlicher Praxis" festgelegt sind, eingehalten.

Meike Katinka Petri

Introduction

This dissertation is submitted as a cumulative thesis according to the doctoral degree regulations of the Faculty of Medicine of the Justus-Liebig-University of Giessen. The thesis includes an interconnection of three original papers.

Table of contents

Table of contents

1. List of papers submitted for thesis

Original papers

(1) Koch P, Petri M, Paradowska A, Stenzinger A, Sturm K, Steger K, Wimmer M.

PTPIP51 mRNA and protein expression in tissue microarrays and promoter methylation of benign prostate hyperplasia and prostate carcinoma.

Prostate 2009; 68(16):1751-62

My contribution to this work: part of writing, evaluation and discussion of the results, immunohistochemical experiments, H&E-stainings.

(2) Petri MK, Koch P, Stenzinger A, Kuchelmeister K, Nestler U, Paradowska A, Steger K, Brobeil A, Viard M, Wimmer M.

PTPIP51, a positive modulator of the MAPK/Erk pathway, is upregulated in glioblastoma and interacts with 14-3-3β and PTP1B *in situ*.

Histology and Histopathology 2011; 26: 1531-1543

My contribution to this work: study design, immunohistochemical experiments, H&E-stainings, PCR experiments, writing, evaluation of the results and discussion.

(3) Petri MK, Brobeil A, Planz J, Bräuninger A, Gattenlöhner S, Nestler U, Stenzinger A, Paradowska A, Wimmer M.

PTPIP51 levels in glioblastoma cells depend on inhibition of the EGF-receptor.

Journal of Neuro-Oncology 2015; DOI 10.1007/s11060-015-1763-8;
Volume 123, Issue 1(2015), 15-25

My contribution to this work: study design, cell culture inhibition experiments, immunohistochemical experiments, evaluation of metabolic rate by Alamar Blue test, PCR experiments, writing, evaluation of the results and discussion.

2. Introduction

2.1 Protein tyrosine phosphatase interacting protein 51

2.1.1 Background

The protein tyrosine phosphatase interacting protein 51 (PTPIP51) was detected 12 years ago by yeast two-hybrid screens used for the identification of potential substrates of the non-receptor tyrosine phosphatases TcellPTP and PTP1B (PTP1B) (Porsche et al, 2001). Up to date, the protein PTPIP51 as well as its gene is discussed in the literature under different synonyms. The gene is also known as FAM82A2, FAM82C, hucep-10, RMD3, hRMD-3, FLJ10579, LOC55177 or ptpip51. Aside from the name PTPIP51, the protein has also been described as cerebral protein 10, TCPTP-interacting protein 51, microtubule-associated protein, regulator of microtubule dynamics 3, family with gene sequence similarity 82, FAM82C or FAM82A2 (Brobeil et al, 2011a).

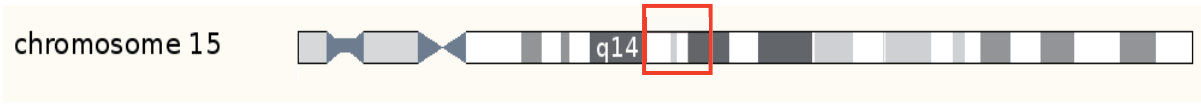

Figure 1: The PTPIP51 gene location on chromosome 15q15.1 (Stenzinger et al 2009)

In humans the PTPIP51 gene is located in chromosome 15 (15q15.1.) [Figure 1]. It comprises 13 exons, of which exons 2-13 are encoding. The whole gene including the non-coding exon has a length of 19.373 basepairs. The full-length sequence encodes a protein of 470 amino acids with a molecular weight of 52,118 kDa (Stenzinger et al, 2009). The protein is phosphorylated in vitro and in situ at Tyr 176 by Src kinase and dephosphorylated by PTP1B (Stenzinger at al 2009). The PTPIP51 protein has a N-terminal transmembrane domain required for its association with membranes, eg to mitochondria. If overexpressed in HeLa and HEK293T cells, mitochondria associated PTPIP51 induces apoptosis (Lv et al, 2006).

Beside the full length form of 52 kDa, there exist several smaller isoforms of PTPIP51 being expressed in different tissues and cells. These isoforms with molecular weights of 45 kDa, 38 kDa and 30 kDa can be explained by alternative initiation codons (Kozak sequences), which give rise to these molecular weight forms (Stenzinger et al, 2009, Brobeil et al 2011a). In addition to these forms, there are further isoforms of shorter length and lower molecular weight, which can not be explained by leaky scanning and are probably the result of alternative splicing. The higher molecular weight forms (75 kDa, 65 kDa and 60 kDa) are posttranslationally modified forms. These variants may explain the different localizations and functions seen for PTPIP51 in different tissues.

PTPIP51 is involved in many different processes. Brobeil and coworkers (2012) described its involvement mitogenic processes (Brobeil et al, 2012b). Mitosis is characterized by four stages: prophase, anaphase, metaphase and telophase (Yao et al, 2012). The mitotic processes are controlled by various checkpoints and there are certain signalling pathways needed for entering mitosis. As Brobeil and coworkers (2012b) demonstrated, PTPIP51 is located at the equatorial region during mitosis, building a PTPIP51/CGI-99 and a PTPIP51/Nuf-2 complex for correct chromosome segregation by the spindle apparatus. The mitogen activated protein kinase (MAPK) pathway plays a critical role in the G2/M transition (Hayne et al, 2000). PTPIP51 interacts with Raf-1 through the scaffolding protein 14-3-3β and thereby stimulating the MAPK cascade (Yu et al, 2008), thus probably regulating G2/M transition [Figure 2]. There are numerous interaction partners linking PTPIP51 to a number of signalling pathways other than the MAPK way. By the diversity of interactions PTPIP51 can regulate and intervene in different processes such as proliferation, differentiation, apoptosis and migration.

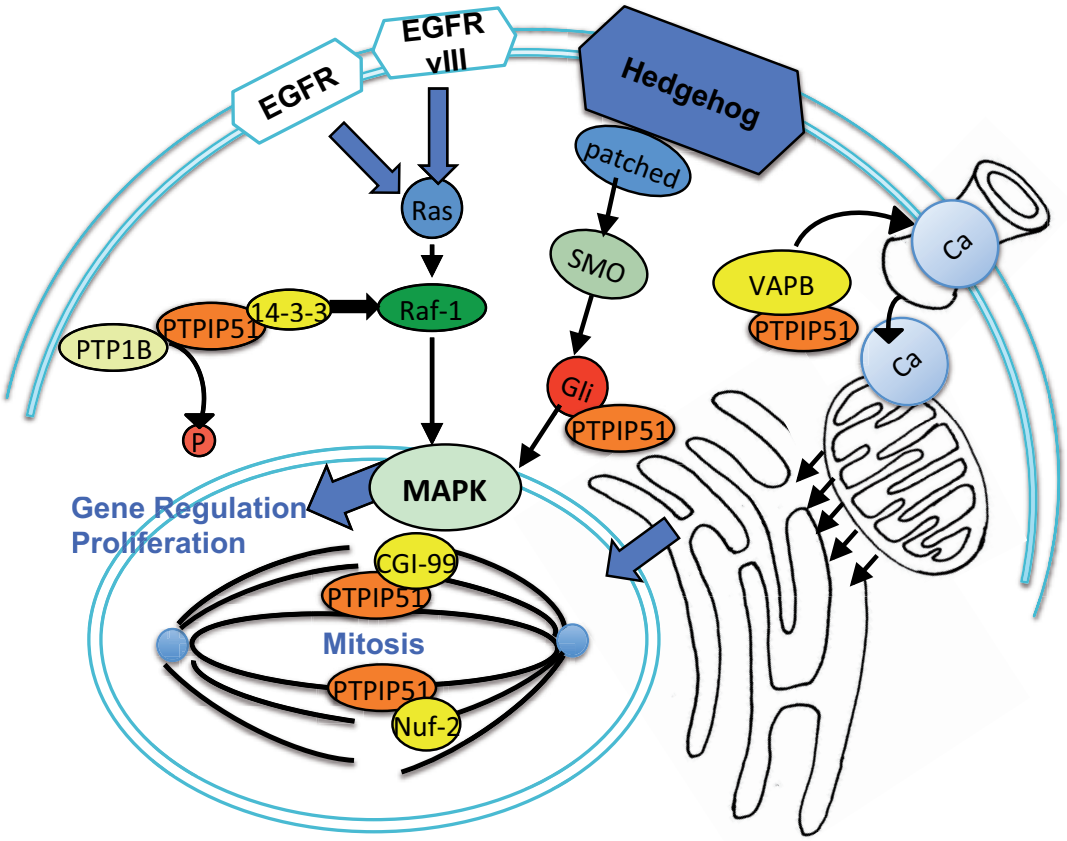

Figure 2: PTPIP51 interacting with 14-3-3β and Raf-1 when dephosphorylated by PTP1B. The complex of PTPIP51, 14-3-3β and Raf-1 stimulates the EGFR/MAPK pathway. The Hedgehog pathway stimulates MAPK, PTPIP51 interaction with Gli is part of this pathway. PTPIP51 influences calcium homeostasis by interaction with VAPB, which links the endoplasmic reticulum to mitochondria in neuronal cells. During mitosis PTPIP51 is located in equatorial region, building a PTPIP51/CGI-99 and a PTPIP51/Nuf-2 complex for correct chromosome segregation by the spindle apparatus.

2.1.2 PTPIP51 tissue expression

Interestingly, PTPIP51 shows specific expression profiles in numerous tissues. It is expressed in different developmental stages of placenta, here in different cell types (Stenzinger et al, 2009), in embryonic tissue e.g. during the development of the eye (Märker et al, 2008), in developing and adult skeletal muscle associated to the type IIa fibers (Barop et al, 2009), in epidermis (Pfeiffer, doctoral thesis, JLU, 2006), in fat tissue (Bobrich et al, 2011) and in diverse types of cells of the blood (Brobeil et al,

2010, 2011b). There was a high expression of PTPIP51 in peripheral nerve fibres and in the ganglia of the autonomous nerve system as identified by co-expression of the neuronal marker PGP9.5 (Koch et al, 2009b). Studies of PTPIP51 in mouse brain revealed its expression to be restricted to neurons, whereas there was no expression of PTPIP51 in glial cells (Koch et al, 2009a).

Many studies confirmed the expression of PTPIP51 mRNA in human tissues e.g. kidney, liver, lung, pancreas, spleen, skeletal muscle, cerebrum, cerebellum and fetal brain (Stenzinger et al 2005, 2007,2009; Lv et al 2006; Barop et al 2009; Koch et al 2009a; Brobeil et al 2010).

2.1.3 Expression of PTPIP51 in human carcinoma

Aside from the expression of PTPIP51 in healthy tissue, Lv et al (2006) detected PTPIP51 mRNA in many human carcinoma cell lines representing bladder, esophagus, liver, lung, kidney, rectum and stomach carcinoma. In situ expression of PTPIP51 is also seen in various human carcinomas. In acute myeloid leukemia (AML) represents a non-solid tumour. The AML blasts express PTPIP51 (Brobeil et al, 2011b). Likewise PTPIP51 is expressed in human keratinocyte carcinoma such as basal cell carcinoma and squamous cell carcinoma as well as Bowen's disease and keratoacanthomas (Koch et al, 2008). Invasive breast cancer cells express high levels of PTPIP51 (Dietel et al, submitted). Comparing prostate carcinoma (PCa) to benign prostate hyperplasia (BPH) revealed a specific expression profile in the tumour samples. Koch and coworkers (2009b) were able to link this upregulated expression to an aberrant promotor methylation status of the PTPIP51 gene in prostate cancer in contrast to benign prostate hyperplasia.

Human neuroepithelial tumours of the human brain display a PTPIP51 expression correlated to the malignancy of the tumour. This applies to glioblastoma (GBM) WHO °IV in comparison to astrocytoma of lower malignancy WHO grade °II (Petri et al 2011) and is now investigated in ependymoma of increasing malignancy (Schmidtchen, personal communication).

2.1.4 Interacting partners of PTPIP51

PTPIP51 intervenes in different signalling pathways by its interaction with specific proteins standing for signalling knots, which also are basic in tumour progression.

The interaction behaviour of PTPIP51 is regulated by its tyrosine 176 phosphorylation status (Brobeil et al 2012a). PTP1B (Protein Tyrosine Phosphatase 1B) and c-Src are responsible for the correct phosphorylation status of PTPIP51 (Stenzinger et al, 2009). Thus, PTPIP51 interacts *in vitro* and *in situ* with the non-transmembrane protein-tyrosine phosphatase, dephosphorylating in vitro and in situ the Tyr176, and with c-Src which accounts for the phosphorylation [Figure 3].

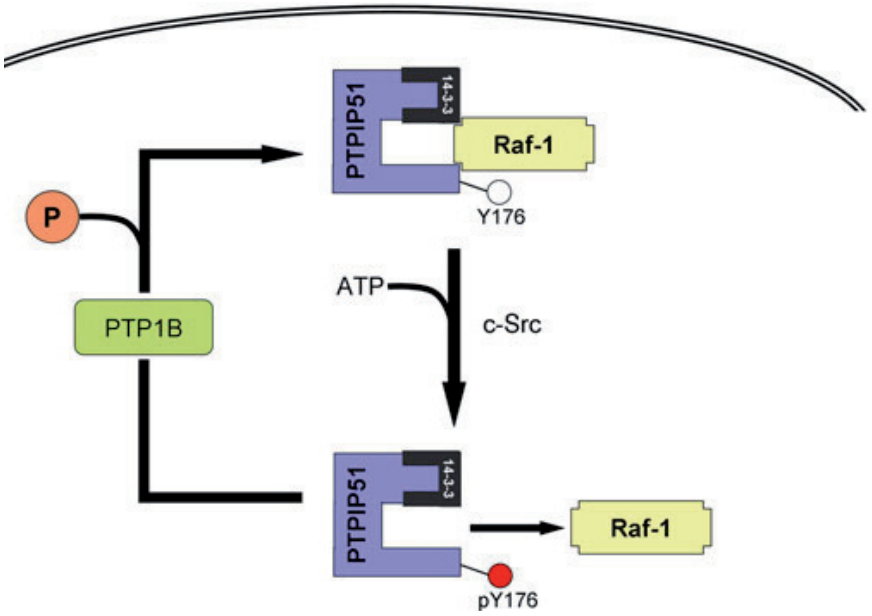

Figure 3: PTPIP51 and 14-3-3β interacting with Raf-1 when dephosphorylated at Tyr 176 by PTP1B, phosphorylation of Tyr 176 by c-Src (Brobeil et al 2012a)

PTP1B contributes to oncogenesis not only by dephosphorylating PTPIP51, but also key signalling proteins (Arias-Romero et al, 2009). PTP1B can activate the MAPK cascade on Ras and c-Src level probably attributed to PTPIP51. The Src kinase activity plays a central role in tumour progression. In prostate carcinoma cell lines Src kinase specific activity is directly correlated to metastatic aggressiveness (Xu et al, 2012). Specific inhibition of Src kinases impairs malignant glioma growth *in vitro* and *in vivo* (Stedt et al, 2012). The protein c-Src mediates the phosphorylation of EGFR, thereby promoting tumour progression (Tice et al, 1999) and regulates

PTPIP51 phosphorylation status balanced by PTP1B activity and in consequence its access to the downstream part of EGFR pathway. This reflects the involvement of PTPIP51 in tumourigenesis (Stenzinger et al, 2009).

Recently, two independent studies by Jin et al (2004) and Ewing et al (2007) described the interaction with 14-3-3β and 14-3-3γ up to then unknown interaction partners of PTPIP51. Meanwhile, further 14-3-3 proteins, namely 14-3-3ζ and 14-3-3τ, are recognized as interacting partners of PTPIP51 (Bandyopadhyay et al. 2010; Ichimura et al. 2013). 14-3-3 proteins, as scaffolding proteins are implicated in numerous cellular processes such as tumourigenesis, cell cycle control and apoptosis (Cao et al, 2008). An upregulation of 14-3-3 proteins is seen in prostate carcinoma (Alaiya et al, 2011). Noteworthy, the expression of 14-3-3β and 14-3-3η is correlated to the grade of malignancy in glioma (Yang et al, 2008). In contrast, normal brain tissue does not express these two isoforms. In glioblastoma we were able to verify the interaction of PTPIP51 with 14-3-3β and corroborated the relation of expression level and malignancy in vivo. This was also detected in prostate carcinoma where we identified a 14-3-3β colocalization with PTPIP51 protein.

Yu and coworkers (2008) linked the PTPIP51/14-3-3 interaction with Raf-1. Thereby PTPIP51 modulates cellular motility and morphology by this access on the mitogen activated protein kinase (MAPK) cascade. This is important in healthy tissue but also has a high clinical relevance for the pathogenesis of carcinoma. The MAPK/ERK pathway is involved in a variety of cellular functions such as growth, proliferation, differentiation, migration and apoptosis. An aberrant regulation of MAPK cascades contributes to cancer. In particular, the extracellular signal-regulated kinase (ERK) of the MAPK pathway has been the subject of intense research (Roberts et al, 2007). ERK is a downstream component of an evolutionarily conserved signalling module that is activated by the Raf serine/threonine kinases. Raf activates the MAPK/ERK kinase (MEK) 1/2 dual-specific protein kinases, which then activate ERK 1/2 (Roberts et al, 2007). ERK activation also promotes an upregulated expression of EGFR ligands, promoting an autocrine growth loop critical for tumour growth. Ras is a downstream effector of the EGFR (Roberts et al, 2007). The EGFR-Ras-Raf-MEK-ERK signalling pathway has been and is still subject of intense analysis to identify new targets for cancer treatment.

PTP1B activates the MAPK cascade on Ras level (Stenzinger et al, 2009) and regulates the phosphorylation status of PTPIP51, which in turn regulates the interaction of PTPIP51 with 14-3-3β. PTPIP51 interacts with Raf-1 through 14-3-3 thereby modulating the MAPK cascade (Yu et al, 2008). These findings underline the important role of PTPIP51 in the EGFR-Ras-Raf-MAPK pathway [Figure 3].

2.1.5 EGFR – MAPK pathway

The ultimate cellular response to the activation of EGFR signalling via MAPK pathway is DNA synthesis and cell division (Halatsch et al, 2004). Amplification of the epidermal growth factor receptor gene (ERBB**1**) is one of the most common oncogenic alterations in GBM (45%), which leads to overexpression of EGFR, thus making it a prime target for therapy (Karpel-Massler et al, 2009).

The epidermal growth factor receptor is a member of the ErbB receptor family, a subfamily of four closely related receptor tyrosine kinases: EGFR (ErbB-1), HER2/c-neu (ErbB-2), Her 3 (ErbB-3) and Her 4 (ErbB-4). Receptors of the ERBB family promote the development of various cancers, and the inhibition of these receptors represents an attractive therapeutic concept. Inhibition of the ERBB1 receptor can inhibit migration of human glioblastoma cells (Staberg et al, 2013).

In about 40-50% of cases of glioblastoma multiforme (GBM) the epidermal growth factor receptor (EGFR) is overexpressed (Ewing et al, 2007; Hegi et al 2012), and almost half of these cases co-express the mutant receptor subtype EGFRvIII. This EGFR variant is constitutively activated, and thereby may contribute to the aggressive and refractory course of GBM, which is associated with a median survival of only 40 to 60 weeks from diagnosis (Loew et al, 2009). However, efforts at targeting the EGFR tyrosine kinase using small molecule inhibitors or antibodies so far have shown disappointing efficacy in clinical trials for newly diagnosed or recurrent glioblastoma (Hegi et al, 2012).

Based on these findings we investigated the expression profile of PTPIP51 and its interaction partner 14-3-3β in brain tumours (low grade astrocytomas and glioblastomas). In a second step we transferred the new informations on glioblastoma cells to get more insights into the effects of EGFR inhibition on PTPIP51and 14-3-3β. The results suggest a correlation between MAPK pathway

inhibition via ERGR and downregulation of PTPIP51 and 14-3-3β expression. Interestingly, this hypothesis argues for a reverse feedback on transcriptional and translational level of both proteins in case of depressed stimulation of EGFR-Ras-Raf-MAPK pathway.

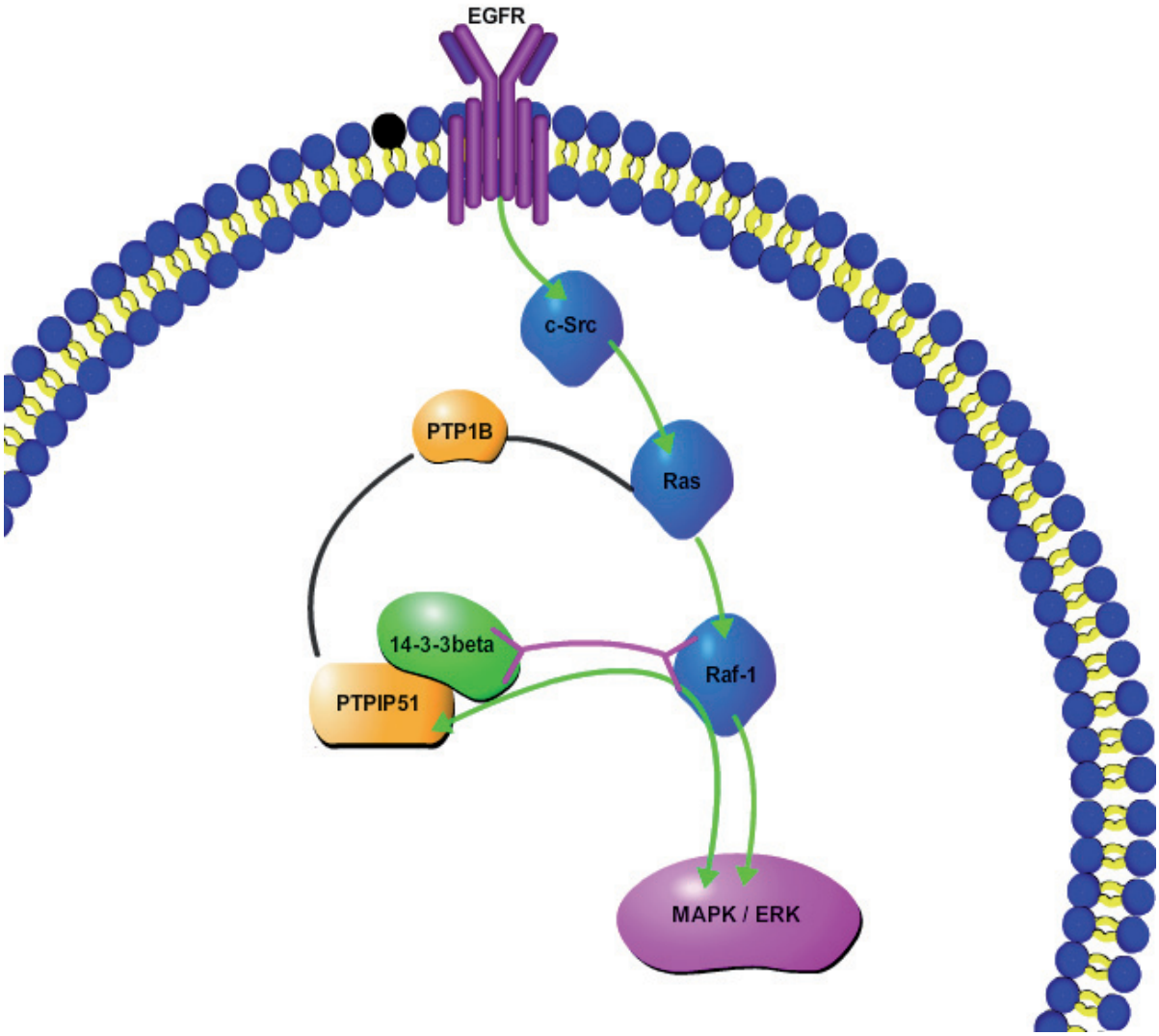

Figure 4: EGFR – MAPK signalling pathway with PTPIP51, 14-3-3β and PTP1B

The tissue specific expression profiles of PTPIP51 and its interactions with important signalling proteins being essential for pathways promoting cancer development and progression argue for an important functional role of PTPIP51 in cancer pathogenesis.

2.2 Prostate carcinoma

2.2.1 Background

Prostate cancer (PCa) is the most common non-skin cancer and the second leading cause of cancer-related death for men in the United States (Farrell et al, 2013; Smith et al, 2009). Compared to other carcinomas, it has a relative low mortality but a high incidence (Farrell et al, 2013). Despite a large increase in prostate cancer incidence, mortality rates have remained relatively constant through improvements in survival. Most patients present with a localized disease, but there are still many who present with an already metastasized stage (Chowdhury et al, 2013). From 1982 to 2006, new cases increased from 80 to 309 per year in Luxembourg, while the incidence (world standard population) rose from 29.5 to 85 per 100 000 men (Lamy et al, 2013). One of 34 patients with diagnosis of prostate carcinoma dies because of the cancer (Crawford, 2003).

Since 1960 the Gleason grading system has become the most commonly used grading system for prostate cancer in the United States and is gaining worldwide acceptance (Guimaraes et al, 2008). Increasing age, ethnic origin, and family history are well-established risk factors for the diagnosis of prostate cancer (Glass et al, 2013). Aside from that increased insulin growth factor (IGF) concentration was detected as a risk factor (Grönberg, 2003; Tsuchiya, 2013).

Most cancers have the potential to metastasize under appropriate conditions, PCa favours the skeleton as the primary site of metastasis, suggesting that the bone microenvironment is conducive to its growth (Hudson et al, 2013).

PCa metastases proceed through a complex series of molecular events that induce angiogenesis at the site of the primary tumour, local migration within the primary site, intravasation into the blood stream, survival within the blood circulation, extravasation of the tumour cells to the target organ and colonization of tumour cells within the new site. One of the mechanisms leading to PCa metastases is the perineural invasion of tumour cells (Martinez et al, 2013). Each one of these steps involves a complicated chain of events that utilize multiple protein – protein interactions, protein signaling cascades and transcriptional changes (Hudson et al, 2013).

Despite PCa is subject to intense research and the urgent need to improve current biomarkers for diagnosis, prognosis and drug resistance, the advances have been very slow. Standard therapy so far includes surgical resection, radiochemotherapy and androgen deprivation therapy (Chowdhury et al, 2013).

2.2.2 Interacting partners of PTPIP51 in prostate carcinoma

The deregulation of the epidermal growth factor receptor (EGFR) pathway plays a major role in the pathogenesis of prostate cancer. However, therapies targeting EGFR have demonstrated limited effectiveness in PCa (Carrion-Salip et al, 2012). A potential mechanism to overcome EGFR blockade in PCa cells is the autocrine activation of alternative receptors of the human EGFR (HER) family through the overexpression of the HER receptors and ligands (Carrion-Salip et al, 2012). This mechanism seems to play a key role in mediating resistance to EGFR inhibition in PCa cells, but is still poorly understood.

C-Src integrates a large number of signal transduction pathways regulating cell division, migration and other aspects of cell physiology. As already mentioned before, c-Src regulates the EGFR/MAPK pathway [Figure 4]. Mutations of Src kinase have not been described in human PCa, but there is evidence for an increased level of expression accompanying cancer progression (Cai et al, 2011). In case of enhanced c-Src expression coupled to the raised expression of androgen receptors, it results in a strong activation of Src kinase activity accompanied by activation of the MAPK pathway and increased activity of the androgen receptors (Cai et al, 2011).

As shown in figure 3, Ras is part of the EGFR/MAPK pathway. To identify additional pathway alterations that cooperate with PTEN (phosphatase and tensin homolog) tumour suppressor gene loss in prostate cancer progression, Mulholland and coworkers (2012) surveyed human prostate cancer tissue microarrays and found that the RAS/MAPK pathway is significantly elevated in both primary and metastatic lesions. Although Ras activation alone cannot initiate prostate cancer development, it significantly accelerates progression caused by PTEN loss, accompanied by epithelial-to-mesenchymal transition (EMT) and macrometastasis with 100% penetrance (Mulholland et al, 2012).

Ren and coworkers postulated the activation of the Ras/Raf/MEK/ERK pathway to be frequent in prostate cancer of Chinese men, with Raf gene copy number gain potentially being the main contributor of this (Ren et al, 2012).

PTP1B stimulates EGFR/MAPK pathway on c-Src and Ras level as described above. PTP1B is induced through the stimulation of androgen receptors in androgen receptor expressing prostate cancer cells at the mRNA and protein level, which increases PTP1B activity (Lessard et al, 2012).

2.2.3 PTPIP51 in prostate carcinoma

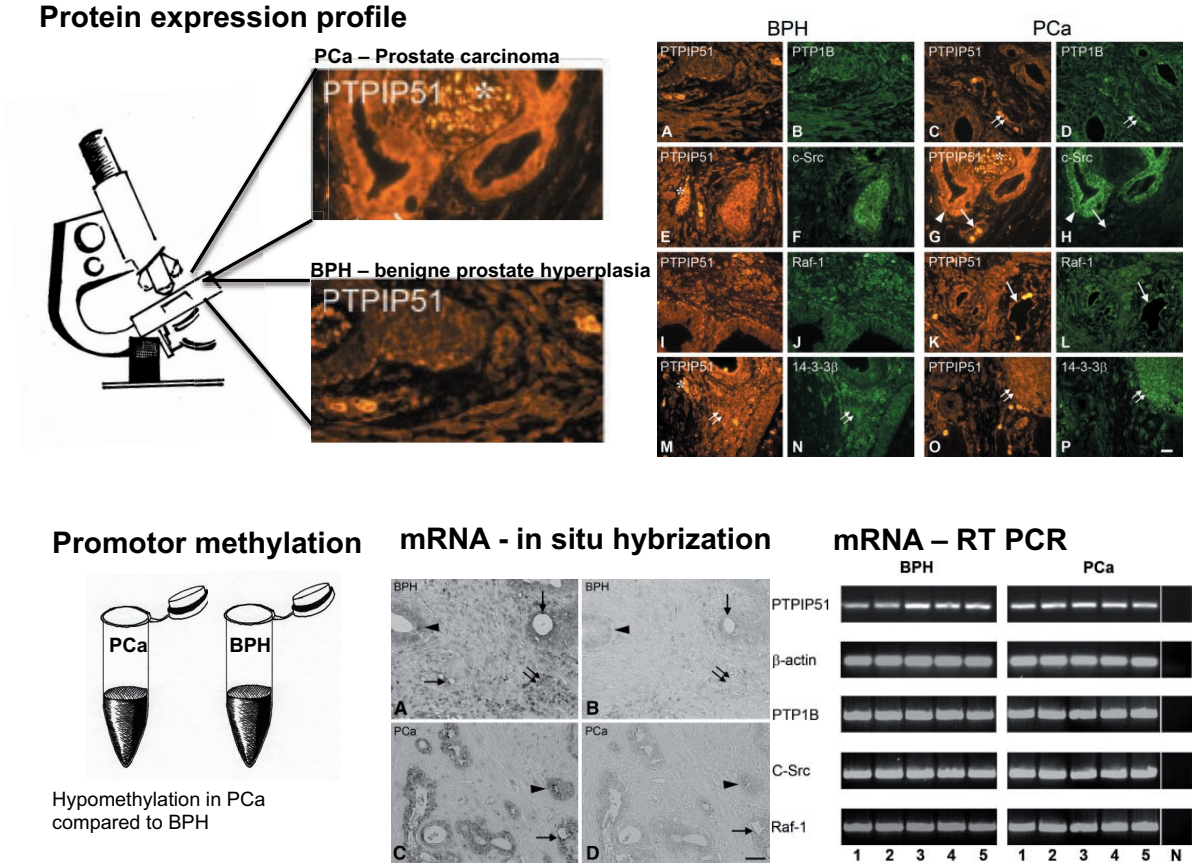

Figure 5: Graphical abstract of the most important results of the first publication submitted for thesis: PTPIP51 mRNA and protein expression in tissue microarrays and promoter methylation of benign prostate hyperplasia and prostate carcinoma (Koch P, Petri MK et al, 2009)

PTPIP51 mRNA and protein expression levels in prostate carcinoma (PCa) compared to benign prostate hyperplasia (BPH) were investigated either by PCR or by immunocytochemistry in tissue microarrays.

This study demonstrated a cell specific expression of PTPIP51 mRNA and protein in BPH and PCa. Quantitative real-time PCR analysis showed slightly elevated levels of PTPIP51 mRNA in the group of PCa specimen when compared to BPH specimen. These findings corroborated the results of in situ hybridization experiments. PTPIP51 protein was investigated by immunohistochemistry. Comparing the protein expression of both investigated groups, a higher expression of PTPIP51 was detected in PCa samples compared to BPH samples. All PCa samples exhibited an increased quantity of ganglia and nerve fibres. All these ganglia and nerve fibres were highly positive for the PTPIP51 protein. In prostate cancer nerve, the nerve fibres play an important role, amongst others being responsible for tumour spreading and supporting tumour growth. As mentioned above, perineural invasion is general mechanism in prostate cancer (Martinez et al, 2013). All ganglia and nerve fibers of the prostate cancer samples as well as of BPH presented with a strong expression of PTPIP51 protein. The observed higher levels of PTPIP51 mRNA and protein in PCa compared to BPH can probably be explained by the higher nerve density reported for PCa as a consequence of cancer-related axogenesis and neurogenesis (Ayala et al, 2008).

PTP1B was partially co-expressed with PTPIP51 in prostatic epithelial cells (BPH) and in prostate tumour cells (PCa). In endothelial cells the co-expression of both antigens was restricted to the PCa samples. This finding may implicate a functional role of PTP1B dephosphorylated PTPIP51. Dephosphorylation allows PTPIP51 to interact with 14-3-3/Raf1 thus activating MAPK signaling (Brobeil et al 2012a) [Figure 3]. This promotes angiogenesis, which is an important prerequisite of pathogenesis in cancer. A stringent cell specific co-expression of PTPIP51 with c-Src was not detected. On subcellular level we found Raf-1 co-expressed with PTPIP51 in the basal part of prostatic epithelial cells (BPH) and in a part of the tumour cells (PCa). Endothelial cells and a subset of immune cells as well displayed a co-expression of both antigens in BPH and in PCa. These findings correlated to

co-expression of PTPIP51 with 14-3-3β, being the precondition for the interference of PTPIP51 in the MAPK pathway.

2.2.4 Promotor methylation in PCa and BPH

The regulation of transcription was examined by investigating the promotor methylation status of PTPIP51 in both BPH and PCa. In general, methylation of the promotor region is associated with gene silencing (Li et al, 2003). In contrast, a lack of methylation is responsible for decondensation of chromatin genomic instability and may cause activation of retrotransposon elements, which results in an aberrant overexpression of certain genes (Jones et al, 1999; Tuck-Muller et al, 2000). Therefore, we investigated PTPIP51 promotor methylation [Figure 6] in samples of BPH and PCa.

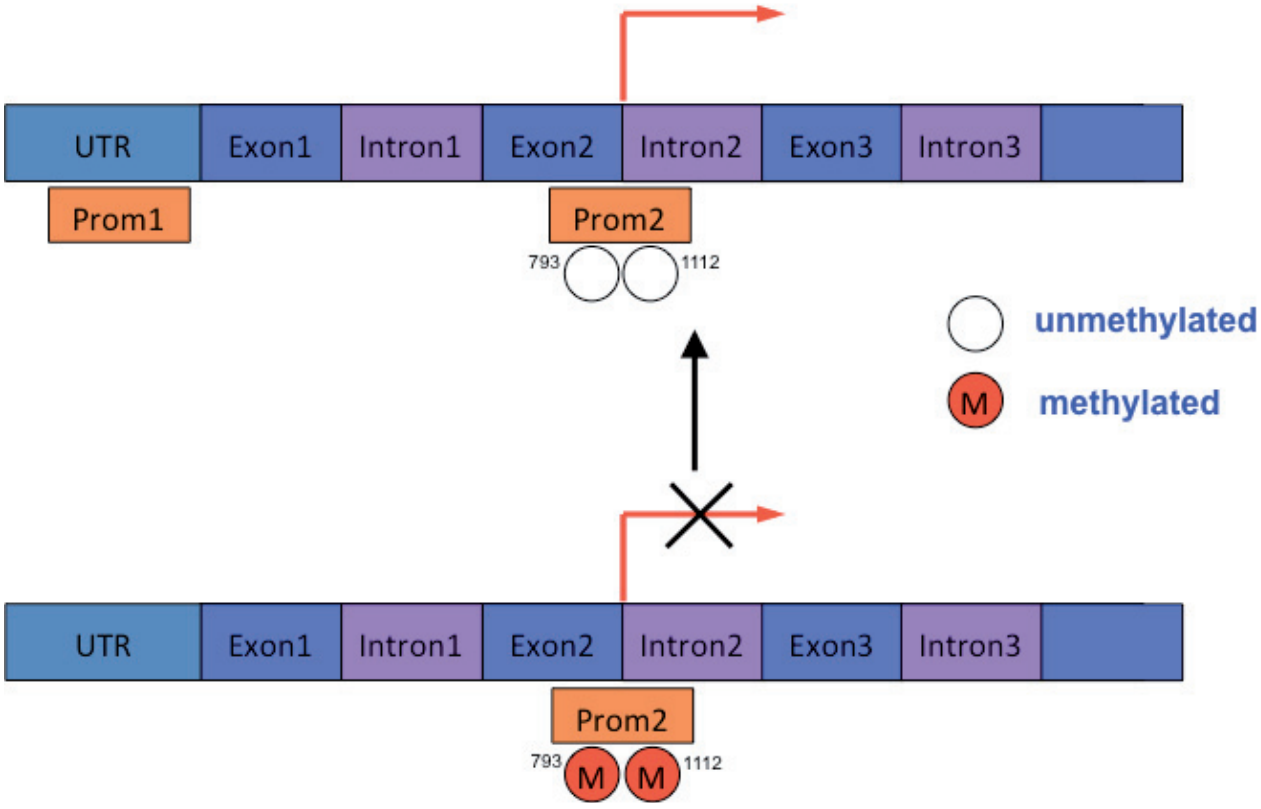

Figure 6: PTPIP51 promotor methylation

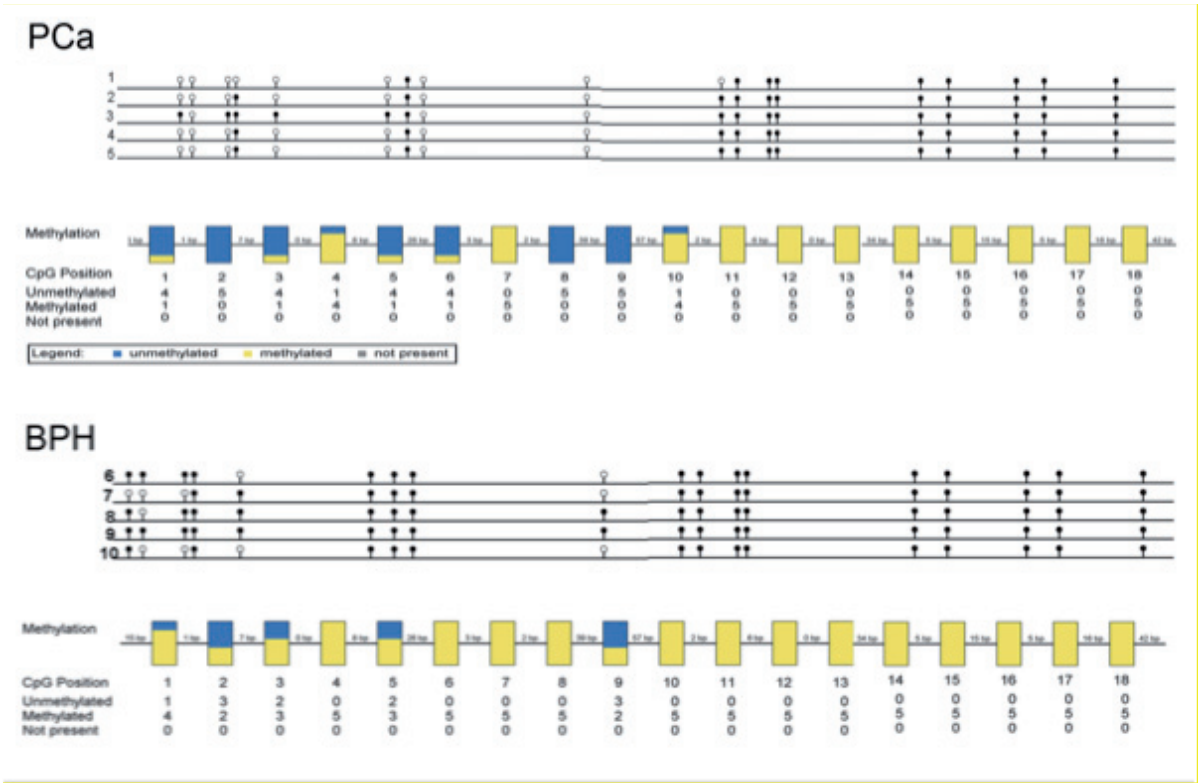

Figure 7: Methylation of PTPIP51 promotor gene in PCa and BPH. Black circles correspond to methylated CpGs, open circles correspond to unmethylated CpGs. Bar diagram demonstrates aggregated representation of methylation data of every CpG nucleotide within the DNA fragment of the PCa and BPH group.

Eighteen CpGs (**C**ytosin-**p**hosphatidyl-**G**uanin) were characterized from each sample by sodium bisulfite sequencing. In contrast to 78% methylated CpGs in BPH, there was a loss of methylation observed in PCa [Figure 7]. Overexpression of PTPIP51 as a result of CpG island hypomethylation might be a potential factor contributing the perineural invasion in PCa.

This study presented differences in PTPIP51 gene methylation in PCa compared to BPH and a tissue-, cell- and pathology specific expression of PTPIP51 protein.

2.3. Glioblastoma

2.3.1 Background

The Glioblastoma (GBM) is the most common and most malignant primary brain tumour. They account for 10-15 % of all intracranial tumours and 50-60 % of the astrocytic gliomas. Every year there are 12 000 glioblastomas diagnosed in the US. The prognosis of GBM is still poor with a median survival of 12 months (Marko et al, 2013). The annual incidence is approximately two to three new cases per 100 000 population. Adult patients are affected most commonly with a peak incidence between 50-70 years of age, but GBMs develop at any age (Reifenberger et al, 2010). GBM is still one of the most lethal cancers in humans. The so called long-term survivors are patients, who are alive after three years from diagnosis.

According to the World Health Organization (WHO) classification of tumours of the central nervous system, including the latest version 2007, GBM belongs to the subgroup of atrocytic tumours which are members of the tumours of neuroepithelial tissue and is grade WHO IV (Louis et al, 2007).

Tumor group	Tumor entity	Grade I	Grade II	Grade III	Grade IV
Astro-cytic tumors	Pilocytic astrocytoma	x			
	Pilomyxoid astrocytoma		x		
	Subependymal giant cell astrocytoma	x			
	Pleomorphic xanthoastrocytoma		x		
	Diffuse astrocytoma		x		
	Anaplastic astrocytoma			x	
	Glioblastoma				x
	Gliomatosis cerebri		(x)	x	(x)

Table 1: WHO grading of tumours of the central nervous system (here only the astrocytic tumor classification shown) (Louis et al, 2007)

The diagnosis of GBM is based on specific histopathological features. Glioblastoma are cellular, highly anaplastic tumours that may be composed of cells with various

morphologies, including fibrillar and gemistocytic cells, fusiform cells, small anaplastic cells and multinuclear giant cells. Atypical nuclei are usually marked, and mitotic activity, including atypical forms, is prominent. The presence of microvascular proliferation and / or necrosis is essential for the diagnosis. Microvascular proliferation often results in GBM–typical so called glomerulum- or garland-like capillary structures (Reifenberger et al, 2010). In glioblastoma primary and secondary GBMs are distinguished. Primary GBMs are newly diagnosed tumours and secondary GBMs develop from astrocytomas of lower malignancy. There are specific molecular aberrations frequently detected in different types of diffusely infiltrating astrocytic gliomas (Reifenberger et al, 2004).

Nuclear p53 immunoreactivity can be detected in 30-40% of all GBMs, with giant cell GBM and secondary GBM being p53 positive in up to 80 % of the cases. Strong expression of the EGFR is found in about 60 % of primary glioblastoma, but is rare in secondary glioblastoma. The MIB 1 (antibody against Ki 67) labelling index is usually high (> 10 %), but often shows marked regional heterogeneity (Reifenberger et al, 2010).

The current standard therapy for GBM is multimodal according to the Stupp protocol, consisting of surgery with targeted macroscopic total resection, radiotherapy with concomitant temozolomide alkylating chemotherapy and six adjuvant temozolomide therapy cycles (Shah et al, 2011). Usually the tumours recur after this therapy. Surgical resection is often limited by involvement of eloquent brain areas. But even in case of macroscopic total resection of the tumours without any gadolinium enhancement in postoperative MRI and the following radiochemotherapy the GBM recidivates in nearly every case.

2.3.2 Interacting partners of PTPIP51 in glioblastoma

Amplification of the epidermal growth factor receptor gene (ERBB**1**) is one of the most common oncogenic alterations in GBM (45%), which leads to overexpression of EGFR, thus making it a prime target for therapy (Karpel-Massler et al, 2009; Hegi et al, 2012). In clinical trials beside standard therapy the therapy with EGFR targeting agents alone in clinical trials has not generated promising results to date (Gao et al, 2013). Strategies are now focusing on blocking the downstream EGFR-

activated metabolic pathways and their key phosphorylated kinase alterations in GBMs (Gao et al, 2013). Almost half of GBM cases with overexpressed EGFR do co-express the mutant receptor subtype EGFRvIII. This EGFR variant is constitutively activated, and thereby may contribute to the aggressive and refractory course of GBM, which is associated with a median survival of only 40 to 60 weeks from diagnosis (Loew et al, 2009).

In GBM, Ras activity is upregulated in the majority of the tumours. Furthermore, the levels of MAPK/ERK, a known downstream effector of Ras, are also increased (Lyustikman et al, 2008). Downregulation of RAS can inhibit glioblastoma cell growth through preventing RAS signaling (Cao et al, 2012).

Lyustikman and coworkers (2008) detected increased levels of Raf-1 and BRAF proteins and Raf kinase activity in human GBM samples. The oncogenic effect of KRas in glioma formation is transduced at least in part through Raf signaling (Lyustikman et al, 2008).

PTP1B contributes to oncogenesis by tyrosine dephosphorylation of key signaling proteins (Arias-Romero et al, 2009) and additionally activates c-Src (Bjorge et al., 2000) and stimulates the MAPK cascade on Ras level. So far its role in GBM pathology only is marginally investigated so far. The vascular endothelial growth factor (VEGF) directly regulates tumour cell invasion negatively through enhanced recruitment of PTP1B (Lu et al, 2012).

In gliomas there is a correlation between the grade of malignancy and the expression levels of 14-3-3β and 14-3-3η (Yang et al, 2008). In contrast, normal brain tissue does not express these both isoforms. The isoforms β and η belong to a superfamily of 14-3-3 proteins, which are differently expressed in many human tissues. 14-3-3 proteins have been implicated in numerous cellular processes, such as tumourigenesis, cell cycle control and apoptosis (Cao et al, 2008).

2.3.3 PTPIP51 in glioblastoma

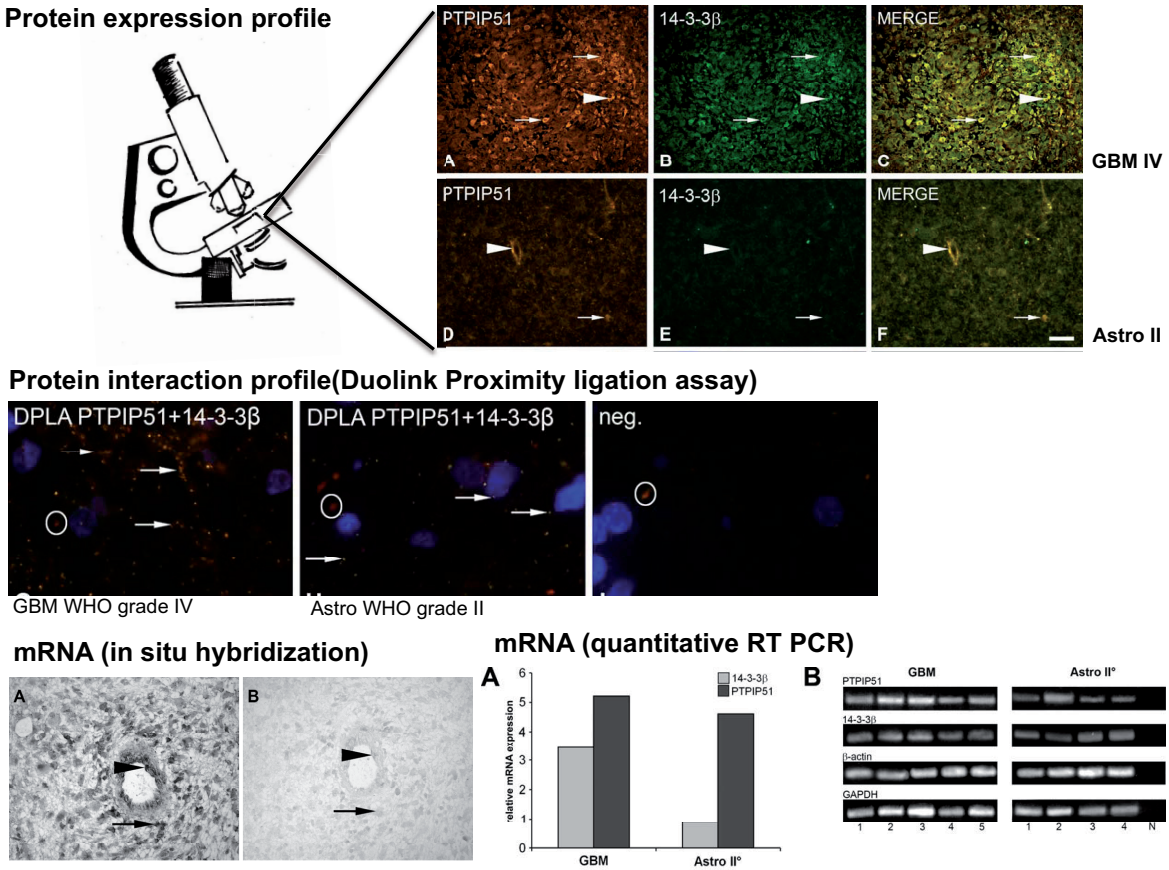

Figure 8: Graphical abstract of the most important results of the second publication submitted for thesis: PTPIP51, a positive modulator of the MAPK/Erk pathway, is upregulated in glioblastoma and interacts with 14-3-3β and PTP1B *in situ*. (Petri et al 2011)

PTPIP51 expression was investigated in glioblastoma on transcriptional and translational level by immunohistochemestry, *in situ* hybridization and RT PCR. Quantitative data of PTPIP51 expression in GBM was compared to the level in WHO grade II astrocytoma by quantitative RT PCR. An *in situ* interaction of PTPIP51 with its expected interacting partners 14-3-3β and PTP1B was verified by Duolink proximity ligation assays [Figure 9: DPLA].

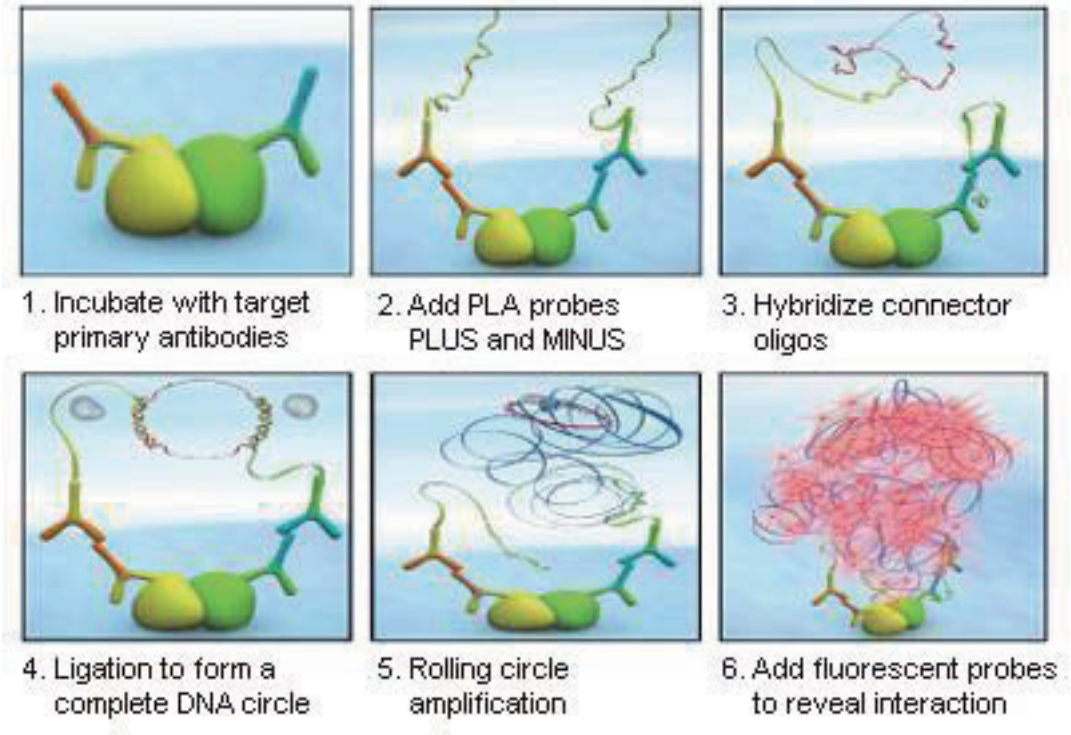

Figure 9: Technique description of Duolink proximity ligation assay (DPLA).

This study revealed a cell specific expression of PTPIP51 mRNA and protein in human glioblastoma. Immunehistochemical experiments and *in situ* hybridization displayed a strong expression of mRNA and PTPIP51 protein in GBM tumour cells, endothelial cells, immune cells within the lumina of tumour vessels as well as in the tumour infiltrating immune cells. In endothelial cells of normal and of pseudoglomerular vessels PTPIP51 protein was restricted to the plasmamembrane and to the nucleus indicating the expression of specific membrane associated PTPIP51 isoforms in these cells. Granulocytes located in capillary lumina or infiltrating the tumour as well as in the necrotic areas displayed a strong cytoplasmic PTPIP51 expression. This is in contrast to B-lymphocytes, which did not show any PTPIP51 expression.

PTPIP51 and 14-3-3β showed a strict co-localization. Both proteins were seen in glioblastoma cells, endothelial cells and granulocytes. The glioblastoma cells displayed a strong cytoplasmic reaction for both proteins. Grade II astrocytoma also displayed a co-localization of PTPIP51 and 14-3-3β, but to a much lower extent [Figure 8].

This was confirmed by a decreased mRNA level of PTPIP51 in WHO grade II astrocytoma compared to glioblastoma [Figure 8]. Comparable observations of a correlation to the grade of malignancy in glioma have already been described for 14-3-3β alone (Yang et al, 2008).

As mentioned above, 14-3-3β mediates the interaction of PTPIP51 with Raf-1, thereby modulating the activity of the MAPK signaling pathway (Lv et al, 2006, Yu et al, 2008; Stenzinger et al, 2009). The MAPK pathway plays an important role in cell migration and thereby seems to be one of the main reasons for recurrence and poor prognosis of GBM. It is considered that migrating tumour cells infiltrate the healthy tissue surrounding the glioblastoma and thereby can escape surgical extirpation as well as radiotherapy and by this way give rise to regrowth.

To sum up, PTPIP51 plays an important role in glioblastoma on the level of EGFR/MAPK pathway by its interaction with 14-3-3β.

2.4 PTPIP51 and EGFR/MAPK pathway – regulatory role in tumour progression

2.4.1 Background

Recently, we detected a tissue specific expression of PTPIP51 in prostate carcinoma. Here we could verify an increased level of PTPIP51 mRNA and protein in carcinoma compared to benign prostate hyperplasia and a hypomethylation of PTPIP51 promotor in cases of PCa. Moreover, PTPIP51 was co-localized with 14-3-3β.

Samples of glioblastoma displayed a tissue specific expression of PTPIP51. In relation to the values seen in low-grade astrocytoma we could verify a higher level of mRNA and protein of PTPIP51 in GBM (WHO grade IV). Beside these identical features for both tumour entities (GBM and PCa), we were able not only to disclose a co-localization of PTPIP51 and 14-3-3β, but also the interaction of both proteins in vivo verified by the Duolink proximity ligation assay.

Taken together, PTPIP51 is highly expressed in carcinomas and thus modifies the EGFR/MAPK pathway of carcinomas as is emphasized by its interaction with 14-3-3β. On cellular level the interaction of PTPIP51 with 14-3-3β leads to a ternary

complex with cRAF (Raf1) stimulating the downstream effector EGFR/MAPK signaling-pathway (Yu et al, 2008). Interestingly, a positive correlation between the grade of tumour malignancy in gliomas with the PTPIP51 interacting partner 14-3-3β has been described before (Yang et al, 2008).

These findings suggest that both proteins may play a functional role in the tumorigenesis of glioblastomas in particular.

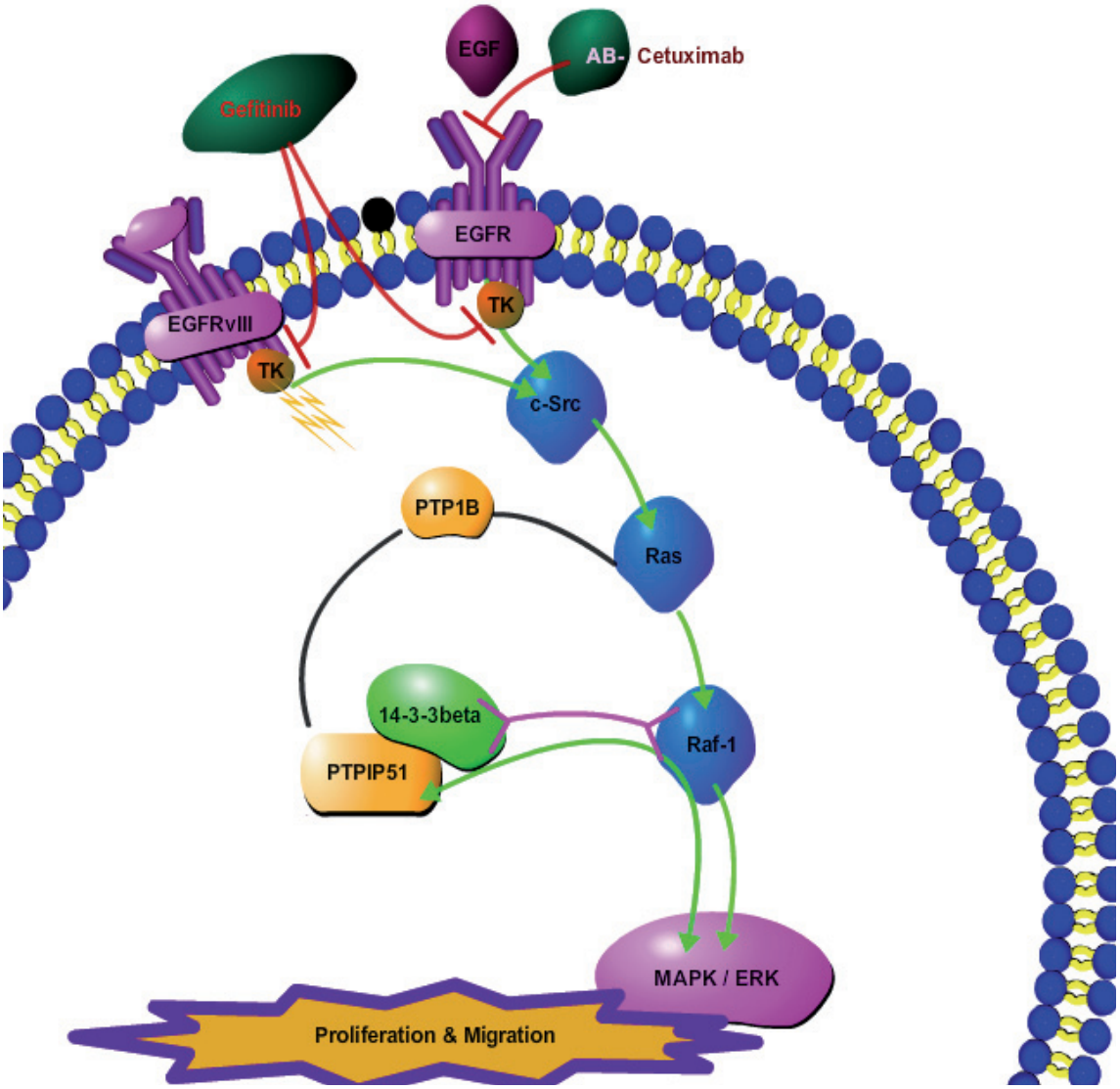

Figure 10: The tyrosine kinase inhibitor Gefitinib and the monoclonal antibody Cetuximab treatment of EGFR – MAPK signalling pathway

2.4.2 PTPIP51 in GBM cells during inhibition of EGFR

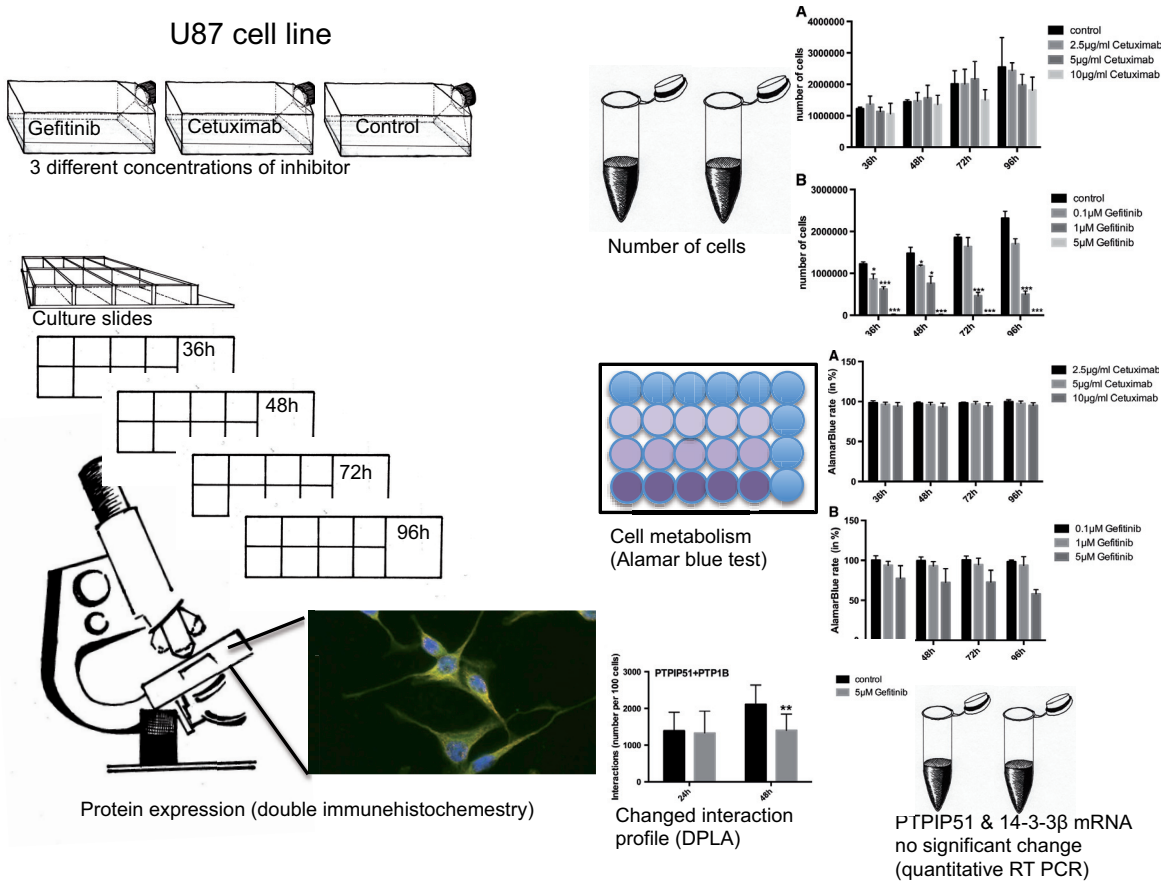

Figure 11: Graphical abstract of the most important results of the third publication submitted for thesis: PTPIP51 levels in glioblastoma cells depend on inhibition of the EGF-receptor (Petri et al, 2015)

Hence, we investigated the interfering effect of the tyrosine kinase inhibitor Gefitinib and the monoclonal antibody Cetuximab on growth factor signaling *in vitro* and *in vivo*. *In vitro* investigations were performed with the U87 cell line as an established model system. To record the *in vivo* effects, primary cells from GBM patients were cultured and treated with either Gefitinib or Cetuximab. Treatment efficiency was controlled by the quantification of cell viability measured by the metabolic rate and by cell counting. PTPIP51 and 14-3-3β expression was evaluated in untreated (control) and treated cells by double immunostainings and its mRNA levels by quantitative real time PCR [Figure 11].

Taken together, Gefitinib treatment of GBM cells resulted in a reduced cell proliferation and cellular metabolic rate. These effects were directly correlated to the time of exposure and to the applied concentration of the tyrosine kinase inhibitor. Interestingly, compared to the untreated reference cells the inhibition by Gefitinib resulted in lower PTPIP51 and 14-3-3β protein expression level correlated to the applied inhibitor concentration. The mRNA level did not show significant change but the PTPIP51 interaction profile changed in correlation to the applied Gefitinib [Figure 11, 12].

.

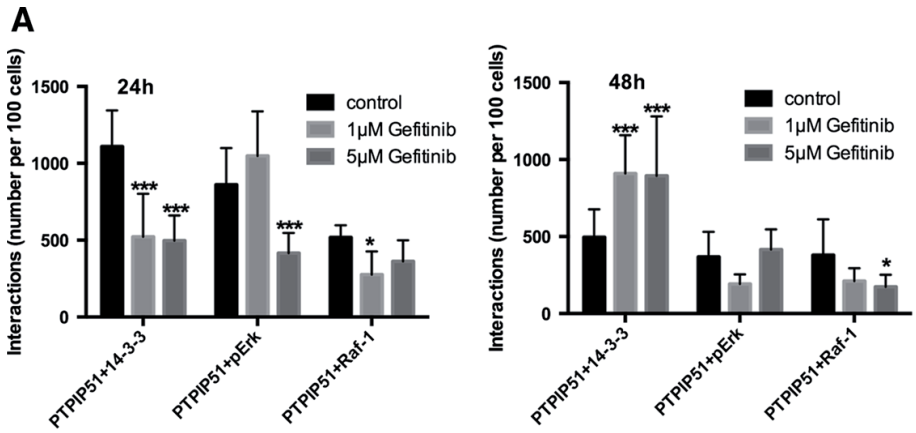

Figure 12: Changes in the interaction profile of PTPIP51 by Gefitinib treatment in a time and dose dependent manner

The use of the monoclonal antibody Cetuximab did not affect the number of viable cells. Their metabolic rate was marginally depressed in relation to the applied Cetuximab concentration. The mRNA and protein expression levels of PTPIP51 as well as of 14-3-3β remained unaffected by Cetuximab treatment.

These findings confirm a direct relation between PTPIP51 and 14-3-3β with the EGFR/MAPK signalling pathway in glioblastoma.

Cetuximab did neither influence PTPIP51 mRNA expression nor tumour cell proliferation rate. As a monoclonal antibody, Cetuximab binds to the extracellular part of the EGFR, thus abolishing the binding of ligands such as EGF. A slight reduction of cellular metabolism was the only dose dependent effect of Cetuximab treatment. This neletible effect of the monoclonal antibody may be explained by the

intrinsic and independent phosphoactivation of mutant EGFR dimer configuration which shows a high prevalence in GBM (Gajadhar et al, 2012).

As a tyrosine kinase inhibitor (TKI) Gefitinib influences this intrinsic EGFR activation of the MAPK pathway. But, despite the distinct effect of Gefitinib treatment in GBM cell culture experiments the clinical context did not reach this effect. Clinical trials using EGFR inhibitors demonstrated only modest improvements in a small percentage of GBM patients, suggesting that many GBMs possess intrinsic resistance or rapidly acquire resistance to EGFR inhibition (Clark et al, 2012).

Our study identified PTPIP51 as a scaffolding protein influencing the EGFR/MAPK pathway in glioblastoma. In consequence, analysis of PTPIP51 expression could indicate the therapeutic response to anti-EGFR therapy by Gefitinib. Further studies are needed to understand the potential of interference in the EGFR phosphorylation independent regulatory circuits, in order to make the MAPkinase pathway sensitive for the knock down of PTPIP51.

2.5 Ongoing Questions

Taking into account the involvement of PTPIP51 in the important MAPK signaling pathway in different tumours, knock down experiments by siRNA are needed to get more insights into the role of PTPIP51 in tumour progression.

The present studies revealed a tissue specific higher expression of PTP1B in glioblastoma. Its stimulating effects on the EGFR/MAPK pathway has previously been described in various malignancies but not in glioma so far. Further studies are needed to explore its importance and relation to PTPIP51 function in this type of tumour to disclose possible intervention mechanisms.

The similarities of PTPIP51 features and that of its interacting partners in prostate carcinoma and glioblastoma suggest a central role of PTPIP51 in the EGFR/MAPK signalling in prostate carcinoma. This hints to a probable common mechanism for affecting both tumour entities on the level of PTPIP51. Thus, the consecutive studies have to be expanded on cultured prostate cancer cells.

PTPIP51 promotor methylation studies are of great importance in pathogenesis and progression of glioma. An investigation of the methylation status in the long-term-survivors of glioblastoma patients would be of enormous interest. This data could become a prognostic predictor for therapy by EGFR inhibitors or PTPIP51 modulating molecules, corresponding to the clinical established MGMT promotor methylation status being a prognostic predictor of therapy with temozolomide.

As a tumour specific expression profile of PTPIP51 was detected in our laboratory, ongoing investigations of PTPIP51 as a molecular marker for ependymoma classification are in progress.

A further analysis of PTPIP51 expression in neuroepithelial tumour entities, being not included in the presented studies aside from diffuse astrocytoma WHO grade II, glioblastoma and several ependymomas, is necessary. These studies probably could help to sub-classify the tumours according to their PTPIP51 expression. What about PTPIP51 expression in oligodendroglial glioma and pilocytic glioma? What is the basis for the high PTPIP51 protein concentration in endothelial cells of neuroepithelial tumours of the choroid plexus tumours?

With the background of high PTPIP51 expression in the nerve fibres of prostate cancer its expression profile in neuroma and schwannoma could be very insightful.

In prostate carcinoma and glioblastoma a strong expression of PTPIP51 was detected in granulocytes in the capillaries of the tumour tissue as well as in the tumour infiltrating granulocytes. PTPIP51 probably plays an important role in the regulation of the immune system. Up to now, this has not been investigated.

The evolutionary conserved protein PTPIP51 has been detected in various different organs, tissues and cell types. This could implicate a basal function in every cell, as for example every cell uses MAP kinase signalling. But, there are some types of cells, which are lacking PTPIP51 e.g. B-lymphocytes. Further studies are needed to explore a correlation of PTPIP51 expression in relation to the cell type.

Latest research findings reported the influence of PTPIP51 on calcium homeostasis in neuronal cells by its interaction with VAPB, thus linking the endoplasmatic reticulum to mitochondria (Stoica et al, 2014). Pertubated calcium signaling can affect tumour growth. Investigation of VAPB interaction will give better insights into tumour growth regulation. Gürsel and coworkers (2015) suggested to target GSK3β in glioblastoma stem-like cells combined with current therapeutic options. Current studies in our laboratory revealed the interaction of PTPIP51 and GSK3β stressing its function as scaffolding protein. Yet, further studies are required to disclose the function of PTPIP51 in GSK3β signaling.

Basing on the growing knowledge of various tumour entities and their characteristic details, e.g. mutation and receptor status and in consequence deteriorated intracellular signalling, there is an increasing demand for personalized therapies. Up to now, there exist several possibilities for such a personalized therapy basing either on specific antibodies, on tyrosine kinase inhibitors or small molecular inhibitors. Most of these therapies intervene very early in the signalling pathways on the upstream region of the se pathways resulting in the development of resistances of the tumour cells to the treatment.

PTPIP51 is a protein being part of numerous signalling knots in many deteriorated tumour relevant signalling pathways. Certainly, there will be crosstalks between some of these tumour relevant pathways. Therefore one of the upcoming questions will be the disclosure of such crosstalks on PTPIP51 level.

Recently, PTPIP51 became drugable by the development of the specific small molecule modulator LDC3 (Brobeil et al, Hoenig et al, submitted). LDC3 affects the

interaction profile of PTPIP51, thus changing the downstream activation of these pathways (Brobeil et al, submitted).

Yet, the presented studies give an important insight in the characteristics of PTPIP51 in glioma and prostate cancer giving the basis for therapeutic options.

3. Summary

3.1 Summary

To sum up, PTPIP51 is overexpressed in prostate carcinoma compared to benign prostate hyperplasia and in glioblastoma WHO grade IV compared to WHO grade II astrocytoma. In both tumour entities PTPIP51 shows a tissue specific expression profile.

For the first time we could link the methylation status of PTPIP51 in prostate carcinoma and benign prostate hyperplasia to the observed altered expression profiles. Here we found a hypomethylation in prostate cancer, which was not seen in benign prostate hyperplasia. This probably explains the higher expression of PTPIP51 in PCa in comparison to BPH on protein level which is reflected on the mRNA level.

The interaction of PTPIP51 with 14-3-3β was identified to lead to a ternary complex with cRAF (Raf1) stimulating the downstream effector of the EGFR/MAPK signaling-pathway. This pathway plays an essential role in cell proliferation and migration, which is especially crucial for the progression of carcinoma. The co-localization of PTPIP51 with 14-3-3β, Raf-1 and PTP1B was as well identified in prostate carcinoma as in glioblastoma. These findings underline the important role of PTPIP51 in the EGFR/MAPK pathway in cancer.

PTP1B is expressed in the investigated tumour samples displaying a similar cellular distribution comparable to that of PTPIP51. As PTP1B regulates the phosphorylation status of PTPIP51, which in turn regulates the interaction of PTPIP51 with 14-3-3β, we postulate a changed interaction profile of PTPIP51 in tumours.

Glioblastoma overexpress EGFR as well as the mutant form EGFRvIII. Therefore, the regulatory potential of PTPIP51 on the downstream part of the EGFR/MAPK pathway was investigated in glioblastoma cells. Interestingly, we were able to demonstrate a direct correlation between the successful inhibition of EGFR by the tyrosine kinase inhibitor Gefitinib treatment led to downregulated expression of PTPIP51 and 14-3-3β on protein level and a changed interaction profile, emphasizing the important influence of PTPIP51 on EGFR signaling in tumours.

In summary, these investigations present an important basis for numerous following studies of PTPIP51 regulation in tumours. Of particular interest is the functional implication of PTPIP51 in neuroepithelial tumours and its clinical relevance as molecular marker in staging or as a target in new therapy strategies.

3.2 Zusammenfassung

Zusammenfassend läßt sich festhalten, dass PTPIP51 sowohl in Prostata Karzinomen verglichen mit benigner Prostata Hyperplasie, als auch in Glioblastomen WHO °IV verglichen mit WHO Grad II Astrozytomen eine erhöhte Expression aufweist. In beiden Tumorentitäten weißt PTPIP51 eine gewebespezische Expressionsverteilung auf, die in den vorgelegten Publikationen zum ersten Mal beschrieben wurde.

In Prostata Karzinomen konnten wir erstmalig einen hypomethylierten Status der Promotorregion des PTPIP51 Gens nachweisen, welche in der benignen Prostata Hyperplasie nicht nachweisbar war. Dies ist eine mögliche Basis für die Überexpression von PTPIP51 in Prostata Karzinomen.

Über die Interaktion mit 14-3-3β bildet PTPIP51 einen Komplex mit Raf-1, was über Raf-1 vermittelt den EGFR/MAPK Signalweg stimuliert. Dieser Signalweg spielt eine wichtige Rolle bei der Proliferation und Migration. Dies sind Prozesse, die essentiell für die Progression von Karzinomen sind. Die Co-Lokalisationen von PTPIP51 mit14-3-3β, Raf-1 und PTP1B konnten sowohl im Prostata Karzinom als auch im Glioblastom nachgewiesen werden. Dies weist auf eine zentrale Rolle des PTPIP51 im EGFR/MAPK Signalweg der Karzinome hin.

PTP1B weist ein ähnliches Verteilungsmuster wie PTPIP51 in den untersuchten Karzinomen auf. Über die Interaktion der PTP1B mit PTPIP51 wird PTPIP51 dephosphoryliert, was wiederum die Interaktion des PTPIP51 mit Raf1 reguliert und somit zu einer erhöhten Aktivierung des MAPK Signalweges in den Karzinomen führt.

Da eine Überexpression von EGFR sowie die Expression einer dauerstimulierten mutierten Form des EGF-Rezeptors, EGFRvIII, besonders in der Pathogenese von Glioblastomen eine Rolle spielt, war ein zentraler Punkt der Untersuchungen die

Frage nach der Regulation von PTPIP51 und dem EGFR/MAPK Signalweg in Glioblastomzellen. Es ließ sich ein direkter Zusammenhang zwischen der erfolgreichen Hemmung des EGFR durch den Tyrosin Kinase Inhibitor Gefitinib und der Expression von PTPIP51 auf Proteinebene, sowie ein verändertes Interaktionsprofil nachweisen.

Diese Arbeiten bilden die Basis für weitere interessante Studien zu PTPIP51. Von besonderem Interesse ist die Beteiligung von PTPIP51 an neuroepithelialen Tumoren und dessen Rolle als molekularer Marker oder Angriffspunkt für klinisch relevante Interventionen, die letztendlich zu einem möglichen Therapieansatz führen könnten.

4. References

Alaiya AA, Al-Mohanna M, Aslam M, Shinwari Z, Al-Mansouri L, Al-Rodayan M, Al-Eid M, Ahmad I, Hanash K, Tulbah A, Bin Mahfooz A, Adra C. Proteomics-based signature for human benign prostate hyperplasia and prostate adenocarcinoma. Int J Oncol. 2011. Apr;38(4):1047-57. doi: 10.3892/ijo.2011.937. Epub 2011 Feb 8

Ayala GE, Dai H, Powell M, Li R, Ding Y, Wheeler TM, Shine D, Kadmon D, Thompson T, Miles BJ, Ittmann MM, Rowley D. Cancer-related axonogenesis and neurogenesis in prostate cancer. Clin Cancer Res. 2008. Dec 1;14(23):7593-603. doi: 10.1158/1078-0432.CCR-08-1164

Arias-Romero LE, Saha S, Villamar-Cruz O, Yip SC, Ethier SP, Zhang ZY, Chernoff J. Activation of Src by protein tyrosine phosphatase 1B Is required for ErbB2 transformation of human breast epithelial cells. Cancer Res. 2009. Jun 1;69(11):4582-8. doi: 10.1158/0008-5472.CAN-08-4001. Epub 2009 May 12

Bandyopadhyay S, Chiang C-Y, Srivastava J, Gersten M, White S, Bell R, et al. A human MAP kinase interactome. Nat. Methods. 2010. Oct;7(10):801–5

Barop J, Sauer H, Steger K, Wimmer M. Differentiation-dependent PTPIP51 expression in human skeletal muscle cell culture. J Histochem Cytochem 2009;57(5):425-35

Bjorge, J. D., Pang, A., and Fujita, D. J. Identification of protein-tyrosine phosphatase 1B as the major tyrosine phosphatase activity capable of dephosphorylating and activating c-Src in several human breast cancer cell lines. Biol. Chem. 2000. 275: 41439–41446

Bobrich M, Brobeil A, Mooren FC, Krüger K, Steger K, Tag C, Wimmer M. PTPIP51 interaction with PTP1B and 14-3-3β in adipose tissue of insulin-resistant mice. Int J Obes (Lond) 2011;Epub Jan 25

Brobeil A, Graf M, Oeschger S, Steger K, Wimmer M. PTPIP51-a myeloid lineage specific protein interacts with PTP1B in neutrophil granulocytes. Blood Cells Mol Dis 2010;45(2):159-68

Brobeil A, Bobrich M, Wimmer M. Protein tyrosine phosphatase interacting protein 51- a-jack-of-all-trades protein. CTR 2011a;doi:10.1007/s00441-011-1146-1

Brobeil A, Bobrich M, Graf M, Kruchten A, Blau W, Rummel M, Oeschger S, Steger K, Wimmer M. PTPIP51 is phosphorylated by Lyn and c-Src kinases lacking dephosphorylation by PTP1B in actue myeloid leukemia. Leukemia Research 2011b; 35(10):1367-75

Brobeil A, Bobrich M, Tag C, Wimmer M. PTPIP51 in protein interactions: regulation and in situ interacting partners. Cell Biochem Biophys. 2012a ;63(3):211-22

Brobeil A, Graf M, Eiber M, Wimmer M. Interaction of PTPIP51 with Tubulin, CGI-99 and Nuf2 During Cell Cycle Progression. Biomolecules 2012b,2,122-142; doi:10.3390/biom2010122

Cai H, Babic I, Wei X, Huang J, Witte ON. Invasive prostate carcinoma driven by c-Src and androgen receptor synergy. Cancer Res. 2011. Feb 1;71(3):862-72. doi: 10.1158/0008-5472.CAN-10-1605. Epub 2010 Dec 6

Carrión-Salip D, Panosa C, Menendez JA, Puig T, Oliveras G, Pandiella A, De Llorens R, Massaguer A. Androgen-independent prostate cancer cells circumvent EGFR inhibition by overexpression of alternative HER receptors and ligands. Int J Oncol. 2012. Sep;41(3):1128-38. doi: 10.3892/ijo.2012.1509. Epub 2012 Jun 6

Cao L, Cao W, Zhang W, Lin H, Yang X, Zhen H, Cheng J, Dong W, Huo J, Zhang X. Identification of 14-3-3 protein isoforms in human astrocytoma by immunohistochemistry. Neurosci Lett 2008;432:94-9

Cao L, Wang YY, Wang XR, Wang XF, Sun G, Luo H, Liu N, You YP. Expression of RAS protein in glioma and its effect on the growth of human glioma cells. Zhonghua Yi Xue Yi Chuan Xue Za Zhi. 2012. Apr;29(2):159-62. doi: 10.3760/cma.j.issn.1003-9406.2012.02.009

Cao WD, Zhang X, Zhang JN, Yang ZJ, Zhen HN, Cheng G, Li B, Gao D. Immunocytochemical detection of 14-3-3 in primary nervous system tumors. J Neurooncol. 2006. Apr;77(2):125-30. Epub 2005 Nov 15

Clark P A, Lida M, Treisman D M, Kalluri H, Ezhilan S, Zomiak M, Wheeler D L, Kuo J S. Activation of Multiple ERBB Family Receptor Mediates Glioblastoma Cancer Stem-like Cell Resistance to EGFR-Targeted Inhibition. Neoplasia. 2012. 14(5): 420-428

Chowdhury S, Kirby R. Advances in the treatment of metastatic prostate cancer. Practitioner. 2013. Apr;257(1760):15-8, 2

Crawford ED. Epidemiology of prostate cancer. Urology 2003;62(6) suppl 1:3-12

Ewing RM, Chu P, Elisma F, Li H, Taylor P, Climie S, McBroom-Cerajewski L, Robinson MD, O'Connor L, Li M, Taylor R, Dharsee M, Ho Y, Heilbut A, Moore L, Zhang S, Ornatsky O, Bukhman YV, Ethier M, Sheng Y, Vasilescu J, Abu-Farha M, Lambert JP, Duewel HS, Stewart II, Kuehl B, Hogue K, Colwill K, Gladwish K, Muskat B, Kinach R, Adams SL, Moran MF, Morin GB, Topaloglou T, Figeys D. Large-scale mapping of human protein-protein interactions by mass spectrometry. Mol Syst Biol 2007;3:89

Farrell J, Petrovics G, McLeod DG, Srivastava S. Genetic and Molecular Differences in Prostate Carcinogenesis between African American and Caucasian American Men. Int J Mol Sci. 2013. Jul 25;14(8):15510-31. doi: 10.3390/ijms140815510

Frank Marko N, Weil RJ, Schroder JL, Sawaya R. 148 Extent of resection of glioblastoma revisited: personalized survival modeling facilitates more accurate individualized survival prediction and supports a "maximum safe resection" approach surgery. Neurosurgery. 2013. Aug;60 Suppl 1:169. doi: 10.1227/01.neu. 0000432739.71828.ce

Gajadhar A S, Bogdanovic E, Munoz D M, Guha A In situ analysis of mutant EGFRs prevalent in glioblastoma multiforme reveals aberrant dimerization, activation, and differential response to anti-EGFR targeted therapy. Mol Cancer Res. 2012. 10(3):428-40

Gao Q, Lei T, Ye F. Therapeutic targeting of EGFR-activated metabolic pathways in glioblastoma. Expert Opin Investig Drugs. 2013. 22(8):1023-1040

Glass AS, Cary KC, Cooperberg MR. Risk-based prostate cancer screening: who and how? Curr Urol Rep. 2013. Jun;14(3):192-8. doi: 10.1007/s11934-013-0319-8

Grönberg H. Prostate cancer epidemiology. Lancet 2003;361(9360):859-64

Guimaraes MS, Quintal MM, Meirelles LR, Magna LA, Ferreira U, Billis A. Gleason score as predictor of clinicopathologic findings and biochemical (PSA) progression following radical prostatectomy. Int Braz J Urol. 2008. Jan-Feb;34(1):23-9

Gürsel DB, Banu MA, Berry N, Marongiu R, Burkhardt JK, Kobylarz K, Kaplitt MG, Rafii S, Boockvar JA. Tight regulation between cell survival and programmed cell death in GBM stem-like cells by EGFR/GSK3b/PP2A signaling. J Neurooncol. 2015. Jan;121(1):19-29

Halatsch ME, Gehrke EE, Vougioukas VI, Bötefür IC, A-Borhani F, Efferth T, Gebhart E, Domhof S, Schmidt U, Buchfelder M. Inverse correlation of epidermal growth factor receptor messenger RNA induction and suppression of anchorage-

independent growth by OSI-774, an epidermal growth factor receptor tyrosine kinase inhibitor, in glioblastoma multiforme cell lines. J Neurosurg. 2004. Mar;100(3):523-33

Hayne C, Tzivion G, Luo Z. Raf-1/MEK/MAPK pathway is necessary for the G2/M transition induced by nocodazole. J. Biol. Chem. 2000, 13,31876-31882

Hegi ME, Rajakannu P, Weller M. Epidermal growth factor receptor: a re-emerging target in glioblastoma. Curr Opin Neurol. 2012. Dec;25(6):774-9. doi: 10.1097/WCO.0b013e328359b0bc

Hudson BD, Kulp KS, Loots GG. Prostate cancer invasion and metastasis: insights from mining genomic data. Brief Funct Genomics. 2013. Jul 22. [Epub ahead of print]

Ichimura T, Taoka M, Shoji I, Kato H, Sato T, Hatakeyama S, et al. 14-3-3 proteins sequester a pool of soluble TRIM32 ubiquitin ligase to repress autoubiquitination and cytoplasmic body formation. J Cell Sci. 2013. May 1;126(Pt 9):2014-26. doi: 10.1242/jcs.122069. Epub 2013 Feb 26

Jin J, Smith FD, Stark C, Wells CD, Fawcett JP, Kulkarni S, Metalnikov P, O'Donnell P, Taylor P, Taylor L, Zougman A, Woodgett JR, Langeberg LK, Scott JD, Pawson T. Proteomic, functional and domain-based analysis of in vivo 14-3-3 binding proteins involved in cytoskeletal regulation and cellular organization. Curr Biol 2004;14:1436-50

Jones PL, Wolffe AP. Relationships between chromatin organization and DNA methylation in determining gene expression. Semin Cancer Biol. Review. 1999. Oct;9(5):339-47

Karpel-Massler G, Schmidt U, Unterberg A and Halatsch M E Therapeutic inhibition of the epidermal growth factor receptor in high-grade gliomas: where do we stand? Mol. Cancer. Res. 2009. 7, 1000-1012

Koch P, Stenzinger A, Viard M, Märker D, Mayser P, Nilles M, Schreiner D, Steger K, Wimmer M. The novel protein PTPIP51 is expressed in human keratinocyte carcinomas and their surrounding stroma. J Cell Mol Med 2008;12:2083-95.

Koch P, Viard M, Stenzinger A, Brobeil A, Tag C, Steger K, Wimmer M. Expression profile of PTPIP51 in mouse brain. J Comp Neurol 2009a;517:892-905

Koch P, Petri M, Paradowska A, Stenzinger A, Sturm K, Steger K, Wimmer M. PTPIP51 mRNA and protein expression in tissue microarrays and promoter methylation of benign prostate hyperplasia and prostate carcinoma. Prostate 2009b;69:1751-62

Lamy S, Wilmart JF, Hein T, Scheiden R, Capesius C. Prostate cancer in Luxembourg from 1982 to 2006. Incidence and mortality. Survival of a hospital cohort. Bull Soc Sci Med Grand Duche Luxemb. 2013;(1):6-19

Lessard L, Labbé DP, Deblois G, Bégin LR, Hardy S, Mes-Masson AM, Saad F, Trotman LC, Giguère V, Tremblay ML. PTP1B is an androgen receptor-regulated phosphatase that promotes the progression of prostate cancer. Cancer Res. 2012. Mar 15;72(6):1529-37. doi: 10.1158/0008-5472.CAN-11-2602. Epub 2012 Jan 26

Li R, Wheeler T, Dai H, Ayala G. Neural cell adhesion molecule is upregulated in nerves with prostate cancer invasion. Hum Pathol. 2003. May;34(5):457-61

Loew S, Schmidt U, Unterberg A, Halatsch M E. The epidermal growth factor receptor as a therapeutic target in glioblastoma multiforme and other malignant neoplasms. Anticancer Agents Med Chem, 2009. 6,703-15

Louis DN, Ohgaki H, Wiestler OD, Cavenee WK. WHO classification of tumours oft he central nervous system. World Health Organization Classification of Tumours. (2007) IARC Press, Lyon, France

.

Lu KV, Chang JP, Parachoniak CA, Pandika MM, Aghi MK, Meyronet D, Isachenko N, Fouse SD, Phillips JJ, Cheresh DA, Park M, Bergers G. VEGF inhibits tumor cell invasion and mesenchymal transition through a MET/VEGFR2 complex. Cancer Cell. 2012. Jul 10;22(1):21-35. doi: 10.1016/j.ccr.2012.05.037

Lv BE, Yu CE, Chen YY, Lu Y, Guo JH, Song QS, Ma DL, Shi TP, Wang L. Protein tyrosine phophatase interacting protein 51 (PTPIP51) is a novel mitochondria protein with an N-terminal mitochondrial targeting sequence and induces apoptosis. Apoptosis 2006;11:1489-501

Lyustikman Y, Momota H, Pao W, Holland EC. Constitutive activation of Raf-1 induces glioma formation in mice. Neoplasia. 2008 May;10(5):501-10

Maerker D, Stenzinger A, Schreiner D, Tag C, Wimmer M. Expression of PTPIP51 during mouse eye development. Histochem Cell Biol 2008;129:345-56

Martinez CH, Williams AK, Chin JL, Stitt L, Izawa JI. Perineural invasion and TRUS findings are complementary in predicting prostate cancer biology. Can J Urol. 2013. Apr;20(2):6696-701

Mulholland DJ, Kobayashi N, Ruscetti M, Zhi A, Tran LM, Huang J, Gleave M, Wu H.

Pten loss and RAS/MAPK activation cooperate to promote EMT and metastasis initiated from prostate cancer stem/progenitor cells. Cancer Res. 2012. Apr 1;72(7):1878-89. doi: 10.1158/0008-5472.CAN-11-3132. Epub 2012 Feb 20

Petri MK, Koch P, Stenzinger A, Kuchelmeister K, Nestler U, Paradowska A, Steger K, Brobeil A, Viard M, Wimmer M. PTPIP51, a positive modulator of the MAPK/Erk

pathway, is upregulated in glioblastoma and interacts with 14-3-3β and PTP1B in situ. Histol Histopathol. 2011 ;26(12):1531-43

Petri MK, Brobeil A, Planz J, Bräuninger A, attenlöhner S, Nestler U, Stenzinger A, Paradowska A, Wimmer M. PTPIP51 levels in glioblastoma cells depend on inhibition oft he EGF-receptor. J Neurooncol.2015, May;123(1):15-25

Porsche A. Identifikation von Interaktionspartnern der T-Zell Protein-Tyrosin-Phosphatase durch das Lex-A Two Hybrid System; thesis (PhD) University of Konstanz. Allensbach: UFO Publishers; 2001. Vol 414

Reifenberger G, Collins VP. Pathology and molecular genetics of astrocytic gliomas. J Mol Med 2004, Oct;82(10):656-670

Reifenberger G, Blümcke I, Pietsch T, Paulus W. Pathology and Classification of tumors of the Nervous System. Book chapter. Oncology of CNS Tumors, DOI: 10.1007/978-3-642-02874-8_1, Springer-Verlag Berlin Heidelberg 2010

Ren G, Liu X, Mao X, Zhang Y, Stankiewicz E, Hylands L, Song R, Berney DM, Clark J, Cooper C, Lu YJ. Identification of frequent BRAF copy number gain and alterations of RAF genes in Chinese prostate cancer. Genes Chromosomes Cancer. 2012. Nov;51(11):1014-23. doi: 10.1002/gcc.21984. Epub 2012 Jul 25

Roberts PJ, Der CJ. Targeting the Raf-MEK-ERK mitogen-activated protein kinase cascade for the treatment of cancer. Oncogene. 2007. May 14;26(22):3291-310

Shah N, Lin B, Sibenaller Z, Ryken T, Lee H, Yoon JG, Rostad S, Foltz G. Comprehensive Analysis of MGMT Promoter Methylation: Correlation with MGMT Expression and Clinical Response in GBM. PLoS One 2011;6(1):e16146

Smith AJ, Karpova Y, D'Agostino R Jr, Willingham M, Kulik G. Expression of the Bcl-2 protein BAD promotes prostate cancer growth. PLoS One 2009;4(7):e6224

Staberg M, Riemer C, Xu R, Dmytriyeva O, Bock E, Berezin V. Identification of a novel antagonist of the ErbB1 receptor capable of inhibiting migration of human glioblastoma cells. Cell Oncol (Dordr). 2013 Jun;36(3):201-11. doi: 10.1007/s13402-013-0128-6. Epub 2013 Apr 12

Stedt H, Alasaarela L, Samaranayake H, Pikkarainen J, Määttä AM, Kholová I, Parker AS, Ylä-Herttuala S. Specific inhibition of SRC kinase impairs malignant glioma growth in vitro and in vivo. Mol Ther Nucleic Acids. 2012. May 1;1:e19. doi: 10.1038/mtna.2012.13

Stenzinger A, Kajosch T, Tag C, Porsche A, Welte I, Hofer HW, Steger K, Wimmer M. The novel protein PTPIP51 exhibits tissue- and cell-specific expression. Histochem Cell Biol 2005;123:19-28

Stenzinger A, Schreiner D, Tag C, Wimmer M. Expression of the novel protein PTPIP51 in rat liver: an immunhistochemical study. Histochem Cell Biol. 2007. Jul;128(1):77-84

Stenzinger A, Schreiner D, Koch P, Hofer HW, Wimmer M. Cell- and molecular biology of the novel protein tyrosine phosphatase interacting protein 51. Int Rev Cell Mol Biol 2009;275:183-246

Stoica R, De Vos KJ, Paillusson S, Mueller S, Sancho RM, Lau KF, Vizcay-Barrena G, Lin WL, Xu YF, Lewis J, Dickson DW, Petrucelli L, Mitchell JC, Shaw CE, Miller CC. ER-mitochondria associations are regulated by the VAPB-PTPIP51 interaction and are disrupted by ALS/FTD-associated TDP-43. NatCommun. 2014. Jun 3; 5:3996

Tice DA, Biscardi JS, Nickles AL, Parsons SJ. Mechanism of biological synergy between cellular Src and epidermal growth factor receptor. Proc Natl Acad Sci U S A. 1999. Feb 16;96(4):1415-20

Tsuchiya N, Narita S, Inoue T, Saito M, Numakura K, Huang M, Hatakeyama S, Satoh S, Saito S, Ohyama C, Arai Y, Ogawa O, Habuchi T. Insulin-like growth factor-1 genotypes and haplotypes influence the survival of prostate cancer patients with bone metastasis at initial diagnosis. BMC Cancer. 2013. Mar 25;13:150. doi: 10.1186/1471-2407-13-150

Tuck-Muller CM, Narayan A, Tsien F, Smeets DF, Sawyer J, Fiala ES, Sohn OS, Ehrlich M. DNA hypomethylation and unusual chromosome instability in cell lines from ICF syndrome patients. Cytogenet Cell Genet. 2000;89(1-2):121-8

Yang SH, Andl T, Grachtchouk V, Wang A, Liu J, Syu LJ, Ferris J, Wang TS, Glick AB, Millar SE, Dlugosz AA. Pathological responses to oncogenic Hedgehog signaling in skin are dependent on canonical Wnt/beta-catenin signaling. Nat Genet 2008;40:1130–5

Yao Y, Dai W. Mitotic checkpoint control and chromatin remodelling. Front Biosci. 2012, 1,976-983

Yu C, Han W, Shi T, Lv B, He Q, Zhang Y, Li T, Zhang Y, Song Q, Wang L, Ma D. PTPIP51, a novel 14-3-3 binding protein, regulates cell morphology and motility via Raf-ERK pathway. Cell Signal 2008;20:2208-20.

Xu W, Allbritton N, Lawrence DS. SRC kinase regulation in progressively invasive cancer. PLoS One. 2012;7(11):e48867. doi: 10.1371/journal.pone.0048867. Epub 2012 Nov 7

5. List of publications

A) Original papers

Koch P, Petri M, Paradowska A, Stenzinger A, Sturm K, Steger K, Wimmer M. PTPIP51 mRNA and protein expression in tissue microarrays and promoter methylation of benign prostate hyperplasia and prostate carcinoma. Prostate 2009; 68(16): 1751-62.

Petri M K, Koch P, Stenzinger A, Kuchelmeister K, Nestler U, Paradowska A, Steger K, Brobeil A, Viard M, Wimmer M. PTPIP51, a positive modulator of the MAPK/Erk pathway, is upregulated in glioblastoma and interacts with 14-3-3β and PTP1B in situ. Histology and Histopathology. 2011; 26: 1531-1543

Petri M K, Brobeil a, Planz J, Bräuninger A, Gattenlöhner S, Nestler U, Stenzinger A, Paradowska A, Wimmer M. PTPIP51 levels in glioblastoma cells depend on inhibition of the EGF-receptor Journal of Neuro-Oncology 2015; DOI 10.1007/s11060-015-1763-8; Volume 123 (1):15-25

Brobeil A, Viard M, Petri M K, Steger K, Tag C, Wimmer M. Memory and PTPIP51 – a new protein in hippocampus and cerebellum. Mol Cell Neurosci. 2015;DOI 10.1016/j.mcn.2014.12.003; Jan, 64:61-73

B) Poster abstracts / Lecture

Petri M, Koch P, Stenzinger A, Kuchelmeister K, Nestler U, Wimmer M. Glioblastoma express PTPIP51, an interacting partner of 14-3-3β.
(GBM International Symposium, Signal Transduction and Diseases, Aachen 2009)

Koch P, Petri M, Stenzinger A, Paradowska A, Wimmer M. PTPIP51 is Expressed in Human Keratinocyte Carcinoma, Prostate Carcinoma and Glioblastoma.

(5th International Conference on Tumor Microenvironment: Progression, Therapy and Prevention, Versailles 2009)

Bobrich M, Kamm M, Petri M, Brobeil A, Viard M, Kuchelmeister K, Wimmer M. PTPIP51 – A new marker for ependymoma? (52th Symposium of the society for Histochemistry, Prag 2010)

Petri M, Planz J, Nestler U, Stenzinger A, Paradowska A, Wimmer M. Inhibtion of the EGFR/MAPK pathway in glioblastoma cell lines at different points of application – inhibition of EGFR's tyrosine kinase via Gefitinib causes depression of PTPIP51. (62. Jahrestagung der DGNC, Hamburg 2011)

Meike Petri, Christoph A. Tschan, Henry W. S. Schroeder, Sonja Vulcu, Michael R. Gaab, Joachim Oertel. Safety and efficiency of endoscopic neurosurgery in children – experience with 164 procedures. (International Society for Pediatric Neurosurgery, 41. Annual Meeting, E-Poster, ISPN Mainz 2013)

Meike Petri, Sebastian Antes, Mohamed Salah, Cristoph A. Tschan, Joachim Oertel. The ShuntScope – new and effective tool for ventricle catheter placement in complex cases of hydrocephalus in pediatric neurosurgery (66. Jahrestagung der DGNC, Lecture, Karlsruhe 2015)

6. Acknowledgements

First of all, I would like to thank Prof. Dr. Monika Wimmer. She was and is still a great supervisor and mentor to me. Her helpfulness, encouragement, spirit and empathy are outstanding. She opened my mind and introduced me to the field of scientific research. She always took time for reviewing abstracts, posters and fruitful discussions. Besides her scientific encouragement, during the last years she helped me through any problems and became a very important person of my personel field. I hope this will last for our lifetime.

Further I would like to thank Prof. Dr. Klaus Steger and his team (Department of Urology and Pediatric Urology, JLU Giessen) for the introductions of methods performed in their laboratory and in particular Dr. Agnieszka Paradowska for help with the realization of the PCR studies.

I am grateful to Prof. Dr. Klaus Kuchelmeister (Department of Neuropathology, University Hospital, Bonn) for his suggestions and help with neurohistopathologic diagnosis of glioma tissues.

I am also very grateful to PD. Dr. Ulf Nestler (Department of Neurosurgery, University Hospital, Leipzig) for his suggestions and help with the realization of the studies about glioblastoma cell lines.

Also I would like to thank the whole team of the Institute of Anatomy and Cell Biology, especially Claudia Tag and Martin Bodenbenner for their kindness and excellent technical support and Karola Michael for help with the photographical preparations.

It was a pleasure for me to work together with several other doctoral candidates at the institute of Anatomy and Cell Biology, especially with Philipp Koch and Albrecht Stenzinger. Both of them always took time for mentoring me. Our inspiring and fruitful discissions helped me enormes to broaden my horizon in scientific research. I am very happy that beside great collaboration a friendship of us resulted from doing research together. I would further like to thank Alexander Brobeil and Manuel Bobrich for inspiring discussions and fruitful collaboration. It was a great time and a lot of fun we shared together.

I would like to thank the whole team of the Department of Neurosurgery (JLU Giessen) for providing an insight into the world of neurosurgery and its research possibilities to me, a field which I hope to remain working in for my lifetime.

I am more than thankful to my friends and especially to Katie, Frederic and Anja, who always kept my spirits high during the last years in Giessen.
I want to express my heartfeld gratitude to Benjamin for his ongoing endurance, encouragement, love and supporting me to indulge my passion for scientific research.
Finally my thanks go to father who always encouraged me to go after my ambitions and to never give up and to my mother who supports me with good advice and love through my whole live and to my sisters.

Der Lebenslauf wurde aus der elektronischen Version der Arbeit entfernt.

The curriculum vitae was removed from the electronic version of the paper.

8. Annexes

Original paper (1)

Koch P, Petri M, Paradowska A, Stenzinger A, Sturm K, Steger K, Wimmer M. **PTPIP51 mRNA and protein expression in tissue microarrays and promoter methylation of benign prostate hyperplasia and prostate carcinoma.** Prostate 2009; 68(16):1751-62.

Original paper (2)

Petri MK, Koch P, Stenzinger A, Kuchelmeister K, Nestler U, Paradowska A, Steger K, Brobeil A, Viard M, Wimmer M. **PTPIP51, a positive modulator of the MAPK/Erk pathway, is upregulated in glioblastoma and interacts with 14-3-3β and PTP1B *in situ*.** Histology and Histopathology 2011; 26: 1531-1543

Original paper (3)

Petri MK, Brobeil A, Planz J, Bräuninger A, Gattenlöhner S, Nestler U, Stenzinger A, Paradowska A, Wimmer M. **PTPIP51 levels in glioblastoma cells depend on inhibition of the EGF-receptor.** Journal of Neuro-Oncology 2015; 123 (1): 15-25

The Prostate 69:1751 – 1762 (2009)

PTPIP51 mRNA and Protein Expression in Tissue Microarrays and Promoter Methylation of Benign Prostate Hyperplasia and Prostate Carcinoma

Philipp Koch,[1]* Meike Petri,[1] Agnieszka Paradowska,[2] Albrecht Stenzinger,[1] Klaus Sturm,[3] Klaus Steger,[2] and Monika Wimmer[1]

[1]*Institute of Anatomy and Cell Biology, Justus-Liebig-University Giessen, Giessen, Germany*
[2]*Department of Urology and Pediatric Urology, Justus-Liebig-University Giessen, Giessen, Germany*
[3]*Department of Pathology, Justus-Liebig-University Giessen, Giessen, Germany*

BACKGROUND. Protein tyrosine phosphatase interacting protein 51 (PTPIP51) shows a tissue-specific expression pattern and is associated with cellular differentiation and apoptosis in several mammalian tissues. Overexpression of the full-length protein enhances apoptosis. It is also expressed in various carcinomas. In this study the expression of PTPIP51 and its in vitro interaction partners was investigated in human benign prostate hyperplasia (BPH) and in prostate carcinoma (PCa).

METHODS. Tissue microarrays of human BPH and PCa were analyzed by immunohistochemistry. For polymerase chain reaction (PCR), cryo samples of BPH and PCa were used. Bisulfite DNA treatment, followed by sequencing of PCR products was performed in order to analyze CpGs methylation within the promoter region of the PTPIP51 gene.

RESULTS. PTPIP51 mRNA and protein expression was detected in prostatic epithelia of BPH and in tumor cells of PCa, respectively, and within smooth muscle cells of the stromal compartment. A stronger expression was present in nerve fibers, particularly in PCa, in immune cells and in smooth muscle and endothelial cells of vessels of BPH and PCa. On mRNA levels, a slightly elevated expression of PTPIP51 was observed in the PCa group as tested by real-time quantitative PCR analyses. Methylation experiments revealed that at least 70% of methylated CpGs in the CpG island of the PTPIP51 gene promoter region were identified in BPH samples. In contrast, a loss of methylation has been found in the PCa group.

CONCLUSION. The promoter methylation status of PTPIP51 seems to influence the expression of PTPIP51, which was seen as elevated in the PCa. *Prostate 69: 1751–1762, 2009.*

KEY WORDS: **PTPIP51; benign prostate hyperplasia; prostate carcinoma; perineural invasion; promoter methylation status; PTP1B**

INTRODUCTION

Protein tyrosine phosphatase interacting protein 51 (PTPIP51, SwissProt accession code Q96SD6) is an evolutionary conserved protein, consisting of 470 amino acids. It was originally detected by a yeast-two-hybrid screen as an interaction partner of two non-transmembrane protein-tyrosine phosphatases, PTP1B and TcPTP [1]. The interaction takes place in the region between amino acids 78 and 214. In vitro and in HEK293 cell, the protein is phosphorylated at Tyr176 by Src kinase. Dephosphorylation is exerted by PTP1B and TcPTP [2].

In mammals, PTPIP51 is expressed in highly differentiated tissue, particularly in follicular and interfollicular epidermis, epithelia, skeletal muscle, testis, and nervous tissue [3]. PTPIP51 protein also plays a role

*Correspondence to: Philipp Koch, Institute of Anatomy and Cell Biology, Justus-Liebig-University, 35385 Giessen, Germany.
E-mail: philipp-sebastian.koch@anatomie.med.uni-giessen.de
Received 25 May 2009; Accepted 1 July 2009
DOI 10.1002/pros.21025
Published online 18 August 2009 in Wiley InterScience (www.interscience.wiley.com).

during mammalian development [4] and both, mRNA and protein could be traced during placental villi formation [5] and in various carcinomas [6,7]. The regulation of the PTPIP51 expression was investigated in immortalized human keratinocytes (HaCaT cells). Epidermal growth factor (EGF), known to promote proliferation, resulted in a reduced PTPIP51 expression, whereas differentiation, promoted by $1,25(OH_2)D_3$, resulted in an enhanced PTPIP51 expression, detected by immunohistochemistry [8].

As demonstrated by Lv et al. [7], PTPIP51 overexpression induces apoptosis in HEK293 cells.

Recent pull-down experiments by Yu et al. [9] described PTPIP51 to interact with Raf-1 through 14-3-3 thereby modulating cellular motility and morphology via the mitogen activated protein kinase (MAPK) cascade.

Data available so far implicate that PTPIP51 is involved in cellular differentiation, motility, cytoskeleton formation, and in apoptosis. These cellular alterations in the epithelium and stroma are implicated in benign prostate hyperplasia (BPH) pathogenesis [10] and the pathogenesis of prostate carcinoma (PCa) essentially results from an aberrant regulation of proliferation and differentiation. Therefore we investigated the PTPIP51-expression profile in BPH and PCa. Since PCa is the most common non-cutaneous malignancy in men and second leading cause of cancer-related deaths [11–13] and BPH is the most common condition associated with ageing in men and often presents with lower urinary tract symptoms such as voiding dysfunction or irritability of the bladder [14], it is certainly of interest to investigate the potential role of PTPIP51 in the pathogenesis of these disorders.

So far the etiology of PCa is not well understood. It is discussed to arise with an intermediate state of proliferative inflammatory atrophy (PIA) [15–17] and prostatic intraepithelial neoplasia (PIN) [18].

The capability of PCa to spread beyond its capsule along nerve fibers is of great importance since the perineural invasion (PNI) is the most common reason of tumor progression [19].

The adhesion of nerve fibers to tumor cells lowers the amount of apoptosis in cancer cells [20,21]. Up to now the process of tumor spreading through the neural capsule and adhering to the nerve fibers is not precisely known.

Epigenetic changes are involved in the regulation of expression of many oncogenes and tumor suppressor genes which contribute to the development and progression of many somatic tumors including prostate cancer. In particular, the role of DNA methylation in oncogenesis is well established for many tumor entities. DNA methylation refers to the addition of methyl (CH_3)-group at the C-5 position of the cytosine ring in the DNA, which is catalyzed by DNA methyltransferases (DNMTs). Methylcytosine residues are often found in short stretches of CpG-rich regions (e.g., CpG islands) that are mostly unmethylated and found in the 5′ region of approximately 60% of genes [22].

Methylation of CpG islands within the promoter region strongly correlates with the transcriptional activity of particular genes. Both hypo- and hypermethylation can lead to chromosomal instability, gene silencing, or gene overexpression. Those epigenetic aberrations have been implicated in a variety of human malignancies, including prostate cancer [23]. We therefore investigated CpG methylation in the promoter region of PTPIP51 as a possible mechanism underlying PTPIP51-dependent cell proliferation during carcinogenesis.

BPH, predominantly involving the stromal compartment of the prostate, is one of the most common condition associated with the ageing male [24,14]. In the United States of America over 80% of men aged 50 years and older are affected, resulting in lower urinary tract symptoms such as bladder outlet obstruction [25]. So far, there is no solid understanding of the pathogenesis of this disorder. Recent studies have discussed the influence of transforming growth factor-β (TGF-β), fibroblast growth factor (FGF), and insulin-like growth factor (ILGF) family members, estrogen/androgen balance, inflammatory processes, and the theory of ageing [26–29].

Our study aimed to elucidate the possible involvement of PTPIP51 in the pathogenesis of BPH and PCa as both are present with a high incidence in men.

MATERIALS AND METHODS

Tissue and Section Preparations

The tissue microarray was constructed using 26 formalin-fixed samples (Ø 4 mm), all taken from radical prostatectomy, 13 resembling PCa and 13 BPH. All samples were obtained from the Department of Pathology, Justus-Liebig-University Giessen. This study was approved by the ethics commission of the Medical Faculty, Justus-Liebig-University Giessen.

The PCa samples were reviewed according to the TNM-classification and Gleason score. BPH was identified by its localization and by means of histopathological analysis.

For immunohistochemistry, paraffin-sections of 4 μm thickness were cut, dried, deparaffinized in xylene, and rehydrated in graded alcohol. Prior to the staining procedure, antigen retrieval using microwave-oven heating (2×5 min, 800 W) in 10 mM standard sodium citrate buffer (pH 6.0) was carried out for all antibodies used in this study.

For sodium bisulfite sequencing, real-time quantitative polymerase chain reaction (PCR) and reverse transcription-PCR (RT-PCR), respectively, DNA and RNA was obtained from cryo-preserved tissue samples of 5 BPH and 5 PCa from patients who underwent prostatectomy at the Department of Urology and Pediatric Urology, University of Giessen.

Immunohistochemistry

Prior to immunostaining non-specific binding sites were blocked with phosphate-buffered saline (PBS) containing 5% bovine serum albumin and 5% normal goat serum. Indirect immunofluorescence was performed by overnight incubation with primary antibodies (see Table I), diluted in PBS at room temperature, followed by washing in PBS and subsequent incubation for 1 hr at room temperature with the appropriate secondary antibodies (see Table I). Then the slides were washed in PBS, coverslipped in carbonate buffered glycerol at pH 8.6.

The polyclonal antibody against PTPIP51, raised as described and characterized in previous studies [3,8], was used in a 1:400 dilution for fluorescence immunohistochemistry.

Primary antibodies were visualized by Alexa fluor 488 and Alexa fluor 555 secondary antibodies. For each series of antibody staining sections were incubated with medium lacking PTPIP51 antibody, serving as an internal negative control. Nuclei were displayed by Dapi.

The Axioplan 2 fluorescence microscope equipped with Plan-Apochromat objectives (Carl Zeiss, Jena, Germany) was used for photographic documentation. For visualization of the secondary antibody Alexa fluor 555 an excitation filter with a range of 530–560 nm and an emission filter with a range 572.5–647 nm were used. Alexa Fluor 488 was visualized by an excitation filter with a range of 460–500 nm and an emission filter with a range of 512–542 nm.

Hematoxyline and Eosin (H&E) and Masson–Goldner Staining

The histomorphological characteristics were evaluated by H&E staining. Collagens of the extracellular tumor matrix were demonstrated by Masson–Goldner staining.

After evaluation of the immunostained samples, the coverslips of each slide was removed and the sections were stained with H&E and evaluated by light microscopy.

In Situ Hybridization

In situ hybridization was performed as described previously [30] using a stringency to achieve hybridization only with a homology greater than 80%. Briefly, 5 μm sections were partially digested with proteinase

TABLE I. Antibodies Applied for This Study

Immunogen	Antibody source	Clone	Dilution	Manufacturer
PTPIP51: Human cDNA sequence encoding amino acids 131–470 of PTPIP51	Rabbit polyclonal		1/400	Prof. HW Hofer, Biochemical Department, University of Konstanz, Germany
PGP9.5: Native, from brain	Mouse monoclonal	31A3	1/100	Biotrend, Germany, Cat #BT78-6310-04
α-Smooth muscle-FITC: N-terminal synthetic decapeptide of α-smooth muscle actin	Mouse monoclonal	1A4	1/500	Sigma, Germany, Cat #F 3777
CK-Pan: Purified human callus cytokeratins	Mouse monoclonal	80	1/40	Acris, Germany, Cat #BM2300
PCNA: Recombinant rat PCNA	Mouse monoclonal	PC10	1/100	BioLegend, USA, Cat #307902
Anti PTP1B: Human recombinant protein tyrosine phosphatise 1B (PTP1B)	Mouse monoclonal	AE4-2J	1/40	Calbiochem, Germany, Cat #PHO2
c-Src: Against full-length recombinant c-Src of human origin	Mouse monoclonal	17AT28	1/100	Santa Cruz, USA, Cat #sc-130124
Raf-1: C-terminus	Mouse monoclonal	E-10	1/100	Santa Cruz, USA, Cat #sc-7267
14-3-3β: C-terminus of 14-3-3β of human origin	Mouse monoclonal	A-6	1/100	Santa Cruz, USA, Cat #sc-25276
Alexa fluor 555	Goat		1/800	Invitrogen, USA, Cat #A21428
Alexa fluor 488	Goat		1/800	Invitrogen, USA, Cat #A11029

K, post-fixed in 4% paraformaldehyde, and exposed to 20% acetic acid. After prehybridization in 20% glycerol, sections were covered with the DIG-labeled sense or antisense cRNA-probes. Production of DIG-labeled cRNA-probes was performed as described previously [30]. PCR conditions were 1 × 94°C for 3 min, 35 × 94°C for 30 sec, 66°C for 30 sec, 72°C for 60 sec, and 1 × 72°C for 8 min using 5′-GTCTCTC-ACCTGAGCTGGCTAGA-3′ as forward primer and 5′-GGATAGCCAAATCCTCCTTCGTGA-3′ as reverse primer. The 247 nucleotide ER-product (nt positions 1126–1372, corresponding to aa 376–457) of the human PTPIP51 gene was subcloned in pGEM-T (Promega, Heidelberg, Germany). Plasmids were transformed in the XL1-Blue *E. coli* strain (Stratagene, Heidelberg, Germany) and extracted by column purification (Qiagen, Hilden, Germany). In vitro transcription of DIG-labeled PTPIP51-cRNA was performed using the 10× RNA-DIG Labeling-Mix (Roche, Mannheim, Germany) and RNA-polymerases T3 and SP6. Vectors containing the PTPIP51 inserts were digested with *Nco*I and *Not*I (New England Biolabs, Frankfurt, Germany) for the production of sense-cRNA and antisense-cRNA, respectively. Both cRNAs were used in a dilution of 1:100 (the optimal concentration was determined by a dot blot test) in hybridization-buffer containing 50% deionized formamide, 10% dextran sulphate, 2× saline sodium citrate (SSC), 1× Denhardt́s solution, 10 μg/ml salmon sperm DNA, and 10 μg/ml yeast t-RNA. Hybridization was performed overnight at 37°C in a humidiWed chamber containing 50% formamide in 2× SSC. Post-hybridization washes were performed according to Lewis and Wells [31]. After blocking with 3% bovine serum albumin, the sections were incubated (overnight at 4°C) with the anti-DIG Fab-antibody conjugated to alkaline phosphate (Roche). Staining was visualized by developing the sections with nitrobluetetrazolium/5-bromo-4-chloro-3-indolylphosphate in a humidified chamber protected from light. Alternatively, the sections were incubated with anti-DIG -fluorescein, Fab fragments (Cat# 11 207 741 910, Roche). For each test negative controls were performed using DIG-labeled cRNA sense-probes.

RNA Extraction

RNA extraction from cryomaterial was performed using the RNA extraction kit RNeasy MINI (Qiagen) according to the manufacturer's instructions.

First Strand Synthesis

First strand synthesis was performed using Omniscript (cryomaterial), according to the manufacturer's protocol (Qiagen).

Reverse Transcription-Polymerase Chain Reaction (RT-PCR)

RT-PCR was performed on an iCycler using SYBR Green Supermix (BioRad, Munich, Germany) to visualize the respective amplicons [32]. Per sample 2 μl cDNA were used. Cycling conditions were 94°C for 2 min, followed by 40 cycles of 94°C (PTPIP51); 58°C (PTP1B); 63°C (c-Src); 63.5°C (Raf-1) for 30 sec, 55°C for 30 sec, and 72°C for 2 min. The following primers were employed: for PTPIP51 as forward primer 5′-AGGGCATCTCGAAACGCATCCA-3′ and as reverse primer 5′-CTTCTAGTTCTTCCAGGTCTTTTTG-3′, for PTP1B as forward primer 5′-GGAGATGGAAAAG-GAGTTC-3′ and as reverse primer 5′-TGCTTTT-CTGCTCCCACAC-3′, for c-Src as forward primer 5′-ATGGTGAACCGCGAGGTGCT-3′ and as reverse primer 5′-GATCCAAGCCGAGAAGC-CGGTCTG-3′, for Raf-1 as forward primer 5′-CAGC-CCTGTCCAG-TAGC-3′ and as reverse primer 5′-GCC-TGACTT-TACTGTTGC-3′.

PCR products were visualized by agarose gel electrophoresis. While amplification of a 90 bp β-actin product served as positive control, negative controls included samples lacking reverse transcriptase.

Real-Time Polymerase Chain Reaction (Real-Time PCR)

The amplification of cDNA from five BPH and five PCa samples was carried out in 25 μl reaction volume on the iCycler iQ Real-Time PCR Detection System (BioRad, Munich, Germany). The final reaction tube contained 100 nM PTPIP51 primers and reference genes β-actin (forward 5′-TTCCTTCCTGGGCATG-GAGT-3′; reverse 5′-TACAGGTCTTTGCGGATGTC-3′), HSPCP (forward 5′-AAGAGAGCAAGGCAAA-GTTTGAG-3′; reverse 5′-TGGTCACAATGCAGCAA-GGT-3′), ATP5b (forward 5′-TCACCCAGGCTGGTT-CAGA-3′; reverse 5′-AGTGGCCAGGGTAGGCTGAT-3′), 12.5 μl iQ SYBR Green Supermix (BioRad) and 2 μl of DNA template. The PCR conditions were 94°C for 3 min followed by 40 cycles for 30 sec, 60°C for 30 sec, and 72°C for 1 min. Melting curves were generated for both genes after amplification. Negative controls were included in each run. The selection of appropriate combination of reference genes for expression analysis of PTPIP51 in PCa and BPH tissue was carried out using NormFinder Program. PCR-products were additional electrophoresed on a 3% agarose gel and visualized by GelRed reagent.

Methylation

From 10 patients (see Table II) who underwent radical prostatectomy, 5 PCa samples, in which at least 70% of

TABLE II. Human Prostate Tissue Samples

Sample	Histological diagnosis	Age	Preoperative PSA value	Gleason score	pTNM staging
1	PCa	72	15 μg/ml	7	pT4 G3 pN1 pR0
2	PCa	70	17 μg/ml	9	pT4 G3 pN0 pR1
3	PCa	67	—	7	pT4 G3 pN0 pR1
4	PCa	67	—	7	pT3a G3 pN0 pR0
5	PCa	64	—	6	pT3a G3 pN0 pR1
6	BPH	64	—	7	pT3a G3 pN0 pR1
7	BPH	72	6.15 μg/ml	7	pT4 G3 pN0 pR0
8	BPH	75	18.66 μg/ml	6	pT2c G2 pN0 pR0
9	BPH	67	—	5	pT3a G3 pN0 pR0
10	BPH	64	—	6	pT3a G3 pN0 pR0

the cells represented cancer epithelial cells, and 5 BPH samples were selected for this study. Additionally, the expression of the tumor epithelial cell marker α-methylacyl-CoA racemase (AMACR) was determined to differentiate between PCa and BPH. For DNA methylation analysis, genomic DNA was isolated from frozen tissue sections using Qiamp DNA Mini Kit (Qiagen).

Genomic DNA (2 μg) was treated with sodium bisulfite using EpiTect Bisulfite Kit (Qiagen) according to manufacturer's instructions. Sodium bisulfite converts unmethylated cytosines to uracils, whereas methylated cytosines remains unaffected. Bisulfite-treated DNA was subsequently amplified using primers specific for bisulfite converted DNA: forward 5′-GAAATGGAGG-TTTGGTTGT-3′, reverse 5′-CCT-AACAAAAAATCC-ACTCAAA-3′. These primers allow the amplification of both the methylated and the unmethylated alleles by spanning a region of 341 bp with 18 differentially methylated CpG nucleotides.

DNA was amplified in a 30 μl volume containing 10 μl of the extracted and bisulfite-treated DNA, PCR buffer gold, 1.5 mM $MgCl_2$, 0.2 mM of each dNTP, 0.66 μM of each primer, and 0.5 μl (2.5 U) of Amplitaq Gold polymerase (Qiagen). After activation of the polymerase at 95°C for 10 min, DNA was amplified in 40 cycles for 45 sec at 95, 56, and 72°C followed by a final extension at 72°C for 10 min. Five milliliters of each PCR product was analyzed on agarose gel and the remaining 25 μl were purified using QIAquick Purification Kit (Qiagen). The probes were then subjected to sequencing using forward primer by Scientific Research and Development GmbH, Oberursel, Germany. The sequencing results were analyzed using BiQ Analyzer, a software tool for DNA methylation available by free download from http://biq-analyzer.bioinf.mpi-inf.mpg.de/.

RESULTS

This study demonstrates for the first time the cell-specific expression of PTPIP51 mRNA and protein in BPH and PCa. Furthermore, this is also the first report providing methylation analysis of BPH and PCa CpG islands in the promoter region of the PTPIP51 gene as a potential mechanism underlying aberrant expression of PTPIP51 mRNA and protein level in prostate cancer. Expression of the PTPIP51 in vitro interaction partners PTP1B, c-Src, and Raf-1 was demonstrated by RT-PCR. Immunohistochemical experiments revealed a co-expression with these in vitro interaction partners in BPH and PCa.

Expression Profile of PTPIP51 in BPH and PCa Samples

Quantitative real-time PCR analysis. PTPIP51 expression levels of five BPH and five PCa samples were assessed by real-time quantitative PCR. Candidate reference genes for normalization and the best combination of two genes was calculated according to their expression stability by the NormFinder program. The best combination of two genes was β-actin and HSPCP, which improved the stability value of 0.026, indicating a more reliable normalization.

Results of expression analysis showed slightly elevated levels of PTPIP51 in the group of PCa when compared with the group of BPH (Fig. 1A). Analyzing each sample of BPH we could observe lower levels of PTPIP51 expression in three out of five patients while in the PCa group all samples represented equally increased expression (Fig. 1B).

In situ hybridization. PTPIP51 mRNA was detected in prostatic epithelia of BPH (Fig. 2A) and in tumor cells of PCa (Fig. 2C). Endothelial cells and smooth muscle

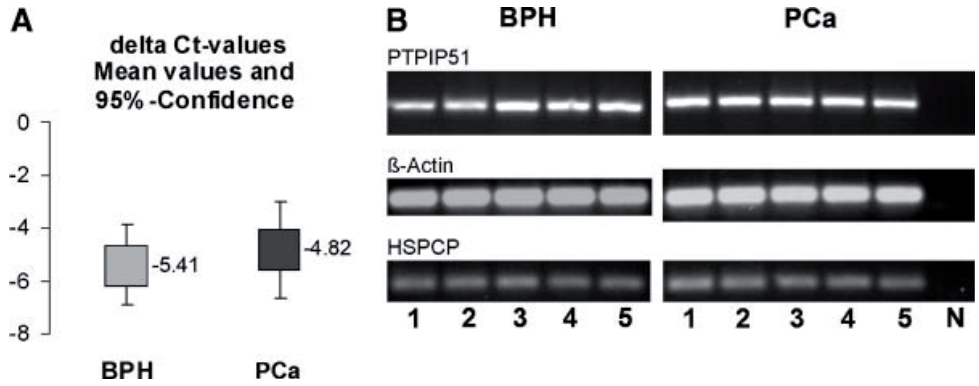

Fig. 1. Real-time PCR analysis of PTPIP5I in BPH and PCa. **A**: Effect of normalization approaches on the expression levels of PTPIP5I gene in malignant (PCa) and non-malignant (BPH) prostate tissue samples. Normalizations were made using reference genes as indicated by Norm-Finder with β-actin and HSPCP as the best combination of two reference genes. **B**: Gels showing expression levels of PTPIP5I in each sample of benign prostate hyperplasia (BPH; 1–5) and prostate carcinoma (PCa; 1–5) as assessed by real-time PCR analyzes. Amplification of β-actin and HSPCP was used as combination of reference genes. Negative control (N).

cells of vessels in BPH and PCa and immune cells infiltrating the BPH stroma strongly expressed PTPIP51 mRNA.

Immunhistochemical detection of PTPIP51 in BPH and PCa. Immunohistochemical staining revealed PTPIP51 expression in both epithelial cells of prostatic glands and in prostatic stromal cells of BPH and PCa. A stronger expression of PTPIP51 protein was present in ganglia and nerve fibers, in immune cells and in smooth muscle and endothelial cells of vessels.

Comparing the PTPIP51 protein levels in BPH and PCa, a stronger expression was seen in PCa as the PCa samples exhibit an increased quantity of ganglia and nerve fibers, all positive to PTPIP51 antibody.

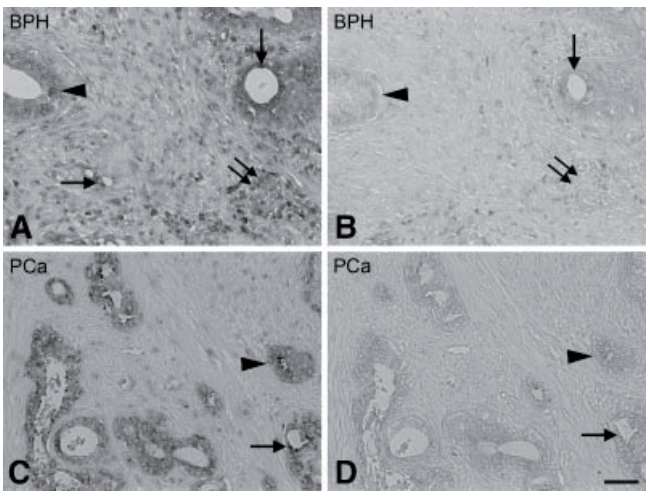

Fig. 2. PTPIP5I in situ hybridization of BPH and PCa. **A**: Antisense probe of BPH. Arrowhead: prostatic epithelia. **B**: Sense probe of BPH. Arrowhead: prostatic epithelia. **C**: Antisense probe of PCa. Arrowhead: tumor cells. **D**: Sense probe of PCa. Arrowhead: tumor cells. Bar: 50 μm. Arrow, endothelial cells; double-arrow, immune cells.

- *Epithelia*: BPH prostatic epithelia (Fig. 3) and PCa tumor cells (Fig. 4), respectively, identified by co-staining with a pan cytokeratin antibody, displayed a faint staining intensity for PTPIP51 protein within the cytoplasm. Occasionally, the plasma membrane reacted strongly with the

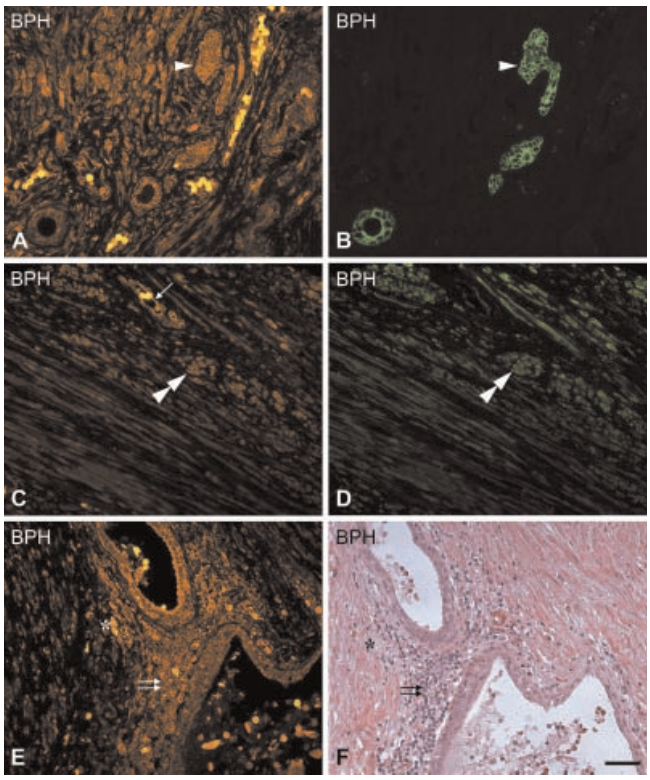

Fig. 3. Immunostaining of PTPIP5I in BPH. **A**: PTPIP5I. **B**: CK-Pan. **C**: PTPIP5I. **D**: α-smooth muscle actin. **E**: PTPIP5I. **F**: H&E. Bar: 50 μm Arrowhead, prostatic epithelia; arrow, endothelial cells; double-arrow, immune cells; double-arrowhead, smooth muscle cells; asteric, nerve.

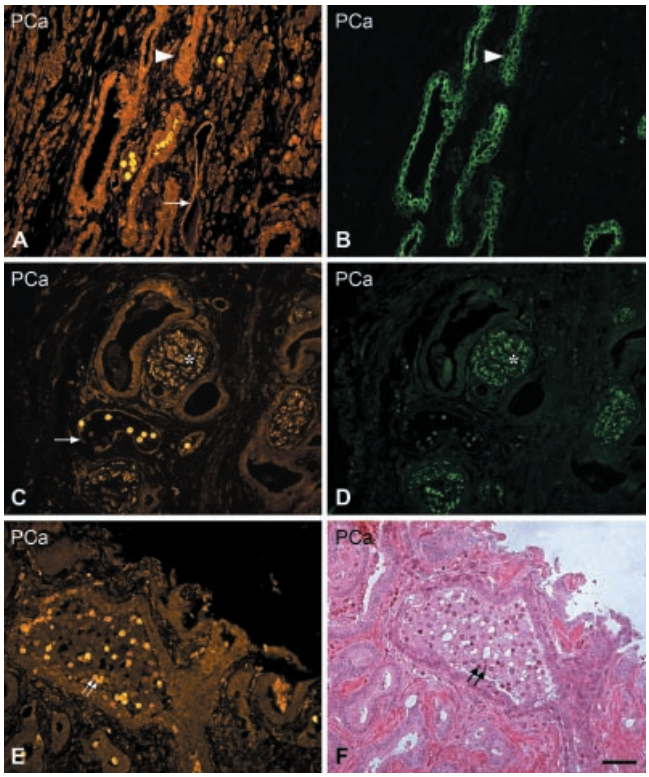

Fig. 4. Immunostaining of PTPIP51 in PCa. **A**: PTPIP51. **B**: CK-Pan. **C**: PTPIP51. **D**: PGP9.5. **E**: PTPIP51. **F**: H&E. Bar: 50 μm Arrowhead, tumor cells; arrow, endothelial cells; double-arrow, immune cells; asteric, nerve.

antibody to PTPIP51 antigen. These cells were found to be quiescent, as no co-expression with proliferating cell nuclear antigen (PCNA), a proliferation marker, was detected (data not shown).

- *Stroma*: Smooth muscle cells, identified by co-expression with α-smooth muscle actin, and fibroblasts comprising the prostatic stroma of BPH (Fig. 3) and PCa (Fig. 4) both reacted positive with the PTPIP51 antibody.
- *Neuronal tissue*: PTPIP51 protein was detected in a higher concentration in the supplying nerve fibers and in the ganglia of the autonomous nerve system as identified by co-expression of PGP9.5, a neuronal marker (Fig. 4).
- *Immune cells*: A strong immune reaction with the antibody to PTPIP51 was detected in the cytoplasm of immune cells (e.g. lymphocytes, granulocytes, and plasma cells), present in BPH (Fig. 3) and PCa (Fig. 4).
- *Vessels*: Endothelial cells lining venous and arterial microvessels and capillaries, were also PTPIP51 positive. Lumina of the vessels, packed with granulocytes and lymphocytes displaying a strong PTPIP51 labeling, were detected quite frequently (Figs. 3 and 4).

Analysis of PTPIP51 promotor methylation in BPH and PCa samples. In the BPH group one out of five samples was completely methylated. Two out of five samples displayed methylation of 14 CpGs. In those patients, loss of methylation was observed in four CpGs. Interestingly, differential methylation was observed in CpGs at positions 1–9. CpGs 10–18 were hypermethylated in all five samples. Analysis of the PCa group revealed that similarly to BPH samples, CpG positions from 10 to 18 were methylated in all five out five PCa samples, however, in the PCa group a significant decrease of methylation could be observed in CpGs at positions 1–9 when compared to the BPH group. Nine out of 18 CpGs were indicated as unmethylated in a single PCa sample. Two PCa samples had more than 7 unmethylated CpGs and a single sample displayed methylation of 15 CpGs. Furthermore, aggregated representation of methylation data from the PCa and BPH groups showed that three CpGs (2, 8, and 9) were entirely unmethylated in PCa while the BPH group had no CpG that was unmethylated in each sample. In contrast to the PCa group, the BPH group displayed 13 completely methylated CpG positions (Fig. 5).

Expression Profile of the In Vitro Interaction Partners of PTPIP51

RT-PCR analysis. The mRNA expression of PTPIP51and its in vitro interaction partners was tested by RT-PCR. As demonstrated in Figure 6 both BPH and PCa express considerable amounts of PTP1B, c-Src, and Raf-1. β-actin amplification served as an internal positive control. Probes lacking reverse transcriptase served as negative controls.

Cellular distribution. Double labeling studies with antibodies to PTPIP51 antigen and the following in vitro interaction partners Src kinase and Raf-1, which take part in the MAP kinase pathway, 14-3-3β and PTP1B revealed different co-expressions patterns.

- *PTP1B* (Fig. 7A–D): PTP1B was partially co-expressed with PTPIP51 in prostatic epithelial cells (BPH) and in tumor cells (PCa). In BPH and in PCa a subset of immune cells co-expressed both antigens. In endothelial cells co-expression of both antigens was restricted to PCa samples.
- *C-Src* (Fig. 7E–H): c-Src was partially co-expressed with PTPIP51 in prostatic epithelial cells (BPH) and in tumor cells (PCa). In endothe-

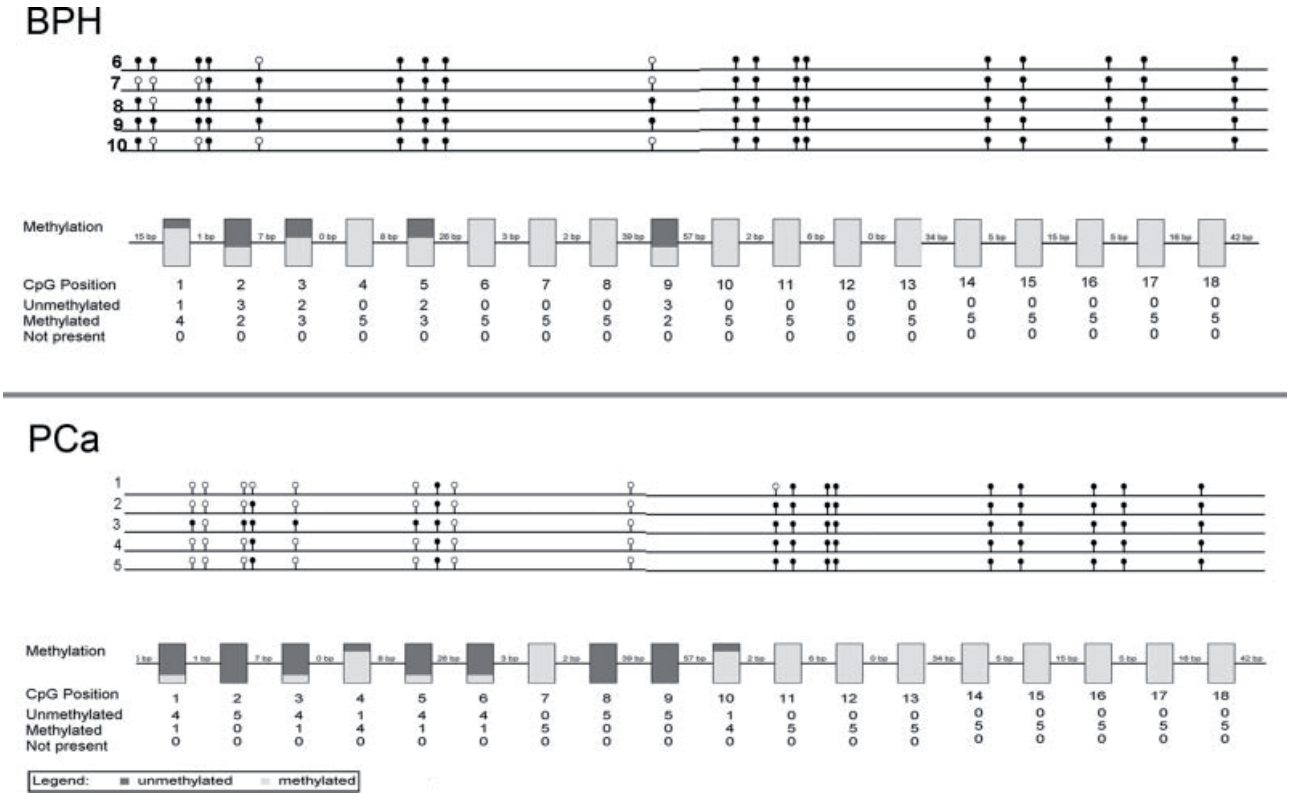

Fig. 5. Methylation profile of PTPIP51 gene promoter in BPH and PCa using sodium bisulfite sequencing. Methylation pattern of five BPH and five PCa samples. Black circles correspond to methylated CpGs, open circles correspond to unmethylated CpGs. Bar diagram demonstrates aggregated representation of methylation data of every CpG nucleotide within the DNA fragment of the BPH and PCa group. Figures were generated using BiQ Analyzer Methylation tool download from http://biq-analyzer.bioinf.mpi-inf.mpg.de/.

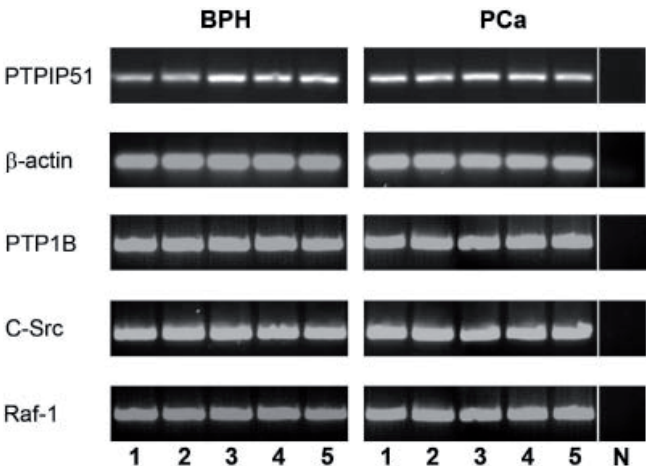

Fig. 6. Expression of PTPIP51 and its in vitro interaction partners as detected by RT-PCR. RT-PCR was performed using primers specific to PTPIP51, PTPIB, c-Src, and Raf-1 as given in Materials and Methods Section. β-Actin was amplified as an internal positive control and probes lacking reverse transcriptase served as negative controls (N). Samples of benign prostate hyperplasia (BPH; 1–5), samples of prostate carcinoma (PCa; 1–5).

lial cells a faint co-expression of both antigens could be found in PCa samples.

- *Raf-1* (Fig. 7I–L): Raf-1 was co-expressed with PTPIP51 in the basal part of prostatic epithelial cells (BPH) and in the apical part of tumor cells (PCa). In BPH and in PCa stromal smooth muscle cells, endothelial cells and a subset of immune cells co-expressed both antigens.
- *14-3-3β* (Fig. 7M–P): 14-3-3β was co-expressed with PTPIP51 in the apical part of the prostatic epithelia (BPH). Tumor cells of PCa displayed a faint staining for both antigens. A stronger expression of both antigens could be found in a subset of immune cells in BPH and PCa.

DISCUSSION

To our knowledge, this study demonstrates for the first time the mRNA expression and cellular localization of PTPIP51 protein in BPH and PCa. Promoter methylation status of PTPIP51 is aberrant in prostate cancer when compared to BPH, this might explain the elevated expression of PTPIP51 in PCa.

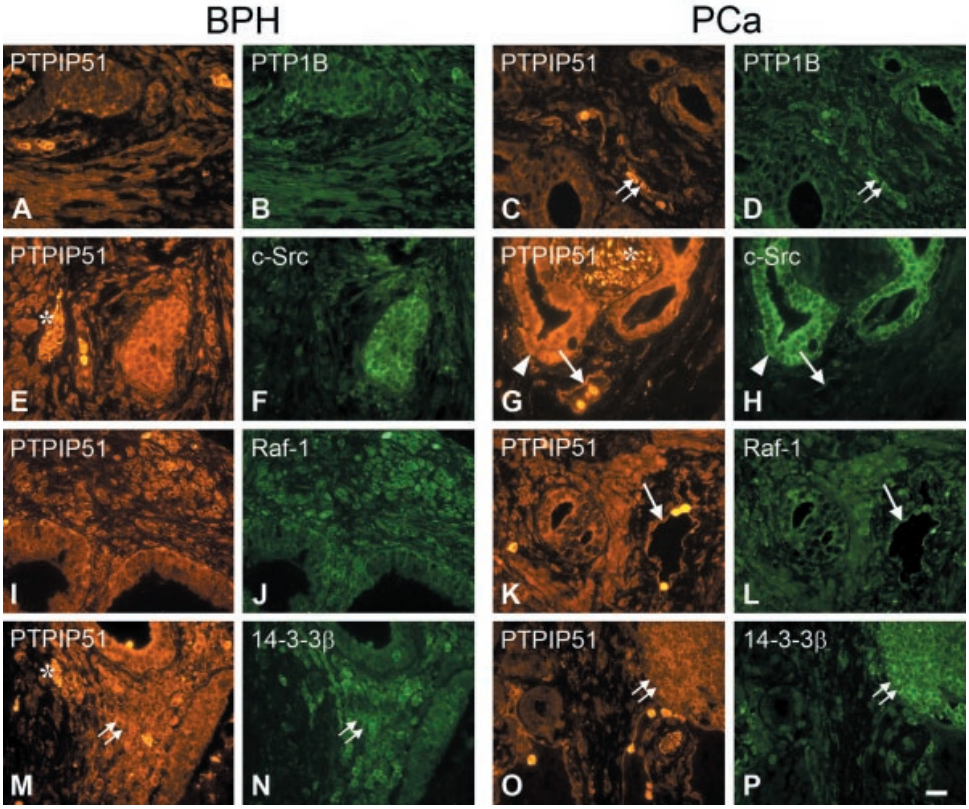

Fig. 7. Co-immunostaining of PTPIP51 and its in vitro interaction partners. Samples of benign prostate hyperplasia (BPH) **A**, **B**, **E**, **F**, **I**, **J**, **M**, and **N**. Samples of prostate carcinoma (PCa) **C**, **D**, **G**, **H**, **K**, **L**, **O**, and **P**, arrowhead: tumor cells. Bar: 20 μm. Arrow, endothelial cells; double-arrow, immune cells; asteric, nerve.

We demonstrated the expression of PTPIP51 in prostate cancer and in BPH within different tissues comprising tumor and peritumoral environment and epithelial and stromal cells of the prostate, respectively. Nerve fibers, immune cells, and vessels displayed a strong immune reaction. Notably, epithelial cells displayed a membranous staining pattern with the PTPIP51 antibody, indicating a putative involvement in the regulation of cell–cell interactions. The latter are known to play a key role in normal and abnormal growth of BPH and PCa [33–35]. A similar subcellular localization of PTPIP51 in keratinocyte carcinomas epithelial cells of non-melanoma skin cancer has been observed recently [6].

In the healthy prostate, interactions of nerves, stromal and epithelial cells play an important role during its development and are relevant for the physiological function of the adult prostate [36,37]. Denervation experiments of the rat prostate resulted in morphological and functional changes of the prostatic glandules, indicating that besides hormonal regulation, the nerval innervation might play a crucial role for the development and functional integrity of the prostate [38,39]. The autonomous innervation of the prostate is organized in the way that prostatic epithelia receives a cholinergic type of innervation while stroma receives a predominantly noradrenergic innervation [40–42].

As PTPIP51 is expressed in both PCa and BPH ganglia and nerve fibers, PTPIP51 might play a role for the functional integrity of the prostatic autonomous nervous system, accordingly essential for the prostatic development and function.

In prostate cancer nerve fibers play an important role, amongst others being responsible for tumor spreading and supporting tumor growth. PNI, driven by the interaction of nerves and tumor cells is a process generally described for prostate cancer, but was also observed in bile duct, pancreatic, head, and neck cancers [19]. PNI is present in more than 85% of PCa [42] and appears to be important for the invasiveness of the tumor. Tumor spreading along nerve fibers is the most common way of tumor spreading.

Our results displayed that all ganglia and nerve fibers of the prostate show a strong expression of PTPIP51 protein in PCa as well as in BPH. Compared with BPH, a stronger expression of PTPIP51 protein in prostate cancer was observed. Corresponding results were observed for the mRNA levels of PTPIP51,

displaying an overexpression in the PCa group. This finding could be explained by the observations made by Ayala et al. [19] who reported cancer-related axonogenesis and neurogenesis leading to an increased nerve density in PCa.

Elevated expression levels of PTPIP51 in PCa and BPH might be explained by data of the methylation analysis of CpGs within the promoter region of the PTPIP51 gene. In general, methylation is associated with gene silencing [43], lack of methylation in contrast is responsible for decondensation of chromatin genomic instability and may cause activation of retrotransposon elements resulting in aberrant overexpression of certain genes [44,45].

Therefore, methylation of five BPH and five PCa samples, parallel with the mRNA and protein expression of PTPIP51 were analyzed in this study. Eighteen CpGs were characterized from each sample using sodium bisulfite sequencing. In BPH samples almost the entire investigated region consisted of methylated CpGs. At least 78% (14 of 18) CpGs were methylated. In PCa, a loss of methylation in the CpG positions 1–3, 5–6, 8–9 was observed. This is the first study presenting differences in the PTPIP51 gene methylation of PCa.

Overexpression of PTPIP51 as a result of CpG island hypomethylation might be a potential factor contributing to PNI of prostate cancer, as DNA hypomethlytion was reported to occur late in prostate carcinogenesis [46].

The reduction of 5′-methylcytosine content in the genome occurs late in prostate cancer progression, appearing only in the stage of metastatic disease. Even though this study includes only five PCa samples with Gleason score between 7 and 9 and five BPH samples, we were able to demonstrate differences in CpG methylation of the PTPIP51 gene promoter. Understanding DNA methylation/demethylation of the PTPIP51 gene in more detail may shed new light on the involvement of PTPIP51 in the carcinogenesis and may help to understand PNI of prostate cancer cells.

Chronic inflammation of the prostate is presumed to be involved in prostate growth either in hyperplastic (BPH) or neoplastic (PCa) changes [47].

Epidemiologic data suggest a high percentage of BPH samples displaying signs of chronic inflammation [48,49]. Inflammation is thought to incite carcinogenesis by causing cell and genome damage, promoting cellular turnover, and creating a tissue microenvironment that can enhance cell replication, angiogenesis, and tissue repair [50].

Recent publications also support the hypothesis that inflammation is a possible factor inducing transition from BPH to PCa [51].

As cells of the innate and adaptive immune system in blood vessels, in lumina of glandules, and also infiltrating the stroma of BPH and PCa reacted strongly positive to PTPIP51 antibody an involvement of PTPIP51 in inflammatory processes seems very likely.

For tumor growth and spreading, the formation of new blood capillaries is essential. Vascular endothelial growth factor (VEGF) is a potent angiogenic peptide effecting in the regulation of hematopoietic stem cell development, extracellular matrix remodeling, and inflammatory cytokine regeneration [52,53]. VEGF has been shown to be expressed in glandular and surrounding stromal cells, regulated by androgens. They are crucial for normal prostate growth and development, as well as for the development of BPH and PCa. Androgen deprivation resulted in a decreased expression of VEGF by prostate cancer [54]. Expression analyses of peptide growth factors made by Soulitzis et al. [55] showed VEGF to be overexpressed in prostate cancer, while there was a downregulation in BPH. Since PTPIP51 is strongly expressed in endothelial cells of the tumor environment, we suggest PTPIP51 to play a role in the process of angiogenesis. This is further supported by the fact that Src-kinase can increase the expression of VEGF through the JaK1–STAT3–VEGF pathway. Apart from that an interaction of Src with steroid receptors was reported. It was shown that low amounts of androgen receptors can lead to an increased Src activation in the cytoplasm [56]. Since Src is partially co-localized with PTPIP51 and PTPIP51 is tyrosine-phosphorylated by c-Src and v-Src in vitro [2] a possible role of PTPIP51 in angiogenesis is likely.

In prostate cancer and in other malignancies increased activity or expression of Src-kinase and other Src family kinases (SFKs) has been reported. SFK-activated pathways are known to be involved in cell growth, tumor adhesion, motility, invasion, and angiogenesis [57]. Therefore, the SFK/Abl inhibitor, dasatinib, is currently being investigated as a new treatment option in prostate cancer and in various other malignancies [58].

CONCLUSIONS

In summary, PTPIP51 is expressed in both, BPH and PCa. Interestingly, PCa samples displayed a higher concentration of PTPIP51 mRNA and protein, compared to BPH samples. These results might be explained by the hypomethylation of the PTPIP51 promoter.

ACKNOWLEDGMENTS

We are grateful to Mrs. K. Michael (Institute of Anatomy and Cell Biology, Giessen) for help with the design of the figures and to Mr. F. Doenges (Department of Pathology, Giessen), Mrs. A. Erkel (Department of Urology and Pediatric Urology,

Giessen), Mrs. B. Fröhlich (Department of Urology and Pediatric Urology, Giessen), and Mrs. C. Tag (Institute of Anatomy and Cell Biology, Giessen) for their excellent technical assistance.

REFERENCES

1. Porsche A. Identifikation von Interaktionspartnern der T-Zell Protein-Tyrosin-Phosphatase durch das Lex-A Two Hybrid System; thesis (Ph.D.), University of Konstanz. Allensbach, UFO Publishers 2001; 414.
2. Stenzinger A, Schreiner D, Koch P, Hofer HW, Wimmer M. Cell- and molecular biology of the novel protein tyrosine phosphatase interacting protein 51 (PTPIP51). Int Rev Cell Mol Biol 2009;275: 183–246.
3. Stenzinger A, Kajosch T, Tag C, Porsche A, Welte I, Hofer HW, Steger K, Wimmer M. The novel protein PTPIP51 exhibits tissue- and cell-specific expression. Histochem Cell Biol 2005;123:19–28.
4. Maerker D, Stenzinger A, Schreiner D, Tag C, Wimmer M. Expression of PTPIP51 during mouse eye development. Histochem Cell Biol 2008;129:345–356.
5. Stenzinger A, Märker D, Koch P, Hoffmann J, Baal N, Steger K, Wimmer M. Protein tyrosine phosphatase interacting protein 51 (PTPIP51) mRNA expression and localization and its in vitro interacting partner protein tyrosine phosphatase 1B (PTP1B) in human placenta of the first, second, and third trimester. J Histochem Cytochem 2009;57:143–153.
6. Koch P, Stenzinger A, Viard M, Märker D, Mayser P, Nilles M, Schreiner D, Steger K, Wimmer M. The novel protein PTPIP51 is expressed in human keratinocyte carcinomas and their surrounding stroma. J Cell Mol Med 2008;12:2083–2095.
7. Lv BF, Yu CF, Chen YY, Lu Y, Guo JH, Song QS, Ma DL, Shi TP, Wang L. Protein tyrosine phosphatase interacting protein 51 (PTPIP51) is a novel mitochondria protein with an N-terminal mitochondrial targeting sequence and induces apoptosis. Apoptosis 2006;11:1489–1501.
8. Stenzinger A, Schreiner D, Pfeiffer T, Tag C, Hofer HW, Wimmer M. Epidermal growth factor-, transforming growth factor-beta-, retinoic acid- and 1,25-dihydroxyvitamin D3-regulated expression of the novel protein PTPIP51 in keratinocytes. Cells Tissues Organs 2006;184:76–87.
9. Yu C, Han W, Shi T, Lv B, He Q, Zhang Y, Li T, Zhang Y, Song Q, Wang L, Ma D. PTPIP51, a novel 14-3-3 binding protein, regulates cell morphology and motility via Raf-ERK pathway. Cell Signal 2008;20:2208–2220.
10. Lee KL, Peehl DM. Molecular and cellular pathogenesis of benign prostatic hyperplasia. J Urol 2004;172:1784–1791.
11. Wu C, Zhang L, Bourne PA, Reeder JE, di Sant'Agnese PA, Yao JL, Na Y, Huang J. Protein tyrosine phosphatase PTP1B is involved in neuroendocrine differentiation of prostate cancer. Prostate 2006;66:1125–1135.
12. Quinn M, Babb P. Patterns and trends in prostate cancer incidence, survival, prevalence and mortality. Part I: International comparisons. BJU Int 2002;90:162–173.
13. Quinn M, Babb P. Patterns and trends in prostate cancer incidence, survival, prevalence and mortality. Part II: Individual countries. BJU Int 2002;90:174–184.
14. Verhamme KM, Dieleman JP, Bleumink GS, van der Lei J, Sturkenboom MC, Artibani W, Begaud B, Berges R, Borkowski A, Chappel CR, Costello A, Dobronski P, Farmer RD, Jiménez Cruz F, Jonas U, MacRae K, Pientka L, Rutten FF, van Schayck CP, Speakman MJ, Sturkenboom MC, Tiellac P, Tubaro A, Vallencien G, Vela Navarrete R. Triumph Pan European Expert Panel. Incidence and prevalence of lower urinary tract symptoms suggestive of benign prostatic hyperplasia in primary care—The Triumph project. Eur Urol 2002;42:323–328.
15. De Marzo AM, Platz EA, Sutcliffe S, Xu J, Grönberg H, Drake CG, Nakai Y, Isaacs WB, Nelson WG. Inflammation in prostate carcinogenesis. Nature 2007;7:256–264.
16. Wagenlehner FME, Elkahwaji JE, Algaba F, Bjerklund-Johansen T, Naber KG, Hartung R, Weidner W. The role of inflammation and infection in the pathogenesis of prostate carcinoma. BJU Int 2007;100:733–737.
17. Fujita K, Ewing CM, Sokoll LJ, Elliott DJ, Cunningham M, De Marzo AM, Isaacs WB, Pavlovich CP. Cytokine profiling of prostatic fluid from cancerous prostate glands identifies cytokines associated with extent of tumor and inflammation. Prostate 2008;68:872–882.
18. Helpap B, Bonkhoff H, Cocket A, Montironi R, Troncoso P, Waters D, Bostwick D. Relationship between atypical adenomatous hyperplasia (AAH), prostatic intraepithelial neoplasia (PIN) and prostatic adenocarcinoma. Pathologica 1997;89:288–300.
19. Ayala GE, Dai H, Powell M, Li R, Ding Y, Wheeler TM, Shine D, Kadmon D, Thompson T, Miles BJ, Ittmann MM, Rowley D. Cancer-related axonogenesis and neurogenesis in prostate cancer. Clin Cancer Res 2008;14:7593–7603.
20. Yang G, Wheeler TM, Kattan MW, Scardino PT, Thompson TC. Perineural invasion of prostate carcinoma cells is associated with reduced apoptotic index. Cancer 1996;78:1267–1271.
21. Ayala GE, Dai H, Ittmann M, Li R, Powell M, Frolov A, Wheeler TM, Thompson TC, Rowley D. Growth and survival mechanisms associated with perineural invasion in prostate cancer. Cancer Res 2004;64:6082–6090.
22. Gardiner-Garden M, Frommer M. CpG islands in vertebrate genomes. J Mol Biol 1987;196:261–282.
23. Pavelić J, Zeljko Z, Bosnar MH. Molecular genetic aspects of prostate transition zone lesions. Urology 2003;62:607–613.
24. Djavan B, Remzi M, Erne B, Marberger M. The pathophysiology of benign prostatic hyperplasia. Drugs Today (Barc) 2002;38: 867–876.
25. Lin VK, Wang SY, Vazquez DV, C Xu C, Zhang S, Tang L. Prostatic stromal cells derived from benign prostatic hyperplasia specimens possess stem cell like property. Prostate 2007;67: 1265–1276.
26. Lucia MS, Lambert JR. Growth factors in benign prostatic hyperplasia: Basic science implications. Curr Urol Rep 2008; 9:272–278.
27. Kramer G, Mitteregger D, Marberger M. Is benign prostatic hyperplasia (BPH) an immune inflammatory disease? Eur Urol 2007;51:1202–1216.
28. Farnsworth WE. Estrogen in the etiopathogenesis of BPH. Prostate 1999;41:263–274.
29. Griffiths K, Eaton CL, Harper ME, Peeling B, Davies P. Steroid hormones and the pathogenesis of benign prostatic hyperplasia. Eur Urol 1991;20:68–77.
30. Steger K, Klonisch T, Gavenis K, Drabent B, Doenecke D, Bergmann M. Expression of mRNA and protein of nucleoproteins during human spermiogenesis. Mol Hum Reprod 1998; 4:939–945.
31. Lewis FA, Wells M. Detection of virus in infected human tissue by in situ hybridization. In: Wilkinson DG, editor. In situ

hybridization: A practical approach. Oxford, England: Oxford University Press; 1992. pp. 121–135.

32. Brehm R, Rüttinger C, Fischer P, Gashaw I, Winterhager E, Kliesch S, Bohle RM, Steger K, Bergmann M. Transition from preinvasive carcinoma in situ to seminoma is accompanied by a reduction of connexin 43 expression in Sertoli cells and germ cells. Neoplasia 2006;8:499–509.
33. Farnsworth WE. Role of estrogen and SHBG in prostate physiology. Prostate 1996;28:17–23.
34. Hudson DL, Guy AT, Fry P, O'Hare MJ, Watt FM, Masters JR. Epithelial cell differentiation pathways in the human prostate. Identification of intermediate phenotypes by keratin expression. Histochem Cytochem 2001;49:271–278.
35. Risbridger G, Wang H, Young P, Kurita T, Wong YZ, Lubahn D, Gustafsson JA, Cunha G. Evidence that epithelial and mesenchymal estrogen receptor-a mediates effects of estrogen on prostatic epithelium. Dev Biol 2001;229:432–442.
36. McVary KT, McKenna KE, Lee C. Prostate innervation. Prostate Suppl 1998;8:2–13.
37. Ventura S, Pennefather J, Mitchelson F. Cholinergic innervation and function in the prostate gland. Pharmacol Ther 2002;94:93–112.
38. Wang JM, McKenna KE, McVary KT, Lee C. Requirement of innervation for maintenance of structural and functional integrity in the rat prostate. Biol Reprod 1991;44:1171–1176.
39. Martínez-Piñeiro L, Dahiya R, Nunes LL, Tanagho EA, Schmidt RA. Pelvic plexus denervation in rats causes morphologic and functional changes of the prostate. J Urol 1993;150:215–218.
40. Abbou CC, Salomon L, Chopin D, Ravery V, Haillot O. The current approach to the management of benign hypertrophy of the prostate. Ann Urol 1996;30:294–310.
41. Andersson KE. The importance of the cholinergic system in neurourology. Eur Urol 1998;34:6–9.
42. Arver S, Sjöstrand NO. Functions of adrenergic and cholinergic nerves in canine effectors of seminal emission. Acta Physiol Scand 1982;115:67–77.
43. Li R, Wheeler T, Dai H, Ayala G. Neural cell adhesion molecule is upregulated in nerves with prostate cancer invasion. Hum Pathol 2003;34:457–461.
44. Jones PA, Laird PW. Cancer epigenetics comes of age. Nat Genet 1999;21:163–167.
45. Tuck-Muller CM, Narayan A, Tsien F, Smeets DF, Sawyer J, Fiala ES, Sohn OS, Ehrlich M. DNA hypomethylation and unusual chromosome instability in cell lines from ICF syndrome patients. Cytogenet Cell Genet 2000;89:121–128.
46. Steinhoff C, Schulz WA. Transcriptional regulation of the human LINE-1 retrotransposon L1.2B. Mol Genet Genomics 2003;270:394–402.
47. Yegnasubramanian S, Haffner MC, Zhang Y, Gurel B, Cornish TC, Wu Z, Irizarry RA, Morgan J, Hicks J, DeWeese TL, Isaacs WB, Bova GS, De Marzo AM, Nelson WG. DNA hypomethylation arises later in prostate cancer progression than CpG island hypermethylation and contributes to metastatic tumor heterogeneity. Cancer Res 2008;68:8954–8967.
48. Sciarra A, Mariotti G, Salciccia S, Gomez AA, Monti S, Toscano V, Di Silverio F. Prostate growth and inflammation. J Steroid Biochem Mol Biol 2008;108:254–260.
49. Krieger JN, Lee SW, Jeon J, Cheah PY, Liong ML, Riley DE. Epidemiology of prostatitis. Int J Antimicrob Agents 2008;31:85–90.
50. Platz EA, De Marzo AM. Epidemiology of inflammation and prostate cancer. J Urol 2004;171:36–40.
51. Vasto S, Carruba G, Candore G, Italiano E, Di Bona D, Caruso C. Inflammation and prostate cancer. Future Oncol 2008;4:637–645.
52. Alcaraz A, Hammerer P, Tubaro A, Schröder FH, Castro R. Is there evidence of a relationship between benign prostatic hyperplasia and prostate cancer? Findings of a literature review. Eur Urol 2009;55:864–875.
53. Moreira VM, Vasaitis TS, Njar VC, Salvador JA. Synthesis and evaluation of novel 17-indazole androstene derivatives designed as CYP17 inhibitors. Steroids 2007;72:939–948.
54. Pradeep CR, Sunila ES, Kuttan G. Expression of vascular endothelial growth factor (VEGF) and VEGF receptors in tumor angiogenesis and malignancies. Integr Cancer Ther 2005;4:315–321.
55. Soulitzis N, Karyotis I, Delakas D, Spandidos DA. Expression analysis of peptide growth factors VEGF, FGF2, TGFB1, EGF and IGF1 in prostate cancer and benign prostatic hyperplasia. Int J Oncol 2006;29:305–314.
56. Chung LW, Baseman A, Assikis V, Zhau HE. Molecular insights into prostate cancer progression: the missing link of tumor microenvironment. J Urol 2005;173:10–20.
57. Chang YM, Bai L, Liu S, Yang JC, Kung HJ, Evans CP. Src family kinase oncogenic potential and pathways in prostate cancer as revealed by AZD0530. Oncogene 2008;27:6365–6375.
58. Nam S, Kim D, Cheng JQ, Zhang S, Lee JH, Buettner R, Mirosevich J, Lee FY, Jove R. Action of the Src family kinase inhibitor, dasatinib (BMS-354825), on human prostate cancer cells. Cancer Res 2005;65:9185–9189.

Histol Histopathol (2011) 26: 1531-1543

http://www.hh.um.es

Histology and Histopathology

Cellular and Molecular Biology

PTPIP51, a positive modulator of the MAPK/Erk pathway, is upregulated in glioblastoma and interacts with 14-3-3ß and PTP1B *in situ*

M.K. Petri[1], P. Koch[1], A. Stenzinger[2], K. Kuchelmeister[3], U. Nestler[4], A. Paradowska[5], K. Steger[5], A. Brobeil[1], M. Viard[1] and M. Wimmer[1]

[1]Institute of Anatomy and Cell Biology, Justus-Liebig-University, Giessen, Germany, [2]Institute of Pathology, University Hospital Heidelberg, Heidelberg, Germany, [3]Institute of Neuropathology, University Hospital Bonn, Bonn, Germany, [4]Department of Neurosurgery, Justus-Liebig-University, Giessen, Germany and [5]Department of Urology and Pediatric Urology, Justus-Liebig-University, Giessen, Germany

Summary. Glioblastoma multiforme (GBM) is the most common and most malignant primary brain tumour. Protein tyrosine phosphatase interacting protein 51 (PTPIP51) is an interaction partner of 14-3-3ß, which correlates with the grade of malignancy in gliomas. In this study PTPIP51 and its interacting partners 14-3-3ß, PTP1B, c-Src, Raf-1 as well as EGFR were investigated in human glioblastoma.

Twenty glioblastoma samples were analyzed on transcriptional and translational level by immunohistochemistry, *in situ* hybridization and RT-PCR. To compare PTPIP51 expression in gliomas of different malignancies, quantitative RT-PCR for grade II astrocytoma and GBM samples was employed. Additionally, we analyzed the correlation between PTPIP51 and 14-3-3ß transcription, and checked for *in situ* interaction between PTPIP51 and 14-3-3ß and PTP1B, respectively.

PTPIP51 and 14-3-3ß mRNA showed a tumour grade dependent upregulation in gliomas. Glioblastoma cells displayed a strong immunoreaction of PTPIP51, which co-localized with 14-3-3ß and PTP1B. The duolink proximity ligation assay corroborated a direct *in situ* interaction of PTPIP51 with both proteins, known to interact with PTPIP51 *in vitro*. The *in vitro* interacting partners Raf-1 and c-Src showed a partial co-localization. Besides, immune cells located in capillaries or infiltrating the tumour tissue and endothelial cells of pseudoglomerular vessels revealed a high PTPIP51 expression.

The upregulation of PTPIP51 and its connection with the EGFR/MAPK pathway by 14-3-3ß via Raf-1 and by PTP1B via c-Src, argue for a functional role of PTPIP51 in the pathogenesis of human glioblastoma.

Key words: Glioblastoma, PTPIP51, 14-3-3ß, EGFR, MAPK, Raf-1, Glioma

Offprint requests to: Meike Katinka Petri, Institute of Anatomy and Cell Biology, Justus-Liebig-University Giessen, 35385 Giessen, Germany. e-mail: meike.petri@anatomie.med.uni-giessen.de

Introduction

The incidence of gliomas is increasing worldwide. 18,820 new cases of human primary central nervous system tumours are diagnosed annually in the United States of America, about 60% are gliomas and 30-40% of these account for glioblastoma (GBM) (Khan et al., 2009). GBM is the most frequent and most malignant form of neuroepithelial tumour. The mean survival time of GBM patients is still around one year, despite significant advances in therapeutic options (McLendon et al., 2007).

PTPIP51 is a novel protein that has been shown to be expressed in many human cancers (Lv et al., 2006; Stenzinger et al., 2009). As demonstrated by Koch et al. (2008, 2009b) PTPIP51 is expressed in human keratinocyte carcinomas and prostate cancer. Comparing benign prostate hyperplasia with prostate carcinoma provided evidence that PTPIP51 expression is partially controlled by promoter methylation. Lv et al. (2006) demonstrated PTPIP51 mRNA-expression in various carcinomas.

PTPIP51 is evolutionary conserved and was shown to interact *in vitro* with the non-transmembrane protein-tyrosine phosphatase, Protein Tyrosine Phosphatase 1B

(PTP1B) (Stenzinger et al., 2005, 2009). The protein is phosphorylated *in vitro* and *in situ* at Tyr176 by Src kinase and dephosphorylated by PTP1B (Stenzinger et al., 2009). In HEK 293 and HeLa cells, PTPIP51 overexpression was shown to enhance apoptosis (Lv et al., 2006).

Recently, two independent studies by Jin et al. (2004) and Ewing et al. (2007) demonstrated the interaction between the two isoforms 14-3-3ß, 14-3-3γ and PTPIP51. The study of Yang et al. (2009) demonstrated a correlation between the grade of malignancy and the expression of 14-3-3ß and 14-3-3η in gliomas. In contrast, normal brain tissue was not found to express these two 14-3-3 isoforms. The isoforms ß and η belong to a superfamily of 14-3-3 proteins, which are differentially expressed in many human tissues. 14-3-3 proteins have been implicated in numerous cellular processes, such as tumourigenesis, cell cycle control and apoptosis (Cao et al., 2008).

Yu and co-workers (2008) reported PTPIP51 to interact with Raf-1 through 14-3-3 protein, thereby modulating cellular motility and morphology by the mitogen activated protein kinase (MAPK) cascade. The MAPK/Erk pathway is involved in a variety of cellular functions such as growth, proliferation, differentiation, migration and apoptosis. This pathway has been extensively studied in glioblastoma cells (Lopez-Gines et al., 2008). The data available so far consider PTPIP51 to play a role in cellular differentiation, motility, cytoskeleton formation and apoptosis.

This study primarily aimed to investigate the PTPIP51-expression profile in GBM, applying RT-PCR, quantitative real time PCR, *in situ* hybridization and immunohistochemistry. Moreover, cell specific co-expression of the proteins 14-3-3ß, Raf-1, PTP1B, c-Src and EGFR were assessed at the mRNA and protein level. Furthermore, the direct interaction of PTPIP51 with 14-3-3ß and PTP1B *in situ* was substantiated.

An earlier study by Koch et al. (2009a) displayed the expression of PTPIP51 to be restricted to neurons in specific areas of normal mouse brain and glial cells did not show an expression of PTPIP51.

Data obtained in the present study will set the base for further studies that aim to investigate the putative role of PTPIP51 in glioblastoma formation.

Material and methods

Samples of twenty glioblastoma cases and samples of four astrocytomas were included in this study (Table 1).

Glioblastoma specimens were stained immunohistochemically for PTPIP51, 14-3-3ß, c-Src, Raf-1, PTP1B, EGFR, apoptosis (TUNEL) and proliferation (Ki67). The cell specific expression of PTPIP51 was corroborated by means of *in situ* hybridization.

Four intraoperatively obtained tissue samples of primary glioblastoma and one of recurrent glioblastoma were examined for mRNA expression of PTPIP51, 14-3-3ß, c-Src, Raf-1 and PTP1B. Moreover, to obtain quantitative data on the transcriptional activity of the 14-3-3ß and PTPIP51 gene in grade II astrocytoma (n=4 paraffin embedded samples) and glioblastoma (n=5 paraffin embedded samples) kinetic PCR was employed.

Immunohistochemistry

The tumour tissue was fixed in neutral-buffered formalin for 48h, embedded in paraffin, sectioned and stained with H&E. The samples were categorized according to the WHO classification and diagnosed as GBM.

Paraffin samples were obtained from the Institute of Neuropathology, University Hospital Bonn. The patients had given informed consent that parts of the histological specimens can be used for research purposes. The sections were deparaffinized in xylene and rehydrated in graded ethanol. Prior to the staining procedure, antigen retrieval using microwave-oven heating (2x5min, 800W) in 10mM standard sodium citrate buffer (pH 6.0) was carried out for all antibodies used in this study.

Nonspecific binding sites were blocked with phosphate-buffered saline (PBS) containing 5% bovine serum albumin and 5% normal goat serum. Immunoreaction with the primary antibodies (Table 2) was performed overnight at room temperature, followed by incubation with the appropriate secondary antibodies

Table 1. Tumour specimens included in the study Tumours.

	Age (years)	Sex	Localization	Tumour specimens	WHO-Grade
1	65	M	central, left	GBM	IV
2	63	F	frontal, right	GBM	IV
3	78	F	frontal, right	GBM	IV
4	72	M	fronto-temporal, left	GBM	IV
5	76	M	temporal, right	GBM	IV
6	70	M	central, right	GBM	IV
7	60	M	temporal, right	GBM	IV
8	66	M	temporo-dorsal, left	GBM	IV
9	72	F	temporo-medial, right	GBM	IV
10	61	M	temporo-parietal, left	GBM	IV
11	42	M	central, left	GBM	IV
12	67	M	frontal, right	GBM	IV
13	78	M	central, right	GBM	IV
14	68	F	temporo-polar, left	GBM	IV
15	52	M	precentral/central, left	GBM	IV
16	33	M	temporo-medial, right	Astrocytoma	II
17	23	F	insula, left	Astrocytoma	II
18	44	F	corpus callosum, left	Astrocytoma	II
19	31	M	insula, right	Astrocytoma	II
20	55	M	occipital, left (hemianopsia)	GBM magnocellular	IV
21	55	F	parietal, right	GBM	IV
22	46	M	parietal/pre-central gyrus, left	GBM, relapse	IV
23	66	M	parietal, occipital right	GBM, relapse	IV
24	76	M	Broca region, left	GBM	IV

No. 1-19 were analyzed by immunocytochemistry and No. 11-19 by quantitative real time PCR. Tumours No. 20-24 were analyzed by reverse transcriptase PCR.

(Table 2) for 1 h at room temperature. Subsequently, the slides were coverslipped in carbonate buffered glycerol at pH 8.6.

The polyclonal antibody against PTPIP51 was raised as described and characterized in previous studies (Koch et al., 2009a).

Primary antibodies were visualized by Alexa fluor 488 and Alexa fluor 555 secondary antibodies. For each series of antibody staining sections were incubated with medium lacking PTPIP51 antibody, serving as an internal negative control. Nuclei were displayed by DAPI.

Apoptosis was detected using the *in situ* cell death detection kit ApopTag (Chemicon International, USA # S7110) which employs an indirect TUNEL method, utilizing an anti-digoxigenin antibody that is conjugated to a fluorescein reporter molecule. It provides indirect immunofluorescence staining. Results were analyzed by using fluorescence microscopy. The kit was used according to the instructions by the manufacturer.

Immunofluorescence analysis and photo-documentation were performed on an Axioplan 2 fluorescence microscope equipped with Plan-Apochromat objectives (Carl Zeiss Jena, Germany). Visualization of the secondary antibody Alexa fluor 555 was achieved with an excitation filter of 530-560 nm and an emission filter with a range 572.5-647 nm. Alexa Fluor 488 was visualized by an excitation filter with 460-500nm and an emission filter 512-542 nm.

Duolink proximity ligation assay (DPLA)

Interaction of PTPIP51 with either PTP1B or 14-3-3ß was detected by the proximity ligation assay kit DuoLink (Olink biosciences, Uppsala, Sweden, PLA probe anti-rabbit minus for the detection of the rabbit PTPIP51 antibody, Cat.# 90602; PLA probe anti-mouse plus for the detection of the mouse anti PTP1B or 14-3-3ß antibody, Cat.# 90701; Detection Kit 563, Cat.# 90134). The DuoLink proximity ligation assay secondary antibodies only hybridise when the two different PLA probes (probe anti-rabbit minus and probe anti-mouse plus) have bound to proteins in proximity closer than 40 nm. This proximity results in ligation forming a circular template and amplification step the fluorophore coupled testing probe binds the amplified oligonucleotide strands. Addition of the fluorescent labelled oligonucleotides that hybridize to the rolling circle amplification (RCA) product leads to a point-shaped signal that is visible in fluorescence microscopy.

Methanol-fixed air-dried samples were per-incubated with blocking agent for 1h. After washing in PBS for 10 min, primary antibodies for PTPIP51 and PTP1B, or PTPIP51 and 14-3-3ß were applied to the samples. The antibodies were diluted in the blocking agent at a concentration of 1:500 and 1:100, respectively.

Table 2. List of the antibodies used in this study.

	Immunogen	Antibody Source	Clone	Dilution	Manufacturer
PTPIP51	Human recombinant PTPIP 51 protein encoding amino acids (aa) 131-470	Rabbit polyclonal		1:400	Prof. HW Hofer, Biochemical Department, University Konstanz, Germany
14-3-3 ß	Epitope mapping the C-terminus of human origin	Mouse monoclonal	A-6	1:100	Santa Cruz Cat# sc-25276
PTP1B	Human recombinant protein tyrosine phosphatase 1B (aa 1 – 321)	Mouse monoclonal	107AT531	1:100	Abgent Cat#AM8411
Glial fibrillary acidic protein	Purified porcine glial filament from spinal cord	Mouse monoclonal	GA5	1:200	Chemicon Cat# MAB3402
Raf-1	Epitope mapping the C-terminus of human origin	Mouse monoclonal	E-10	1:50	Santa Cruz Cat# sc-7267
c-Src	Full-length human recombinant c-Src	Mouse monoclonal	17AT28	1:100	Santa Cruz Cat# sc-130124
EGFR	Plasma membranes of A431 cells	Mouse monoclonal	2E9	1:75	Santa Cruz Cat# sc-57091
Ki67	Human recombinant peptide corresponding to a 1002 bp Ki-67 cDNA fragment	Mouse monoclonal	MIB-1	1:100	Dako Cytomation Cat# M 7240
CD20	CD20 protein	Mouse monoclonal	B9E9	1:100	Thermo Scientific Cat # MA1-7634
CD34	CD34 protein from human endothelial vesicles	Mouse monoclonal	QBEND-10	1:100	ThermoScientific Cat.# Ma35170
Granulocyte marker SPM250	nuclei from Pokeweed nitrogen-stimulated human peripheral blood lymphocytes	Mouse monoclonal	his48	1:100	Santa Cruz Cat# sc-65523
α-smooth muscle actin- FITC antibody	N-terminal synthetic decapeptide of α-smooth muscle actin	Mouse monoclonal	clone 1A4	1:100	SigmaAldrich Cat# F3777
Alexa fluor 555 Coupled to anti-rabbit antibody	IgG heavy chains from rabbit	Goat		1:800	Invitrogen Cat# A21428
Alexa fluor 488 Coupled to anti-mouse antibody	IgG heavy chains from mouse	Goat		1:800	Invitrogen Cat# A11029
ApopTag® Fluorescein *In Situ* Apoptosis Detection Kit					Chemicon International S7107

Incubation was done overnight in a pre-heated humidity chamber. Slides were washed three times in PBS for 10 min. Duolink PLA probes detecting rabbit or mouse antibodies were diluted in the blocking agent at a concentration of 1:5 and applied to the slides following incubation for 2h in a pre-heated humidity chamber at 37°C. Washing three times in PBS for 10 min removed unbound PLA probes. For hybridization of the two Duolink PLA probes Duolink Hybridization stock was diluted 1:5 in high purity water and slides were incubated in a pre-heated humidity chamber for 15 min at 37°C. The slides were washed in TBS-T for 1 min under gentle agitation. The samples were incubated in the ligation solution consisting of Duolink Ligation stock (1:5) and Duolink Ligase (1:40) diluted in high purity water for 90 min at 37°C. Detection of the amplified probe was done with the Duolink Detection kit. Duolink Detection stock was diluted 1:5 in high purity water and applied for 1 h at 37°C. Final washing steps were done by SCC buffer and 70% ethanol.

H&E

The histomorphological characteristics were evaluated by hematoxylin and eosin staining.

In situ hybridization

In situ hybridization was performed as described previously (Koch et al., 2009a).

Reverse transcriptase-polymerase chain reaction (RT-PCR)

For assessment of RT-PCR five glioblastoma tissue specimens were obtained during neurosurgical resection. The tissue samples were immediately transferred into RNA-later (Qiagen, Hilden, Germany) and stored deep frozen at -20°C according to the manufacturer's instructions. All tissue samples used for RT-PCR were obtained from the Department of Neurosurgery, Justus-Liebig-University, Giessen. Prior to resection, patients had given informed consent to using parts of the histological specimen for research purposes.

The RNA extraction was performed using the RNA extraction kit RNeasy MINI (Qiagen, Hilden, Germany) according to the manufacturer's instructions.

Qualitative reverse transcriptase PCR was performed on an iCycler using SYBR Green Supermix (BioRad, Munich, Germany) to visualize the respective amplicons. 2 μl cDNA were used per sample. Cycling conditions were 94°C for 2 min, followed by 40 cycles of 94°C (PTPIP51); 58°C (PTP1B); 63°C (c-Src); 63.5°C (Raf-1) and 60°C (14-3-3ß) for 30 sec, 55°C for 30 sec and 72°C for 2 min. The primers were employed for PTPIP51, PTP1B, c-Src, Raf-1 and 14-3-3ß (Table 3).

PCR products were visualized by agarose gel electrophoresis. While amplification of a 90 bp ß-actin

Table 3. Primer used for RT-PCR and for quantitative real time PCR.

	Primer RT-PCR (fresh tissue specimen)	size	template
PTPIP51	forward 5´-GCAGGTGGTGCTATCAGGTC-3´ reverse 5'-AGCTCCAGGGCCAACTTCATC-3'	232 BP	1294-1525
PTP1B	forward 5'-GGAGATGGAAAAGGAGTTC-3' reverse 5'-TGCTTTTCTGCTCCCACAC-3'	311 BP	177-487
14-3-3ß	forward 5'-ATTCGTCTTGGTCTGGCACT-3' reverse 5'-CAGGCTACAGGCCTTTTCAG-3'.	78 BP	689-766, 784-861
c-Src	forward 5'-ATGGTGAACCGCGAGGTGCT-3' reverse 5'-GATCCAAGCCGAGAAGCCGGTCTG-3'	244 BP	1753-1996
Raf-1	forward 5'-CAGCCCTGTCCAGTAGC-3' reverse 5'-GCCTGACTTTACTGTTGC-3'	614 BP	1287-1900
ß-actin	forward 5'-TTCCTTCCTGGGCATGGAGT-3' reverse 5'-TACAGGTCTTTGCGGATGTC-3'	90 BP	2439-2528
	Primer quantitative RT-PCR (paraffin embedded tissue)		
PTPIP51	forward 5'-TCAAGGAGCATGTGGACAAA-3' reverse 5'-ATAGCACCACCTGCCAAGAA-3'	80 BP	1228-1307
14-3-3ß	forward 5'-ATTCGTCTTGGTCTGGCACT-3' reverse 5'-CAGGCTACAGGCCTTTTCAG-3'.	78 BP	689-766, 784-861
ß-actin	forward 5'-TTCCTTCCTGGGCATGGAGT-3' reverse 5'-TACAGGTCTTTGCGGATGTC-3'	90 BP	2439-2528
GAPDH	forward 5'-ATGCCAGTGAGCTTCCCGTTCA-3' reverse 5'-TGGTATCGTGGAAGGACTCATGA-3'	189 BP	628-794

product served as positive control, negative controls included samples lacking reverse transcriptase.

Quantitative real time PCR

Five paraffin-embedded GBM tissues and four samples from patients with grade II astrocytoma were used for quantification of mRNA. The purification of RNA was done using the QIAamp DNA FFPE tissue kit (Qiagen, Hilden, Germany) according to the manufacturer's instruction.

The amplification of cDNA was carried out in 25 μl reaction volume on the iCycler iQ Real-Time PCR Detection System (Bio Rad, Munich, Germany). The final reaction tubes contained 100nM as PTPIP51, 14-3-3ß and reference genes ß-actin and GAPDH (Table 3), 12.5 μl iQ SYBR Green Supermix (Bio Rad) and 2 μl of DNA template. The PCR conditions were 94°C for 3 min followed by 40 cycles for 30 sec, 60°C for 30 sec and 72°C for 1min. Melting curves were generated for both genes after amplification. Negative controls were included in each run. The selection of appropriate combination of reference genes for expression analysis of PTPIP51 in GBM and astrocytoma II tissue was carried out using NormFinder Program. PCR-products were additionally electrophoresed on a 3% agarose gel and visualized by GelRed reagent.

Results

This study demonstrates for the first time the cell-specific expression of PTPIP51 mRNA and protein in human glioblastoma. Immunohistochemical experiments and *in situ* hybridization revealed a strong expression of PTPIP51 in GBM tumour cells and endothelial cells and immune cells. Additionally, the PTPIP51 expression profile was assayed in apoptosis by TUNEL and in proliferation with Ki67 by double immunostaining. Furthermore, we explored the interacting partners of PTPIP51, 14-3-3ß, Raf-1, PTP1B, c-Src and EGFR. The transcription of the respective signalling partners was shown by qualitative reverse transcriptase PCR. The correlation of the tumour grade of gliomas with the quantitative expression of both, PTPIP51 and 14-3-3ß, was examined by quantitative real time PCR comparing GBM and grade II astrocytoma.

In situ expression profile of PTPIP51 mRNA and protein

Immunohistochemical staining of 15 GBM samples revealed PTPIP51 protein expression in tumour cells as identified by subsequent H&E staining of the sections (Fig. 1A-C). Probing glioblastoma samples with both PTPIP51 antibody and GFAP antibody confirmed the expression of PTPIP51 in malignant glial cells (Fig. 1D-

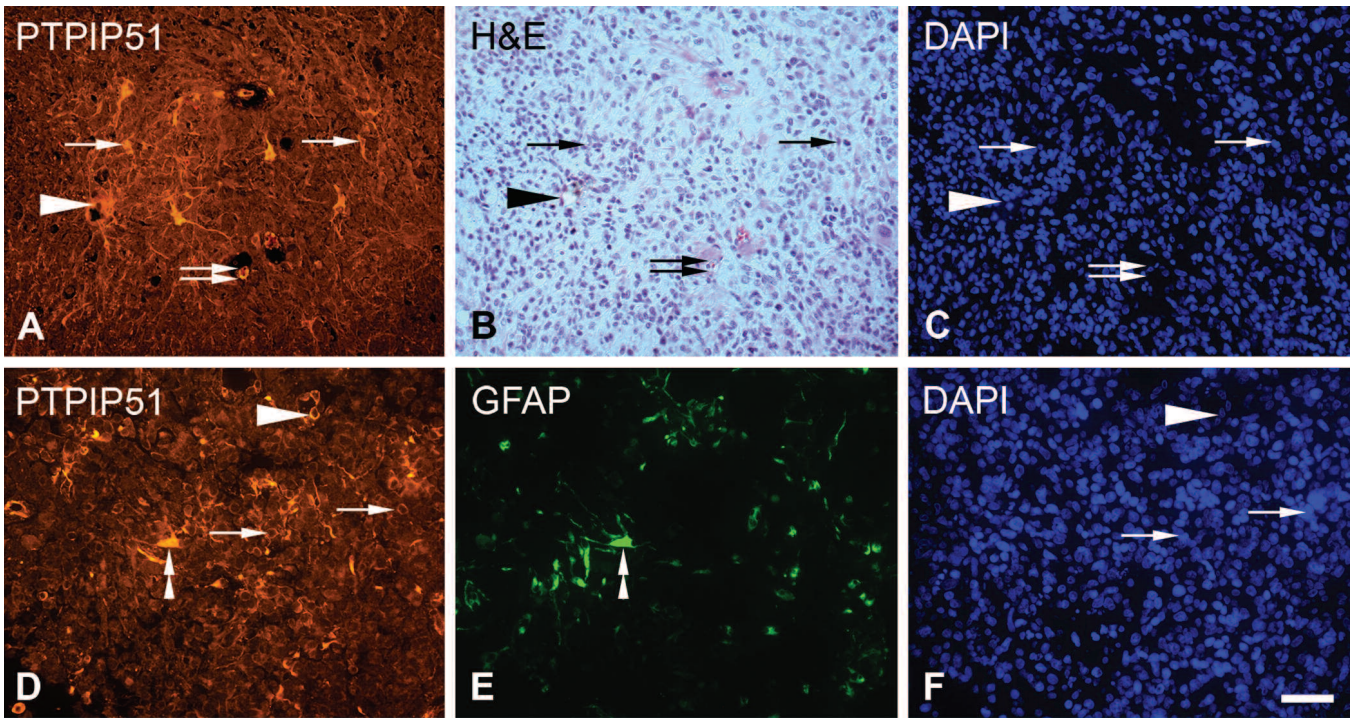

Fig. 1. Immunostaining of PTPIP51 in sections of human glioblastoma. **A.** PTPIP51 immunostaining. **B.** H&E staining of section A. **C.** DAPI staining of section A. **D.** PTPIP51 immunostaining. **E.** GFAP staining of section D. **F.** DAPI staining of section D. Arrows: PTPIP51 positive glioblastoma cells, arrowheads: PTPIP51 positive endothelial cells, double arrowheads: PTPIP51 and GFAP positive reactive astrocyte, double arrow: PTPIP51 positive immune cell (neutrophil granulocyte). Bar: 50 μm.

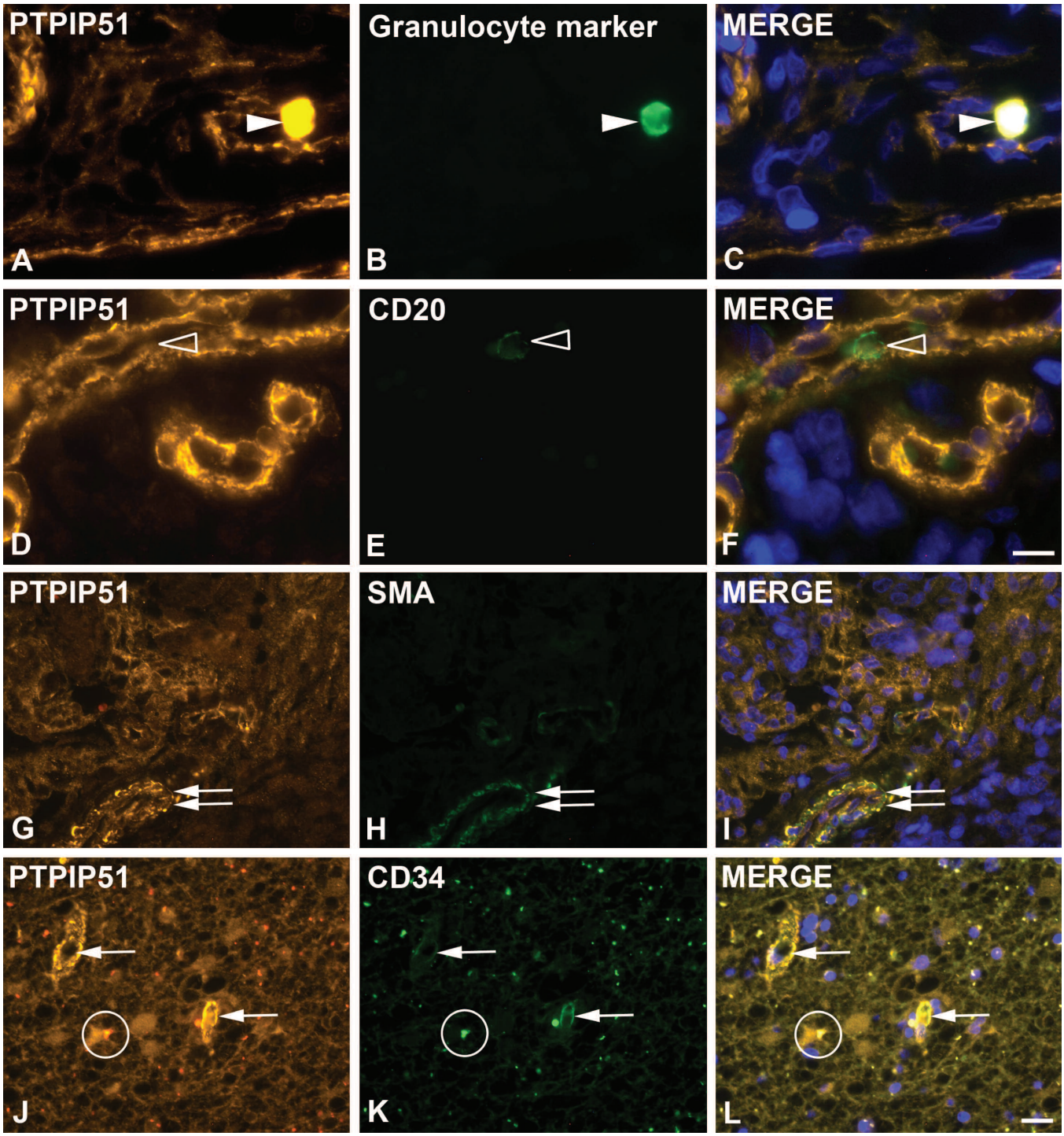

Fig. 2. PTPIP51 expression in immune cells, smooth muscle cells and endothelial cells. **A.** PTPIP51 immunostaining. **B.** granulocyte marker of section A. **C.** Merge of A, B and DAPI. **D.** PTPIP51 immunostaining. **E.** B lymphocyte in section D detected by CD20. **F.** Merge of D, E and DAPI. **G.** PTPIP51 immunostaining. **H.** α-sma of section G. **I.** Merge of G,H and DAPI. **J.** PTPIP51 immunostaining. **K.** Endothelial cells detected by CD34 in section J. **L.** Merge of J, K and DAPI. Arrowhead: neutrophil granulocytes; blank arrowhead: B lymphocytes; double arrow: smooth muscle cells; arrow: endothelial cells; white circle: lipofuscin granula . Bars: A-F, 10 μm; G-L, 20 μm.

F). Endothelial cells (Fig. 2J-L), smooth muscle cells (Fig. 2G-I) and immune cells also showed PTPIP51 expression. In endothelial cells of normal and of pseudoglomerular vessels PTPIP51 protein was restricted to the plasmamembrane and to the nucleus. Granulocytes located in capillary lumina or infiltrating the tumour, as well as the necrotic tissue, displayed a strong PTPIP51 immunoreaction (Fig. 2A-C). In contrast to granulocytes, B lymphocytes did not show any PTPIP51 expression (Fig. 2D-F).

Matching the protein expression profile, PTPIP51 mRNA was found in the cytoplasm of tumour cells and in the cytoplasm of endothelial cells as detected by *in situ* hybridization (Fig. 3).

In situ expression profile of PTPIP51 and its interacting partners

PTPIP51 and 14-3-3ß showed a strict co-localization. Both proteins were found in glioblastoma cells, endothelial cells and in immune cells. The glioblastoma cells displayed a strong cytoplasmic reaction (Fig. 4A-C). In astrocytoma, a co-localization for PTPIP51 and 14-3-3ß was seen, but to a much lower extent (Fig. 4D-F).

To corroborate the interaction of PTPIP51 and 14-3-3ß, a duolink proximity ligation assay was applied to GBM and astrocytoma sections. In all investigated samples, hybridized and amplified antibody-linked

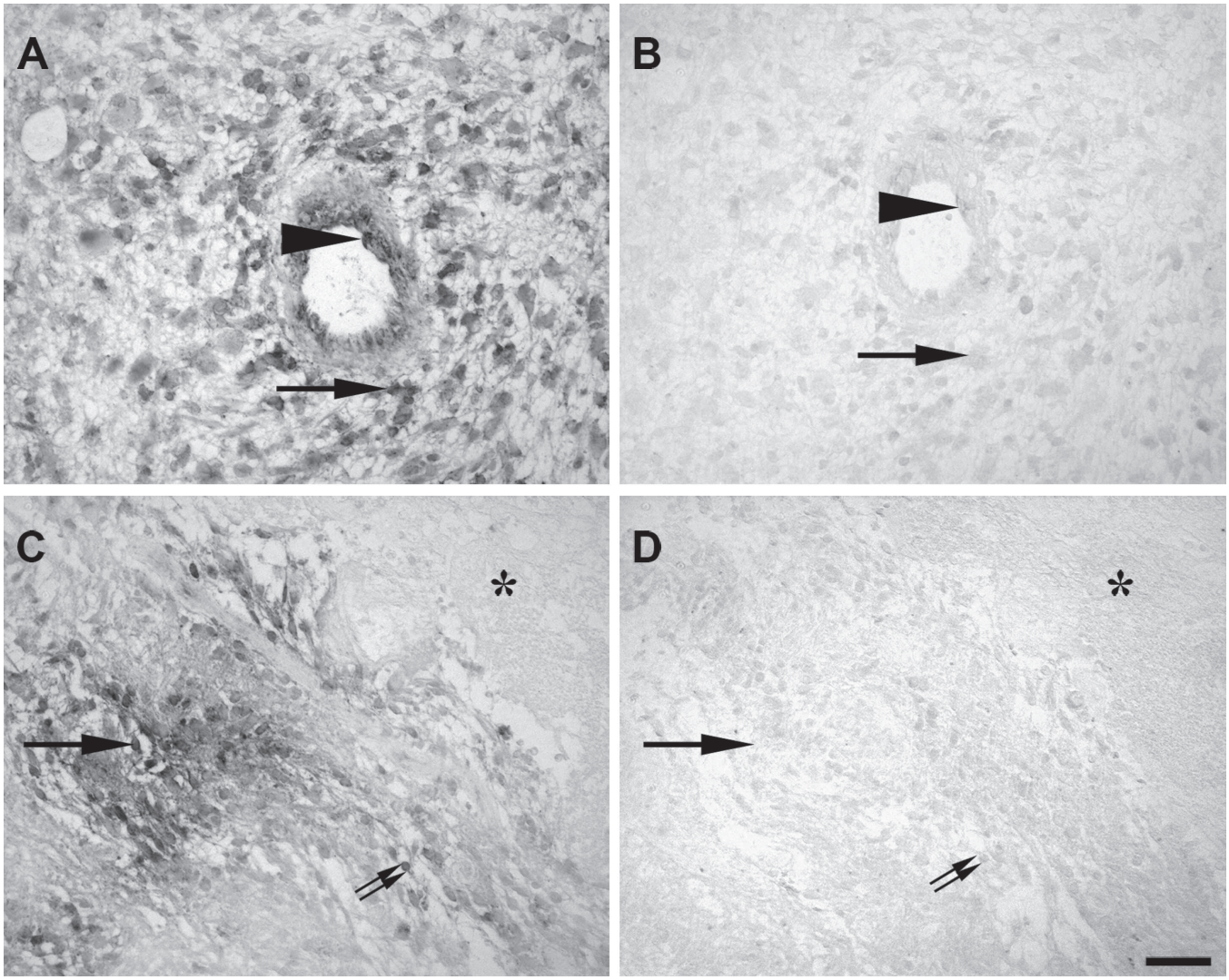

Fig. 3. *In situ* hybridization of PTPIP51 in sections of human glioblastoma. **A.** Anti-sense probe. **B.** Sense probe of parallel section to A. **C.** Anti-sense probe. **D.** Sense probe in parallel section to C. Arrows: PTPIP51 mRNA in glioblastoma cells, arrowhead: PTPIP51 mRNA in endothelial cells, double arrow: immune cells, asterisk: necrotic tissue. Bar: 50 μm.

nucleotide strands were detected. Every dot corresponds to an interaction between PTPIP51 and 14-3-3ß.

As seen in Figure 4G and H, glioblastoma and astrocytoma cells displayed hybridized and amplified antibody-linked nucleotide strands, revealing the *in situ* interaction between PTPIP51 and 14-3-3ß.

GBM tumour cells situated around pseudo-glomerular vessels, as well as endothelial cells and immune cells, displayed a co-localization of PTPIP51 with PTP1B (Fig. 5A-C). To confirm an *in situ* interaction of PTPIP51 and PTP1B, a duolink proximity ligation assay was performed. As seen in Figure 5D glioblastoma cells displayed hybridized and amplified antibody-linked nucleotid strands, revealing the interaction between PTPIP51 and PTP1B.

Raf-1 and PTPIP51 displayed a strong co-localization in the vessels surrounding tumour cells (Fig. 6A-C).

There was only a partial co-localization of PTPIP51 and c-Src (Fig. 6D-F). In contrast to high PTPIP51 expression in the cytoplasm of tumour and immune cells c-Src is only present in some of these cells.

A majority of tumour cells displayed a co-localization of PTPIP51 and EGFR (data not shown).

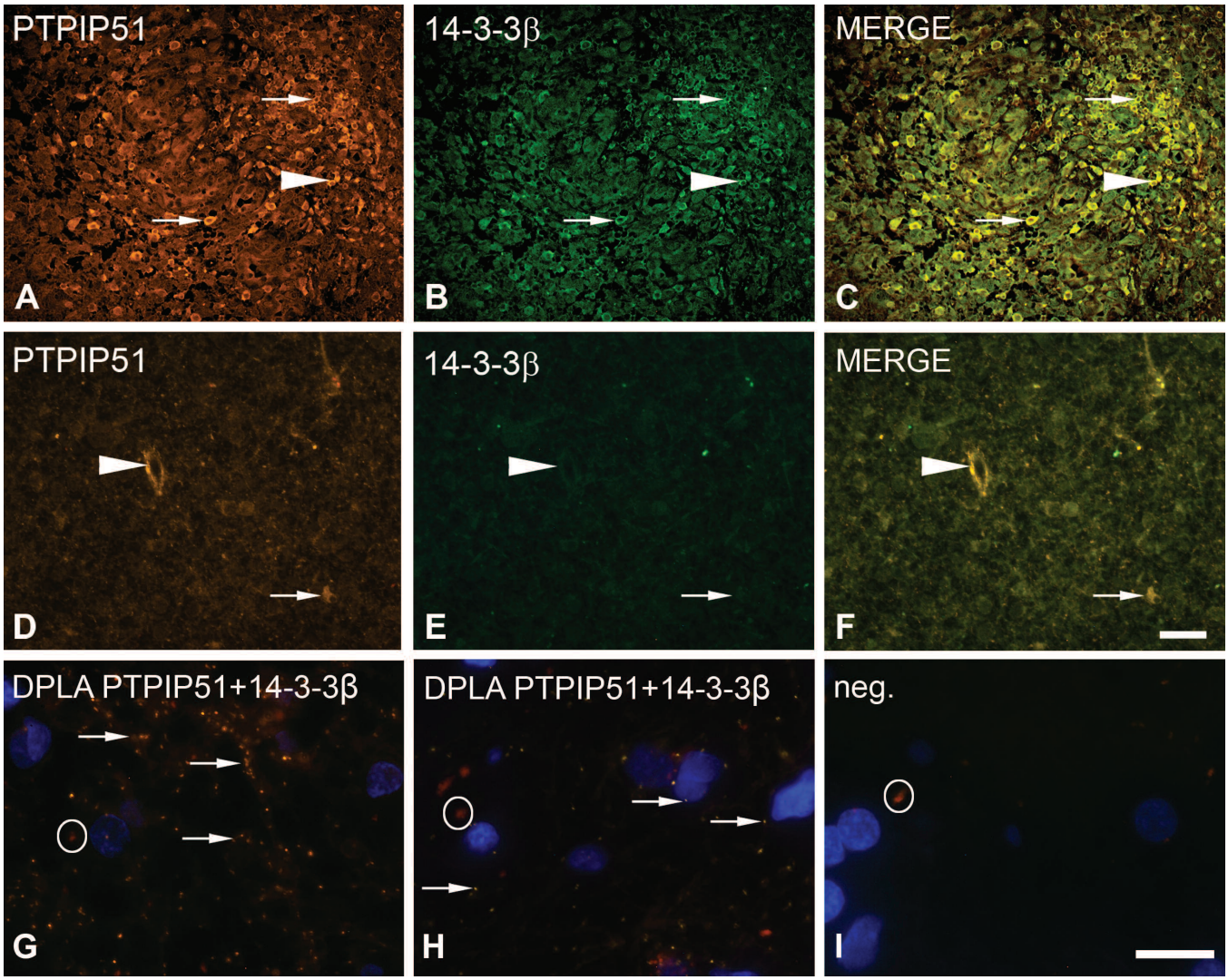

Fig. 4. PTPIP51 and its interacting partner 14-3-3ß - *in situ* co-localization analysis and Duolink proximity ligation assay in sections of human glioblastoma and astrocytoma. **A.** PTPIP51 immunostaining GBM. **B.** 14-3-3ß immunostaining of section A. **C.** Merge of A and B. **D.** PTPIP51 immunostaining astrocytoma. **E.** 14-3-3ß immunostaining of section D. **F.** Merge of D and E. Arrows: PTPIP51 positive glioblastoma cells, arrowheads: PTPIP51 positive endothelial cells, double-arrows: immune cells. **G.** GBM duolink proximity ligation assay for PTPIP51 and 14-3-3ß. **H.** astrocytoma duolink proximity ligation assay for PTPIP51 and 14-3-3ß. Interaction of both proteins is seen as orange dots (arrows). **I.** Negative control. White circles: lipofuscin granules. Bars: A-F, 50 μm; G-I, 10 μm.

Stained by Ki-67, proliferating cells showed a strong expression of PTPIP51 in the cytoplasm with elevated concentration near the plasmamembrane (Fig. 7A-C).

TUNEL assay analysis of GBM sections did not show PTPIP51 positive cells executing apoptosis (Fig. 7D-F).

mRNA expression of PTPIP51 and its interaction partners

Qualitative reverse transcriptase PCR analysis: The mRNA expression of PTPIP51 and its *in vitro* interaction partners was tested by reverse transcriptase PCR. As demonstrated in Figure 8, the samples 1, 2, 3 and 5 expressed a considerable amount of PTPIP51, PTP1B, 14-3-3ß, Raf-1 and c-Src. A different expression pattern was observed in sample number 4, which had been obtained from a patient with a recurrent GBM. The histopathological findings of this specimen showed healthy cerebral tissue with only singular tumour cells. In this case attenuated expression of PTPIP51 and PTP1B was found, c-Src was barely detectable, and Raf-1 was lacking (Fig. 8).

Comparison of PTPIP51 expression levels in grade II astrocytoma and glioblastoma by quantitative PCR

PTPIP51 expression levels of 5 GBM and 4 grade II astrocytoma samples were assessed by quantitative PCR. Candidate reference genes for normalization and the best

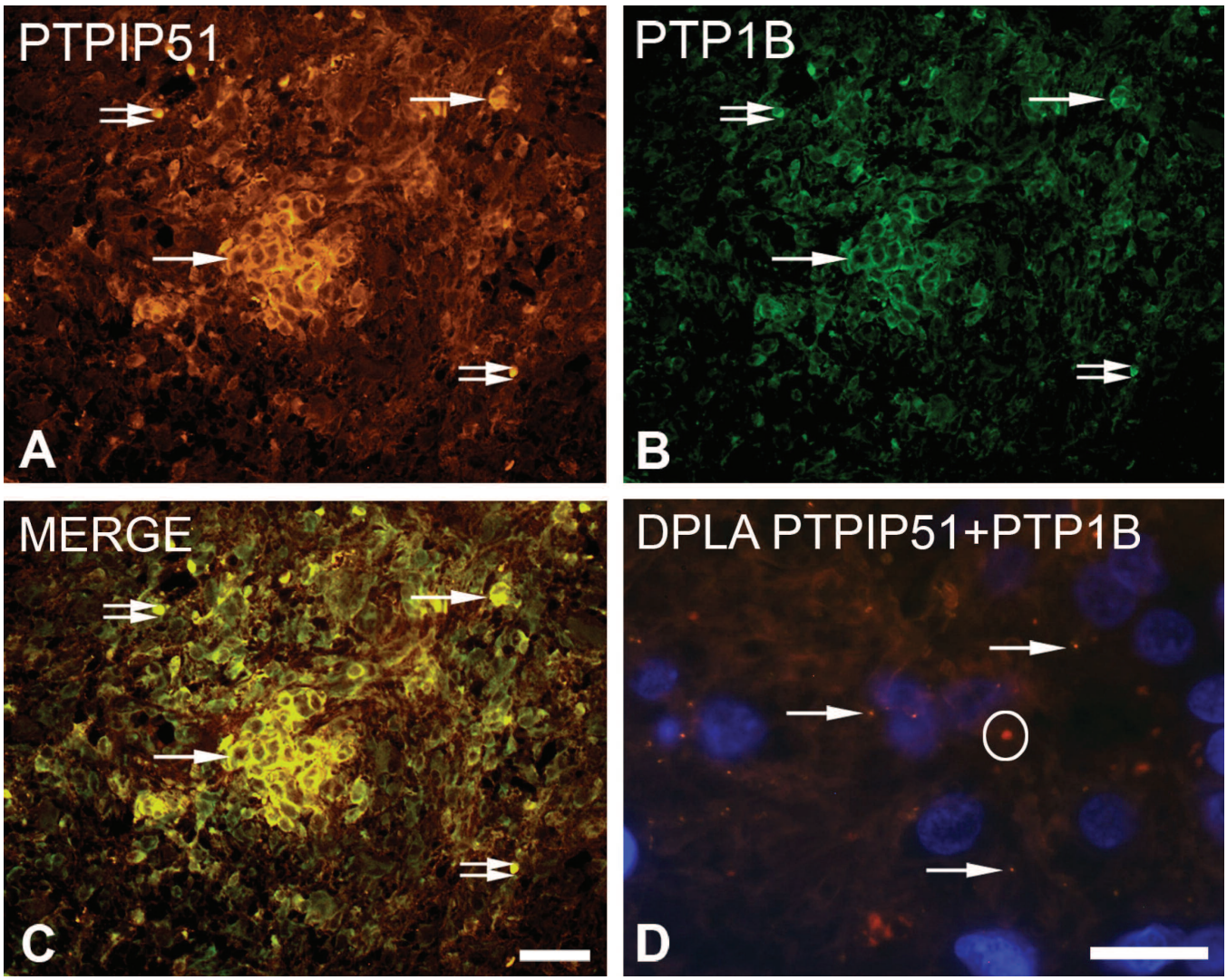

Fig. 5. PTPIP51 and its interacting partner PTP1B in sections of human glioblastoma. **A.** PTPIP51 immunostaining. **B.** PTP1B immunostaining of section A. **C.** Merge of section A and B. Arrows: PTPIP51 positive glioblastoma cells; Double arrows: immune cells. **D.** Duolink proximity ligation assay for PTPIP51 and PTP1B. Interaction of both proteins is seen as orange dots (arrows). Bars: A-C, 20 μm; D, 10 μm.

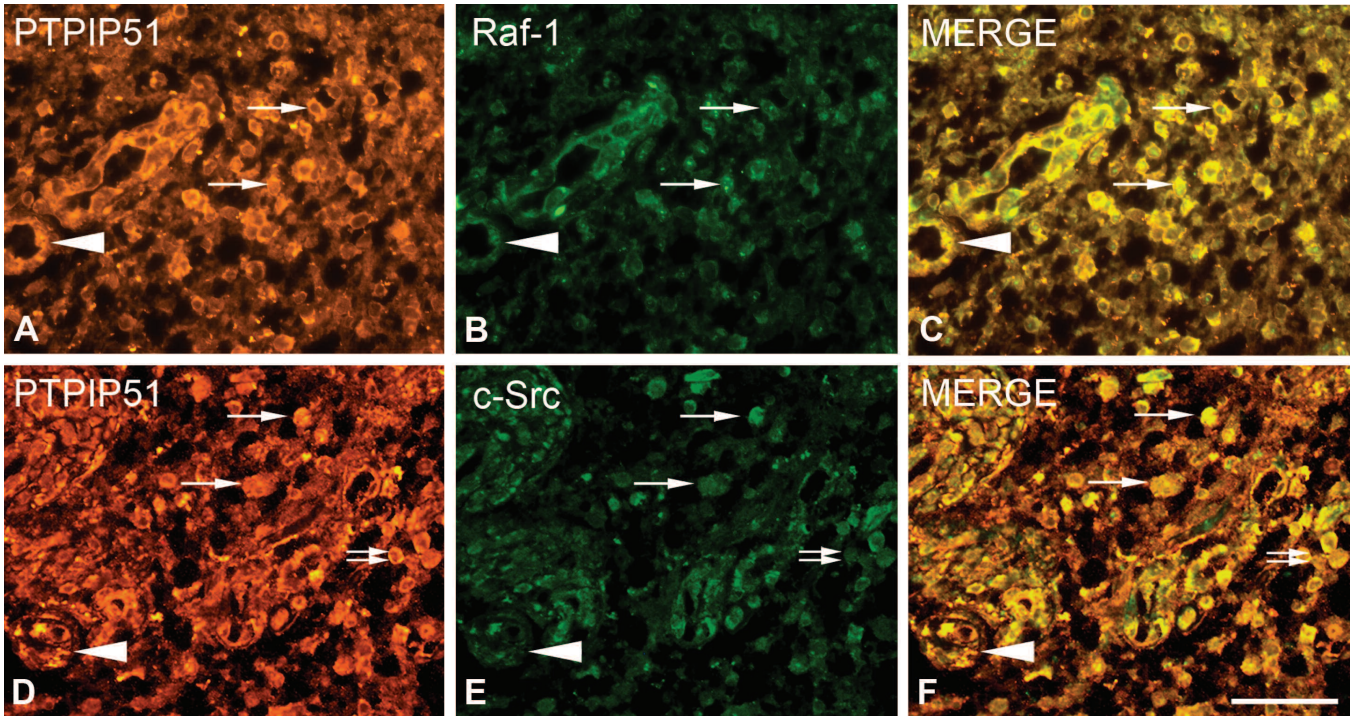

Fig. 6. PTPIP51 and its interacting partners Raf-1 and c-Src in sections of human glioblastoma. **A.** PTPIP51 immunostaining. **B.** Raf-1 immunostaining of section A. **C.** Merge of A and B. **D.** PTPIP51 immunostaining. **E.** c-Src immunostaining of section D. **F.** Merge of D and E. Arrows: PTPIP51 positive glioblastoma cells, arrowheads: PTPIP51 positive endothelial cells, double-arrows: immune cells. Bar: 50 μm.

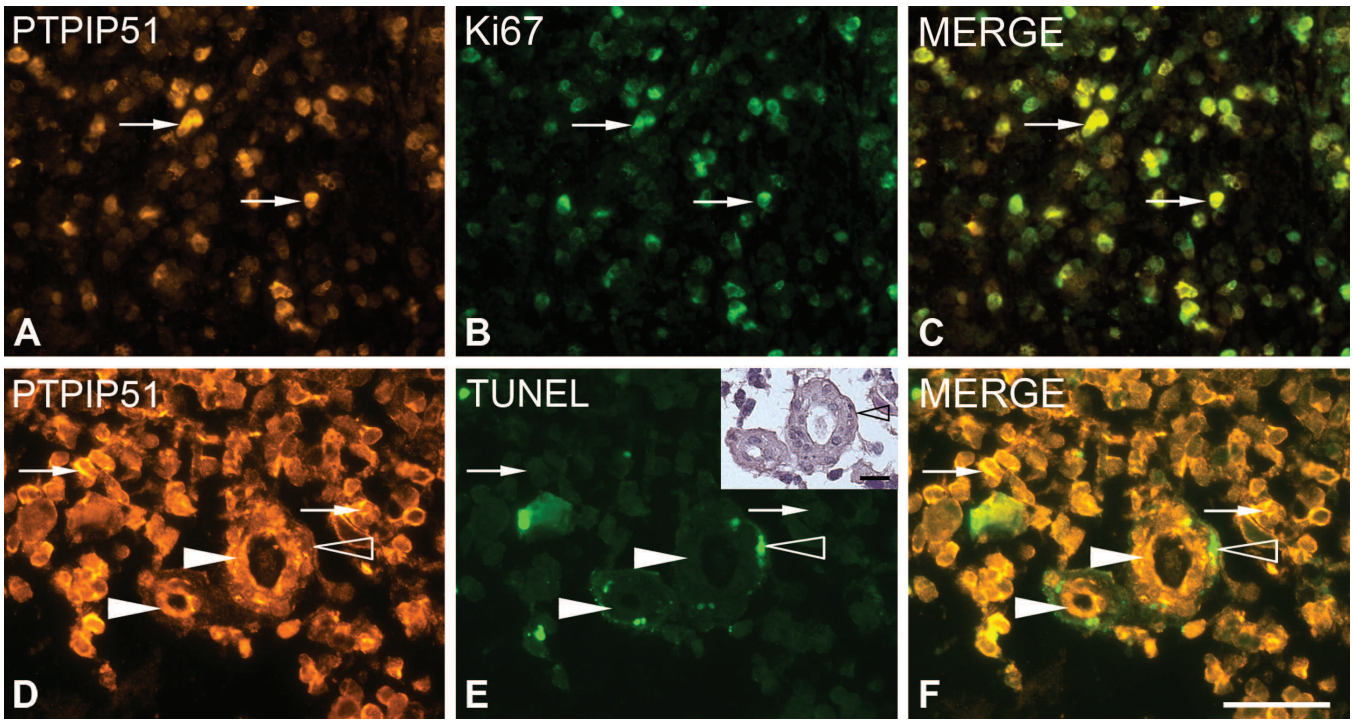

Fig. 7. PTPIP51 protein expression and investigation of proliferation and apoptosis by Ki67 antibody and TUNEL-assay. **A.** PTPIP51 immunostaining. **B.** Ki67 immunostaining of section A. **C.** Merge of A and B. **D.** PTPIP51 immunostaining. **E.** TUNEL-assay of section D, insert: H.E. staining of detail **F.** Merge of D and E. Arrows: PTPIP51 positive glioblastoma cells, arrowheads: PTPIP51 positive endothelial cells, blank arrowhead: apoptotic pericyte. Bar: 50 μm.

combination of two genes were calculated according to their expression stability by the NormFinder program. The best fitting combination proved to be ß-actin with GAPDH.

The results of expression analysis showed slightly elevated levels of PTPIP51 (mean value 5.23±1.01) in the group of GBM when compared to low grade astrocytoma (mean value 4.62±1.49). 14-3-3ß expression in glioblastoma (mean value 3.42±1.10) was significantly higher than in grade II astrocytoma samples (mean value 0.88±2.74) (Fig. 9).

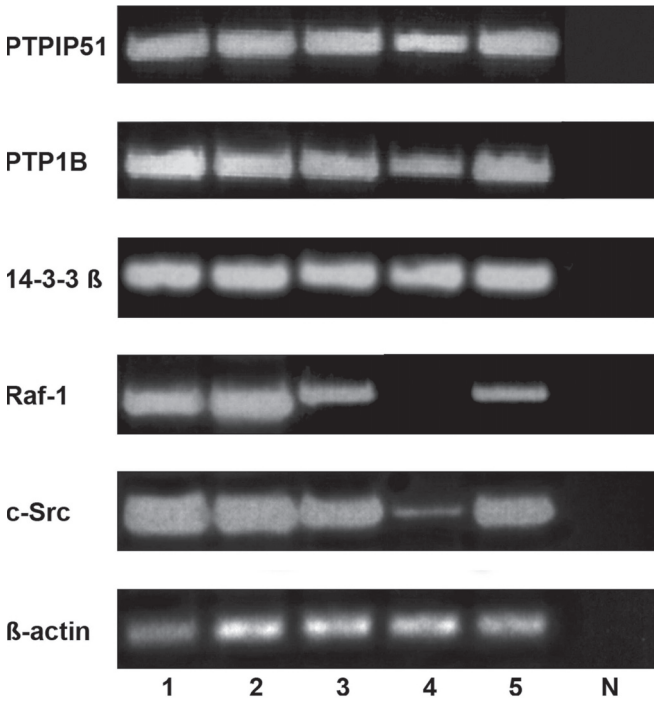

Fig. 8. Expression of PTPIP51 and its interaction partners as detected by reverse transcriptase-PCR in tissues of human glioblastoma. Qualitative reverse transcriptase-PCR was performed using primers specific to PTPIP51, PTP1B, Raf-1, c-Src and 14-3-3ß as given in Materials and Methods section. ß-actin was amplified as an internal positive control and probes lacking reverse transcriptase served as negative controls (N).

Discussion

Our results revealed elevated levels of PTPIP51 expression in GBM (grade IV glioma) samples when compared to low grade astrocytomas (grade II glioma), which correlated with the expression levels of 14-3-3ß. This is consistent with recent studies displaying a tumour grade dependent expression of two isoforms of 14-3-3ß and 14-3-3η in gliomas. Healthy cerebral tissue is completely lacking in both isoforms (Yang et al., 2009). The upregulation of 14-3-3 proteins seems to be associated with the reduced capacity of apoptosis, as antagonizing 14-3-3 or silencing its expression induces apoptosis in cultured glioma cells (Cao et al., 2010).

14-3-3ß and 14-3-3γ mediate the interaction of PTPIP51 and Raf-1, thereby modulating the activity of the MAPK-cascade (Lv et al., 2006; Yu et al., 2008; Stenzinger et al., 2009). The MAPK pathway plays an important role in cell migration and seems to be one of the main reasons for recurrences and poor prognosis of glioblastoma. It is considered that migrating tumour cells infiltrate the healthy tissue surrounding the glioblastoma and in this way can escape surgical extirpation and give rise to regrowth. With regard to these findings the interaction of PTPIP51 with 14-3-3ß, which was confirmed by the duolink proximity ligation assay, may mirror the role of PTPIP51 protein in migration and proliferation of GBM tumour cells.

A strong co-localization and interaction of PTPIP51 and 14-3-3ß was also found in all endothelial cells of GBM-typical glomerulum-like vessels of glioblastoma.

This interaction may contribute to the well known

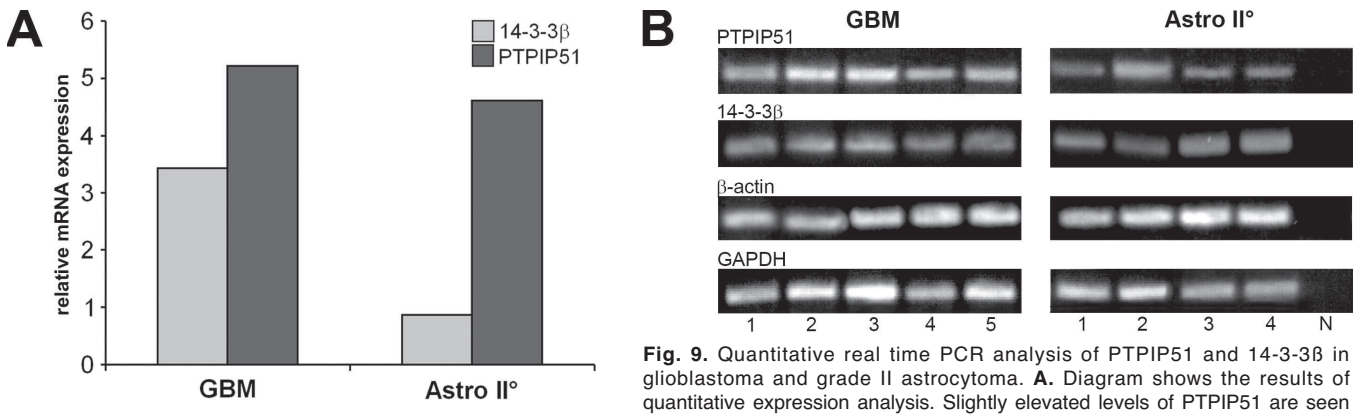

Fig. 9. Quantitative real time PCR analysis of PTPIP51 and 14-3-3ß in glioblastoma and grade II astrocytoma. **A.** Diagram shows the results of quantitative expression analysis. Slightly elevated levels of PTPIP51 are seen in the group of glioblastoma (GBM) when compared to low grade astrocytoma. 14-3-3ß expression in glioblastoma was significantly higher than in grade II astrocytoma samples. Amplification of ß-actin and GAPDH was used as a combination of reference genes. **B.** Gel: bands exclusively detecting mRNA with the expected amplification size with the primers used in 7A. Negative control (N).

high activation of the MAPK/Erk pathway via EGFR, resulting in dysfunction of cell cycle control and upregulation of proliferation in GBM.

The non-transmembrane Protein Tyrosine Phosphatase 1B (PTP1B), a known interacting partner of PTPIP51, is able to activate the MAPK cascade on c-Src and Ras level (Dubé et al., 2004; Dubé and Tremblay, 2004; Tonks and Muthuswamy, 2007; Zhao et al., 2008; Stenzinger et al., 2009). Reichardt and coworkers (2003) were unable to detect DNA amplification of PTP1B in human gliomas. However, in our study PTP1B expression was upregulated and highly co-localized with the PTPIP51 protein. The observed upregulation is consistent with the data reported by Akasaki and co-workers (2006), who also reported PTP1B to be overexpressed in gliomas. Furthermore, a direct *in situ* interaction of PTPIP51 and PTP1B in glioblastoma cells was corroborated by the duolink proximity ligation assay. These results underline the significance of our observations of upregulated PTPIP51 expression levels in glioblastomas.

PTP1B contributes to oncogenesis by the loss of tyrosine phosphorylation of key signalling proteins or by up-regulation of two growth-promoting pathways (Arias-Romero et al., 2009). In human mammary cells PTP1B links an important oncogenic receptor tyrosine kinase, namely ErbB2, to signalling pathways that promote aberrant cell division and survival by activation of Src and inducing a Src-dependent transformed phenotype. It deactivates the Ras/MAPK pathway inhibitor (Tonks and Muthuswamy, 2007).

C-Src mediates the phosphorylation of EGFR, thereby promoting tumour progression (Tice et al., 1999). The ultimate cellular response to the activation of EGFR signalling cascade via MAPK pathway is DNA synthesis and cell division (Halatsch et al., 2004). In our samples PTPIP51 and EGFR were partly co-localized, suggesting a synergistic effect on cell proliferation, migration and oncogenic transformation. This may be exerted by sharing the same final signalling pathway, PTPIP51 via 14-3-3ß interaction with Raf-1 and EGFR activating the Ras/Raf/MAPK/ERK pathway. Compared to secondary GBM, developed by progression from lower grade gliomas, EGFR gene amplification has been shown to be five times higher in primary glioblastoma, which leads to overexpression in 40% of GBM (Karpel-Massler et al., 2009). Besides this EGFR overexpression, EGFR is expressed as the mutated EGFRvIII (epidermal growth factor receptor variant III) form of the receptor in 20% of GBM cases (Jutten et al., 2009). This constitutively active mutant form of the EGFR, which is commonly expressed in glioblastoma, is also detected in a number of epithelial cancers (Yoshimoto et al., 2008; Hama et al., 2009) also known to express high concentrations of PTPIP51, e.g. non melanoma skin cancer, prostate cancer (Koch et al., 2008; 2009b) and breast cancer. EGFR signalling cascade via MAPK pathway is modulated by PTP1B through c-Src and by 14-3-3ß through Raf-1 (Yu et al., 2008), both interaction partners of PTPIP51. This *in situ* interaction in GBM was substantiated in our study by duolink proximity ligation assay (Gajadhar and Guha, 2010).

Glial malignant transformation might be correlated to the status of PTPIP51 gene promotor methylation, since high grade gliomas (GBM) also presented a higher mRNA expression of PTPIP51 in comparison to low grade gliomas (grade II astrocytoma).

To sum up, in neuroepithelial tumours, PTPIP51 expression increases with the grade of malignancy and PTPIP51 interacts *in situ* with 14-3-3ß and PTP1B. The data presented in this study suggest an important role of PTPIP51 in glioblastoma formation.

Acknowledgements We are grateful to Mrs. K. Michael (Institute of Anatomy and Cell Biology, Giessen) for help with the design of the figures and to Mrs. A. Peters (Department of Neurosurgery, Giessen) for help in providing the glioblastoma samples. The excellent techncial assistance of Mrs. A. Erkel, Mrs. B. Fröhlich (Department of Urology and Pediatric Urology, Giessen), Mrs. A. zur Mühlen (Institute of Neuropathology, Bonn) and Mrs. C. Tag (Institute of Anatomy and Cell Biology, Giessen) is gratefully acknowledged.

References

Akasaki Y., Liu G., Matundan H.H., Ng H., Yuan X., Zeng Z., Black K.L. and Yu J.S. (2006). A peroxisome proliferator-activated receptor-gamma agonist, troglitazone, facilitates caspase-8 and -9 activities by increasing the enzymatic activity of protein-tyrosine phosphatase-1B on human glioma cells. J. Biol. Chem. 281, 6165-6174.

Arias-Romero L.E., Saha S., Villamar-Cruz O., Yip S.C., Ethier S.P., Zhang Z.Y. and Chernoff J. (2009). Activation of Src by protein tyrosine phosphatase 1B is required for ErbB2 transformation of human breast epithelial cells. Cancer Res. 69, 4582-4588.

Cao L., Cao W., Zhang W., Lin H., Yang X., Zhen H., Cheng J., Dong W., Huo J. and Zhang X. (2008). Identification of 14-3-3 protein isoforms in human astrocytoma by immunohistochemistry. Neurosci. Lett. 432, 94-99.

Cao W., Yang X., Zhou J., Teng Z., Cao L., Zhang X. and Fei Z. (2010). Targeting 14-3-3 protein, difopein induces apoptosis of human glioma cells and suppresses tumor growth in mice. Apoptosis 15, 230-241.

Dubé N. and Tremblay M.L. (2004). Beyond the metabolic function of PTP1B. Cell Cycle. 3, 550-553.

Dubé N., Cheng A. and Tremblay M.L. (2004). The role of protein tyrosine phosphatase 1B in Ras signalling. Proc. Nat. Acad. Sci. USA 101, 1834-1839.

Ewing R.M., Chu P., Elisma F., Li H., Taylor P., Climie S., McBroom-Cerajewski L., Robinson M.D., O'Connor L., Li M., Taylor R., Dharsee M., Ho Y., Heilbut A., Moore L., Zhang S., Ornatsky O., Bukhman Y.V., Ethier M., Sheng Y., Vasilescu J., Abu-Farha M., Lambert J.P., Duewel H.S., Stewart I.I., Kuehl B., Hogue K., Colwill K., Gladwish K., Muskat B., Kinach R., Adams S.L., Moran M.F., Morin G.B., Topaloglou T. and Figeys D. (2007). Large-scale mapping of human protein-protein interactions by mass spectrometry. Mol. Syst. Biol. 3, 89.

Gajadhar A. and Guha A. (2010). A proximity ligation assay using transiently transfected, epitope-tagged proteins: application for *in*

situ detection of dimerized receptor tyrosine kinases. Biotechniques. 48, 145-152

Halatsch M.E., Gehrke E.E., Vougioukas V.I., Bötefür I.C., A-Borhani F., Efferth T., Gebhart E., Domhof S., Schmidt U. and Buchfelder M. (2004). Inverse correlation of epidermal growth factor receptor messenger RNA induction and suppression of anchorage-independent growth by OSI-774, an epidermal growth factor receptor tyrosine kinase inhibitor, in glioblastoma multiforme cell lines. J. Neurosurg. 100, 523-533.

Hama T., Yuza Y., Saito Y., Ouchi J., Kondo S., Okabe M., Yamada H., Kato T., Moriyama H., Kurihara S. and Urashima M. (2009). Prognostic significance of epidermal growth factor receptor phosphorylation and mutation in head and neck squamous cell carcinoma. Oncologist 14, 900-908.

Jin J., Smith F.D., Stark C., Wells C.D., Fawcett J.P., Kulkarni S., Metalnikov P., O'Donnell P., Taylor P., Taylor L., Zougman A., Woodgett J.R., Langeberg L.K., Scott J.D. and Pawson T. (2004). Proteomic, functional, and domain-based analysis of *in vivo* 14-3-3 binding proteins involved in cytoskeletal regulation and cellular organization. Curr. Biol. 14, 1436-1450.

Jutten B., Dubois L., Li Y., Aerts H., Wouters B.G., Lambin P., Theys J. and Lammering G. (2009) Binding of cetuximab to the EGFRvIII deletion mutant and its biological consequences in malignant glioma cells. Radiother. Oncol. 92, 393-398.

Karpel-Massler G., Schmidt U., Unterberg A. and Halatsch M.E. (2009). Therapeutic inhibition of the epidermal growth factor receptor in high-grade gliomas: where do we stand? Mol. Cancer. Res. 7, 1000-1012.

Khan M.K., Hunter G.K., Vogelbaum M., Suh J.H. and Chao S.T. (2009). Evidence-based adjuvant therapy for gliomas: current concepts and newer developments. Indian J. Cancer 46, 96-107.

Koch P., Stenzinger A., Viard M., Märker D., Mayser P., Nilles M., Schreiner D., Steger K. and Wimmer M. (2008). The novel protein PTPIP51 is expressed in human keratinocyte carcinomas and their surrounding stroma. J. Cell. Mol. Med. 12, 2083-2095.

Koch P., Viard M., Stenzinger A., Brobeil A., Tag C., Steger K. and Wimmer M. (2009a). Expression profile of PTPIP51 in mouse brain. J. Comp. Neurol. 517, 892-905.

Koch P., Petri M., Paradowska A., Stenzinger A., Sturm K., Steger K. and Wimmer M. (2009b). PTPIP51 mRNA and protein expression in tissue microarrays and promoter methylation of benign prostate hyperplasia and prostate carcinoma. Prostate 69, 1751-1762.

Lopez-Gines C., Gil-Benso R., Benito R., Mata M., Pereda J., Sastre J., Roldan P., Gonzalez-Darder J. and Cerdá-Nicolás M. (2008). The activation of ERK1/2 MAP kinases in glioblastoma pathobiology and its relationship with EGFR amplification. Neuropathology 28, 507-515.

Lv B.E., Yu C.E., Chen Y.Y., Lu Y., Guo J.H., Song Q.S., Ma D.L., Shi T.P. and Wang L. (2006). Protein tyrosine phophatase interacting interacting protein 51 (PTPIP51) is a novel mitochondria protein with an N-terminal mitochondrial targeting sequence and induces apoptosis. Apoptosis 11, 1489-1501.

McLendon R.E., Turner K., Perkinson K. and Rich J. (2007). Second messenger systems in human gliomas. Arch. Pathol. Lab. Med. 131, 1585-1590.

Reichardt W., Jung V., Brunner C., Klein A., Wemmert S., Romeike B.F., Zang K.D. and Urbschat S. (2003). The putative serine/threonine kinase gene STK15 on chromosome 20q13.2 is amplified in human gliomas. Oncol. Rep. 10, 1275-1279.

Stenzinger A., Kajosch T., Tag C., Porsche A., Welte I., Hofer H.W., Steger K. and Wimmer M. (2005). The novel protein PTPIP51 exhibits tissue- and cell-specific expression. Histochem. Cell. Biol. 123, 19-28.

Stenzinger A., Schreiner D., Koch P., Hofer H.W. and Wimmer M. (2009). Cell- and molecular biology of the novel protein tyrosine phosphatase interacting protein 51. Int. Rev. Cell. Mol. Biol. 275, 183-246.

Tice D.A., Biscardi J.S., Nickles A.L. and Parsons S.J. (1999). Mechanism of biological synergy between cellular Src and epidermal growth factor receptor. Proc. Nat. Acad. Sci. USA 96, 1415-1420.

Tonks N.K. and Muthuswamy S.K. (2007). A brake becomes an accelerator: PTP1B - a new therapeutic target for breast cancer. Cancer Cell 11, 214-216.

Yang X., Cao W., Lin H., Zhang W., Lin W., Cao L., Zhen H., Huo J. and Zhang X. (2009). Isoform-specific expression of 14-3-3 proteins in human astrocytoma. J. Neurol. Sci. 276, 54-59.

Yoshimoto K., Dang J., Zhu S., Nathanson D., Huang T., Dumont R., Seligson D.B., Yong W.H., Xiong Z., Rao N., Winther H., Chakravarti A., Bigner D.D., Mellinghoff I.K., Horvath S., Cavenee W.K., Cloughesy T.F. and Mischel P.S. (2008). Development of a real-time RT-PCR assay for detecting EGFRvIII in glioblastoma samples. Clin. Cancer Res. 14, 488-493.

Yu C., Han W., Shi T., Lv B., He Q., Zhang Y., Li T., Zhang Y., Song Q., Wang L. and Ma D. (2008). PTPIP51, a novel 14-3-3 binding protein, regulates cell morphology and motility via Raf-ERK pathway. Cell. Signal. 20, 2208-2220.

Zhao Y., Xiao A., Dipierro C.G., Abdel-Fattah R., Amos S., Redpath G.T., Carpenter J.E., Pieper R.O. and Hussaini, I.M. (2008). H-Ras increases urokinase expression and cell invasion in genetically modified human astrocytes through Ras/Raf/MEK signalling pathway. Glia 56, 917-924.

Accepted June 15, 2011

J Neurooncol (2015) 123:15–25
DOI 10.1007/s11060-015-1763-8

LABORATORY INVESTIGATION

PTPIP51 levels in glioblastoma cells depend on inhibition of the EGF-receptor

M. K. Petri[1] · A. Brobeil[2] · J. Planz[1] · A. Bräuninger[2] · S. Gattenlöhner[2] · U. Nestler[3] · A. Stenzinger[4] · A. Paradowska[5] · M. Wimmer[1]

Received: 5 February 2014 / Accepted: 1 April 2015 / Published online: 11 April 2015

Abstract Protein tyrosine phosphatase interacting protein 51 (PTPIP51) is upregulated in glioblastoma multiforme (GBM) and expression levels correlate with the grade of malignancy in gliomas. A similar correlation was reported for its interacting partner 14-3-3β, which has been shown to facilitate the interaction of PTPIP51 with cRAF (Raf1). Since the interaction of these signalling partners stimulates growth factor signalling downstream of the epidermal growth factor receptor (EGFR), a major drug target in GBM, we here investigated the impact of EGFR inhibition by small molecule inhibitors or monoclonal antibody on PTPIP51. The effect of EGFR inhibition on PTPIP51 mRNA, protein expression and its interaction profile in GBM was analyzed using the U87 cell line as model system. The transferability of the results to in vivo conditions was evaluated in cultured tumour cells from GBM patients. Cells were treated either to the small molecule tyrosine kinase inhibitor of EGFR Gefitinib or the monoclonal antibody Cetuximab in a time and dose dependent manner. Gefitinib treatment decreased the proliferation rate and induced apoptosis in U87 and primary tumour cells. The PTPIP51 interaction profile changed in correlation to the applied Gefitinib. Despite unchanged mRNA levels PTPIP51 protein was reduced. In contrast, treatment with Cetuximab had no effects on PTPIP51 expression. In conclusion, our results demonstrate the impact of EGFR inhibition by Gefitinib on PTPIP51 protein expression, a downstream regulator of MAPK signalling. These data will serve as a basis to unravel the precise role of PTPIP51-mediated signalling in GBM and its potential implications for Gefitinib-mediated therapy in future studies.

Keywords PTPIP51 · 14-3-3β · Glioblastoma · EGFR · Gefitinib · Cetuximab

Introduction

Despite powerful therapy regimens comprising neurosurgery, radiation and temozolomide, Glioblastoma (GBM) is still one of the most lethal human cancers. Clinical trials using EGFR targeting agents as mono therapy did not generate promising results [1]. Current approaches are focusing on blocking the downstream EGFR-activated metabolic pathways and their key kinase alterations [1].

Amplification of the epidermal growth factor receptor gene (ERBB2) is one of the most common oncogenic alterations in GBM (45 %), which leads to overexpression of EGFR [2, 3]. Almost half of these cases co-express the mutant receptor subtype EGFRvIII. This EGFR variant is constitutively activated, and thereby may contribute to the aggressive and refractory course of GBM, which is

Electronic supplementary material The online version of this article (doi:10.1007/s11060-015-1763-8) contains supplementary material, which is available to authorized users.

✉ M. K. Petri
meike.petri@gmx.de

[1] Institute of Anatomy and Cell Biology, Justus-Liebig-University, 35385 Giessen, Germany

[2] Institute of Pathology, Justus-Liebig-University, Giessen, Germany

[3] Department of Neurosurgery, Justus-Liebig-University, Giessen, Germany

[4] Institute of Pathology, University Hospital Heidelberg, Heidelberg, Germany

[5] Department of Urology and Pediatric Urology, Justus-Liebig-University, Giessen, Germany

associated with a median survival of only 40 to 60 weeks from diagnosis [4].

Therapeutic strategies targeting EGFR rely either on tyrosine kinase inhibitors such as Gefitinib or on monoclonal antibodies, e.g. Cetuximab. Thus, EGFR inhibition can be achieved by two different strategies: either preventing ligand binding to the receptor or by directly blocking the activity of the EGFR tyrosine kinase [5]. Cetuximab is a monoclonal antibody that targets the extracellular domain of EGFR thereby preventing the interaction with adequate ligands, and in turn intracellular EGFR signalling. Besides, its direct effect on the MAPK pathway, Cetuximab stimulates the internalization and degradation of EGFR [5].

The small molecule inhibitor Gefitinib selectively inhibits tyrosine kinase activity of EGFR by binding to its ATP-binding site and is currently approved as first line therapy in patients with non-small-cell lung cancer harboring activating epidermal growth factor receptor mutation [6]. The efficacy of Gefitinib-mediated EGFR-inhibition in GBM is being evaluated in a clinical phase II trial [7–9].

However, despite the fact that Gefitinib reaches high concentrations in the tumour tissue, it does not seem to be sufficient to entirely shut down MAPK pathway activity [10].

Clinical trials using EGFR inhibitors demonstrated only modest improvements in a small percentage of GBM patients, suggesting that many GBMs possess primary intrinsic resistance mechanisms or rapidly acquire secondary resistance to EGFR inhibition [11, 12].

Recently, we reported the expression of protein tyrosine phosphatase interacting protein 51 (PTPIP51) in gliomas and showed PTPIP51 expression levels to correlate with the grade of tumour malignancy [2]. Interestingly, a similar correlation was observed for its interacting partner 14-3-3β [13, 14]. This direct interaction of PTPIP51 and 14-3-3 proteins was demonstrated in glioblastoma [2]. On the molecular level, the interaction of PTPIP51 and 14-3-3β leads to a ternary complex with cRAF (Raf1), which in turn stimulates the downstream signalling of the EGFR/MAPK signalling-pathway [15]. PTPIP51 interaction is regulated by its Tyr176 phosphorylation in vitro and in situ at by Src kinase and by its dephosphorylation through PTP1B [16]. Interestingly, both, the PTPIP51/14-3-3β and 14-3-3β/Raf1 interactions are inversely correlated with the PTPIP51 phosphorylation level [17]. Besides 14-3-3 mediated effect of PTPIP51 on Raf1, PTPIP51 can directly interact with EGFR [17, 18]. Taken together, these findings suggest a functional role of PTPIP51 in the tumourigenesis of gliomas and glioblastomas in particular.

Since PTPIP51 is an important positive regulator of EGFR downstream signalling at different levels, which may contribute to mechanisms impairing the efficacy of therapeutic EGFR interference, we investigated the effect of EGFR inhibition on PTPIP51 expression levels in U87 cells and primary GBM cell lines.

Materials and methods

Cell culture

The human glioblastoma cell line U87 (American Type Culture Collection) and cell cultures from five GBM patients were kindly provided by the Neurosurgical-Neurooncologic Laboratory, Justus-Liebig-University, Giessen, Germany. The patients had given informed consent for research use of the surplus material not used for pathology. The material was obtained during neurosurgery and the cells were washed in a solution of trypsin/medium 1:1 for 1 h and plated into cell culture vials. They were cultivated in DMEM High Glucose 4,5 g/l medium with 2-mmol/L glutamine supplemented with 10 % FCS and 1 x 10^5 IU/L penicillin, 100 mg/l streptomycin until reaching a logarithmic growth phase (less than three passages). Culture conditions were humidified 5 % CO_2 atmosphere and a temperature of 37 °C. When reaching near confluency the cells were harvested by adding 5 ml trypsin and 5 ml PBS (Dulbecco) and subsequently counted. Then the cells were resuspended in medium into flasks and part of them were seeded into 24-microwellplates for the evaluation of the metabolic rate by the Alamar Blue test (AbD Serotec, BUF012B, UK). Part of the cells were seeded on culture slides to perform immunofluorescence analyzis after the experiments.

Inhibitors

All inhibitors were dissolved as stock solution in DMSO. Prior to use they were diluted in DMEM. DMSO treated cells were used as controls.

Gefitinib (#PKI-GFTB2-200, Biaffin, Kassel, Germany) was applied in three different inhibitor concentrations 0.1, 1, 5 μM and for four different time periods (36, 48, 72, 96 h). The effects of the concentration gradient (0.1, 1, 2, 3, 4, 5 μM) of Gefitinib were analyzed after 24 h of inhibitor treatment by quantitative real time PCR.

Cetuximab (Erbitux®, Merck) interacts exclusively with domain III of soluble extracellular region of EGFR (S Li, 2005). It was applied in three different concentrations 2.5, 5, 10 μg/ml and for four different time periods (36, 48, 72, 96 h).

Erlotinib (LC Laboratories #E-4997) is a selective inhibitor of the tyrosine kinase domain of EGFR. It was applied to glioblastoma cells in different concentrations (0.1, 1, 10, 20 μM) for 24 h as well as 96 h.

Metabolic rate evaluation

The Alamar Blue test (AbD Serotec, BUF012B, UK) was performed in 24-well-plates. The test was applied to 20000, 10000, 5000 and 2500 cells, respectively. Alamar blue is a nontoxic substrate for living cells giving a linear relationship between the reduction of the blue substrate to a pink product and the level of cell metabolism. After an incubation of 36, 48, 72 and 96 h the remaining unmetabolized blue substrate was determined photometrically by its absorption at 630 nm. Higher absorption values corresponded to a reduced metabolic activity indicating cell death. The metabolic rate was calculated and was correlated to the internal standard (10,000 cells). The values were corrected by subtracting the absorption of the negative control. Tests with U87 cells for every inhibitor concentration for every treatment time were repeated five times ($n = 5$). Hamid et al. reported the Alamar blue test to be a more sensitive proliferation assay than the well known MTT test [19].

Immunohistochemistry

The polyclonal antibody against PTPIP51 was raised as described and characterized in previous studies [10, 13]. The specificity of the PTPIP51 antibody was tested by ELISA and by immunoblotting of the isolated purified recombinant protein staining bands with 52, 34, and 30 kDa. Immunoblotting of homogenates from porcine spleen tissue revealed bands of 48, 40, and 29 kDa. The antibody binds to the EGFP fusion PTPIP51 protein expressed in HEK293. Preabsorbing the PTPIP51 antibody against its antigen completely abolished the immune reaction in all tested samples [15]. Double–immunostainings were performed according to a standard protocol. After fixation with methanol for 2 min the slides were washed with phosphate buffered saline (PBS, pH 7.4). The nonspecific binding sites were blocked with 5 % bovine serum albumin and 5 % normal goat serum in PBS. Incubation with the primary antibodies (PTPIP51 = rabbit polyclonal, 1:400 dilution, generated by Prof. H W Hofer, Biochemical Department, University Konstanz, Germany; 14-3-3β = mouse monoclonal, 1:100 dilution, from Santa Cruz, Cat #sc-25276) was performed overnight at room temperature, followed by the incubation for 1 h with the appropriate secondary antibodies (Alexa fluor 488 coupled to anti-mouse antibody, Invitrogen Cat #A11029 and Alexa fluor 555 coupled to anti-rabbit antibody, Invitrogen Cat #A21428) at room temperature. Subsequently the slides were coverslipped in carbonate buffered glycerol (pH 8.6). Nuclei were visualized by DAPI. For each staining series appropriate controls were performed. The results were visualized using an excitation filter of 530 - 560 nm wave length (Alexa fluor 555) and an emission filter with a range 572.5–647 nm wavelength. Alexa fluor 488 was visualized by an excitation filter with 460–500 nm wave length and an emission filter 512–542 nm wavelength. Immunofluorescence analysis and photo-documentation was performed with an Axioplan 2 fluorescence microscope equipped with Plan-Apochromat objectives (Carl Zeiss Jena, Germany).

Quantitative real time PCR

Cells were harvested by trypsination and transferred into RNA later (Qiagen) for storage at −20 °C. cDNA amplification was performed in 25 µl reaction volume on the iCycler iQ Real-Time PCR Detection System (Bio Rad, Munich, Germany). Primers were chosen as described previously [2]. The final reaction tube contained 100nM as PTPIP51, 14-3-3β and reference genes β-actin and GAPDH, 12.5 µl iQ SYBR Green Supermix (Bio Rad) and 2 µl of DNA template. The PCR conditions were 94 °C for 3 min followed by 40 cycles for 30 s, 60 °C for 30 s and 72 °C for 1 min. Melting curves were generated for both genes after amplification. Negative controls were included in each run. The appropriate combinations of reference genes for the expression analysis of PTPIP51 and 14-3-3β in U87 and primary GBM cells, were selected by the NormFinder Program.

Statistical analyses: In U87 cells the examination of every inhibitor concentration at every treatment time was repeated five times ($n = 5$). The values were subsequently analyzed by GraphPad Software (San Diego, California) version 6.00 using the Dunnett's multiple comparison test. Results were considered as significant with $p < 0.05$.

Analysis of the EGFR status

U87 Cells and the five primary cell cultures were analyzed for mutations in EGFR (exons 1, 8 and 18–21) by Sanger sequencing. Extraction of genomic DNA was performed by proteinase K digestion using a fully automated purification system (QIASymphony SP; Qiagen, Hilden, Germany). DNA content was measured using a spectrophotometer (NanoDrop; Thermo Scientific, Wilmington, DE, USA). For PCR amplification the following primers were used. EGFR: 5′-agcgctcctggcgctgc-3′ (exon 1), 5′-acttgcggacgccgtcttcc-3′ (exon 8), 5′-gctgaggtgacccttgtctc-3′ (exon 18 forward), 5′-acagcttgcaaggactctgg-3′ (exon 18 reverse); 5′-gctggtaa catccacccaga-3′ (exon 19 forward), 5′-gagaaaaggtgggcct gag-3′ (exon 19 reverse); 5′-catgtgcccctccttctg-3′ (exon 20 forward), 5′-gatcctggctccttatctcc-3′ (exon 20 reverse); 5′- cagagcttcttcccatgatga-3′ (exon 21 forward), 5′-cctggt gtcaggaaaatgct-3′ (exon 21 reverse). Direct sequencing of the PCR amplicons was performed for both strands on a 3500 Genetic Analyzer using the BigDye Terminator v1.1 Cycle Sequencing Kit (both Applied Biosystems, Life Technologies, Carlsbad, CA, USA).

Immunoblotting

Immunoblot samples of GBM cell lysates were separated on a NuPAGENovex 4–12 % Bis–Tris Gel (Life Technologies GmbH, Darmstadt, Germany Cat #NP0329BOX). Transfer on an Immobilon P membrane (Millipore, Billerica, USA, Cat #IPVH07850) was performed according to Towbin et al. [20]. The membrane was blocked with 1 × Rotiblock for 1 h at room temperature. Incubation with monoclonal rabbit anti-Phospho-p44/42 MAPK (Erk1/2) (Thr202/Tyr204) (D13.14.4E) XP® (Cell Signalling #4370), monoclonal rabbit anti-total p44/42 MAPK (Erk1/2) (137F5) (Cell Signalling Cat #4695), polyclonal rabbit anti-PTPIP51 (Prof. HW Hofer, Biochemical, Department, University Konstanz, Germany), polyclonal guinea pig anti-phosphoTyr176-PTPIP51 (BioLux, Stuttgart, Germany) and anti-beta actin (Cell Signalling Cat #4967) was done overnight at 4 °C. HRP-conjugated anti-guinea pig or HRP-conjugated anti-rabbit immunoglobulins were applied for 1 h at room temperature diluted in 1 × Rotiblock. The reaction was visualized with the ECL prime substrate. For documentation an Amersham Hyperfilm ECL (GE Healthcare Lifescience, Freiburg, Germany, Cat #28-9068-36) was used. Calibration was performed with a molecular weight marker suitable for chemiluminescence (Life Technologies GmbH, Darmstadt, Germany, Cat #LC5602).

Duolink II proximity ligation assay (DPLA)

The downstream effects on the in situ interactions were detected by the proximity ligation assay kit Duolink II (Olink Bioscience, Uppsala, Sweden; PLA probe anti-rabbit minus, Cat #92005-0100; PLA probe anti-mouse plus, Cat #92001-0100; Detection Kit Orange, Cat #92007-0100). The DPLA probe anti-rabbit minus binds to the PTPIP51 antibody, whereas the PLA probe anti-mouse plus binds to the antibody of 14-3-3β, pErk, Raf1 and PTP1B. The DPLA secondary antibodies only generate a signal when the two DPLA probes have bound, which only takes place if both the proteins are closer than 40 nm, indicating their interaction. PFA-fixed U87 cells were preincubated with blocking agent for 1 h. After washing in PBS for 10 min, primary PTPIP51 antibody (1:1000) was applied to the samples. Primary antibodies of the interacting partners were used for proving the interaction by co-incubation with the PTPIP51 antibody. Incubation was done overnight in a preheated humidity chamber. Culture slides were washed three times in PBS for 10 min. DPLA probes detecting rabbit or mouse antibodies were diluted in the blocking agent in a concentration of 1:5 and applied to the slides followed by incubation for 1 h in a preheated humidity chamber at 37 °C. Unbound DPLA probes were removed by washing twice in PBS for 5 min. The samples were incubated with the ligation solution consisting of Duolink II ligation stock (1:5) and Duolink ligase (1:40) diluted in high purity water for 30 min at 37 °C. After ligation, the Duolink amplification and detection stock, diluted 1:5 with addition of polymerase (1:80), was applied to the slides for 100 min. Dapi was used to identify the nuclei. After the final washing steps, the slides were dried and cover slips were applied.Quantification was done with the Duolink Image Tool (Olink Bioscience, Uppsala, Sweden, v1.0.1.2). The signal threshold was adjusted to 135 and pixel size for spot detection to five pixels for each picture. The quantified DPLA spots were calculated per cell (number of dots/cell) for each picture.

Statistical analyses: The quantified DPLA spots were calculated per cell (number of dots/cell) for each picture. The results were standardized to the number of interactions/100 cells. The values were subsequently analyzed by GraphPad Software (San Diego, California) version 6.00 using the Dunnett's multiple comparison test. Results were considered as significant with $p < 0.05$.

Results

Cellular vitality under Cetuximab treatment

Treatment of U87 cells either with 2.5, 5 or 10 μg/ml Cetuximab for 36 h had no effect on the number of cells compared to the controls. 48 h of treatment with 2.5, 5 or 10 μg/ml Cetuximab did not change the number of cells compared to controls. Application of 2.5, 5 or 10 μg/ml Cetuximab for either for 72 or 96 h had no effect on the number of cells compared to controls (Fig. 1a). The same hold true for all primary cell cultures (Supplement A1 A).

Cellular vitality under Gefitinib treatment

Treatment of U87 cells either with 0.1, 1 and 5 μM Gefitinib for 36 h reduced the cell number in a concentration dependent manner (Fig. 1b). For each concentration these reductions in cell number were statistically significant in comparison to the control. 48 h of treatment with 0.1, 1 and 5 μM Gefitinib significantly reduced the number of cells in a concentration dependent manner compared to controls. Application of 0.1, 1 and 5 μM Gefitinib either for 72 or 96 h had the same statistically significant concentration dependent effect on the number of cells compared to controls. Treatment with 5 μM Gefitinib resulted in an almost complete reduction of viable cells at every time of incubation (Fig. 1b). The same hold true for all primary cell cultures (Supplement A1 B).

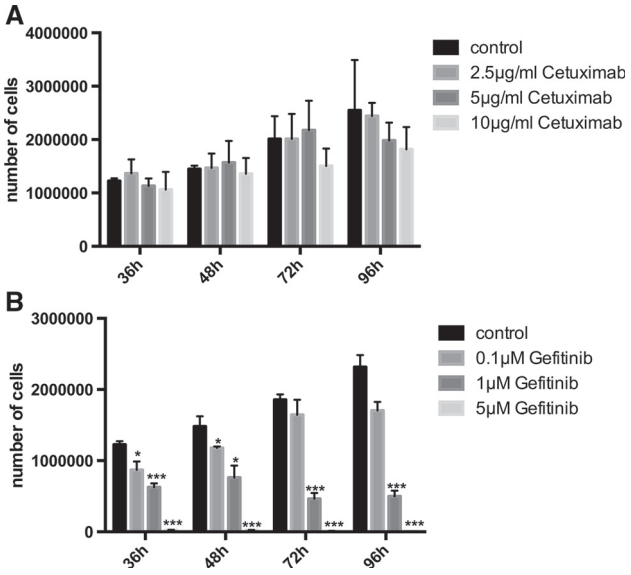

Fig. 1 Cell proliferation. **a** Cetuximab: Number of cells after 36, 48, 72 and 96 h after adding Cetuximab in following concentrations: IC1 (2,5 µg/ml), IC2 (5 µg/ml) and IC3 (10 µg/ml). Every group started with 500,000 cells. Application of the monoclonal antibody to EGFR Cetuximab did not lead to a reduction in cell numbers independent of the applied concentration or incubation time in the five probed primary cultures. Only in U87 (N = 5) there was a slight decrease of inhibited cells compared to the reference group after 96 h (Fig. 2b). **b** Gefitinib: Number of cells after 36, 48, 72 and 96 h after adding Gefitinb. Every group started with 500,000 cells. The not inhibited reference group reached a higher amount of cell number than the others at every time. The number of treated cells was negatively correlated to the applied inhibitor concentration for 0.1 and 1 µM being the result of a reduced proliferation rate compared to the reference group. Application of 5 µM Gefitinib led to a decreased number of cells, which cannot be explained by complete inhibited proliferation alone. Values were analyzed by using the Dunnett's multiple comparison test. *$p < 0.05$, **$p < 0.01$ and ***$p < 0.001$

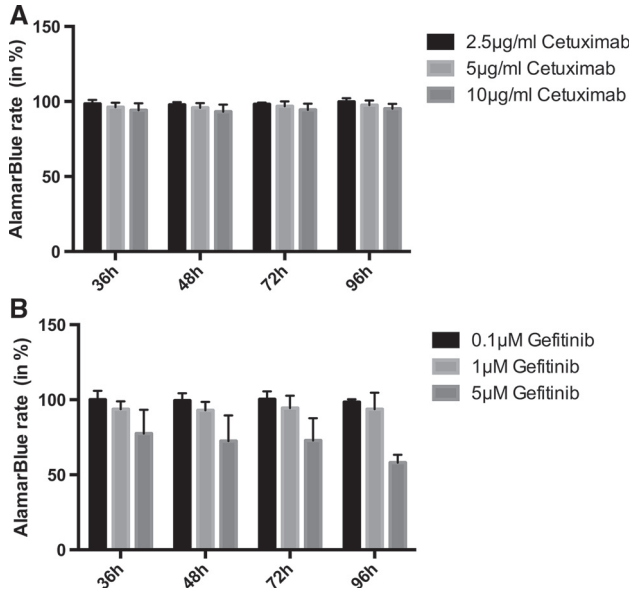

Fig. 2 Cell metabolism. **b** Gefitinib: Metabolic rates were reduced in a dose dependent manner by the application of 1 (IC2) and 5 µM (IC3) Gefitinib. Concentration of 0.1 µM (IC1) Gefitinib had no effect on the metabolic rate. Only the IC3 group displayed a time dependent decrease in the metabolic rate. **a** Cetuximab: Inhibtion with IC1 (2.5 µg/ml), IC2 (5 µg/ml) and IC3 (10 µg/ml) Cetuximab led to a marginal reduction in the metabolic rate in a dose dependent matter. This reduction was independent from the application time. Control values represent 100 %

Cellular metabolism under Cetuximab treatment

Treating U87 cells with 2.5, 5 or 10 µg/ml Cetuximab for 36 h had no significant effect on cellular metabolism compared to controls as tested by Alamarblue. This indicates high normal cell vitality as seen in Fig. 2a. Control values correspond to 100 %. The values of treated cells are given in percent of the control value (Fig. 2a). Prolonging the incubation time to 48, 72 or 96 h had no significant effect on cell viability neither under the influence of 2.5, 5 or 10 µg/ml Cetuximab in relation to the controls.

Cellular metabolism under Gefitinib treatment

As tested by Almarblue, treating U87 cells with 0.1, 1 and 5 µM Gefitinib for 36 h reduced cellular metabolism in a strictly concentration dependent manner in relation to controls. This indicates a reduced cell vitality as seen in Fig. 2b. Control values correspond to 100 %. The values of treated cells are given in percent of the control value. Prolonging the incubation time to 48 and 72 h also let to a concentration dependent reduction of cell vitality the magnitude of which was the same as seen after 36 h. Incubating the cells for 96 h with 0.1, 1 and 5 µM Gefitinib reduced cell viability in a concentration dependent manner. The reduction of cell vitality after 96 h incubation with the 5 µM Gefitinib was significant.

Protein expression

Immunofluorescence assays of PTPIP51 and 14-3-3β protein in U87 cells (Fig. 3) displayed high levels of both proteins in the control group. High concentrations of PTPIP51 were seen perinuclear area and granules of the protein at the cell membrane (Fig. 3a). 14-3-3β displayed an evenly cytoplasmic distribution (Fig. 3b). Both proteins were partially colocalized (Fig. 3c).

Treatment with 10 µg/ml Cetuximab for 72 h did not alter the PTPIP51 and 14-3-3β protein expression (Fig. 3d, e) compared to control cells (Fig. 3a, b). The subcellular distribution of both proteins remained the same. A partial cololalization of both proteins was displayed in Cetuximab treated cells comparable to the controls (Fig. 3f).

Application of 5 µM Gefitinib for 72 h resulted in a pronounced reduction of PTPIP51 as well as 14-3-3β

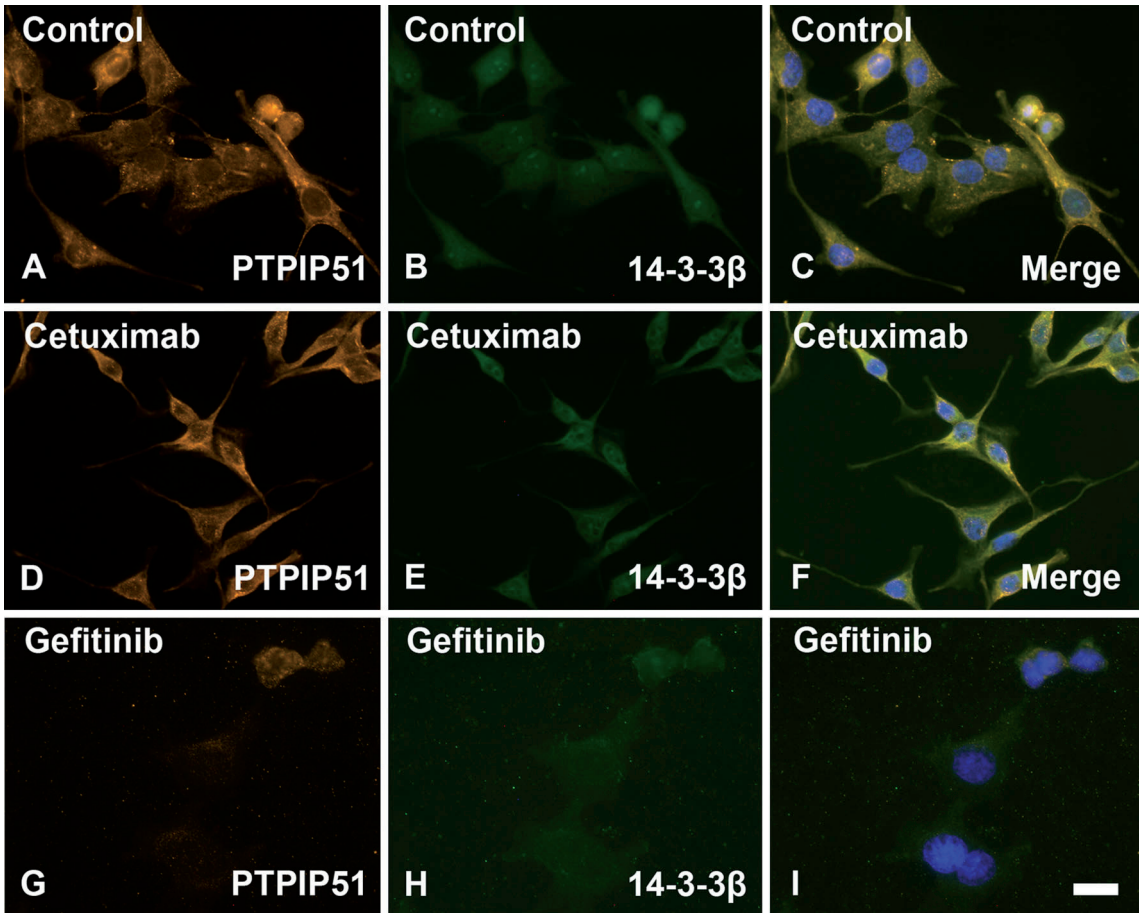

Fig. 3 Double immunostaining of protein expression. Staining of PTPIP51 and 14-3-3β in U87 cells. Untreated tumour cells (control) show high concentrations of PTPIP51 (**a**) and 14-3-3β (**b**) which are colocalized as shown in the merge picture (**c**) and highly expressed in the cytoplasm of tumour cells. In contrast to the control (**a**–**c**) and the Cetuximab treated cells (**d**–**f**), Gefitinib treated cells had lower levels of PTPIP51 (**g**) and 14-3-3β (**h**). The nuclei are additional shown by DAPI in the merged photographies (**c**, **f**, **i**). In **i** is a less number of cells compared to **c** and **f**, which was already explored by the proliferation rates. Treating U87 cells with Cetuximab did not alter the PTPIP51 expression pattern compared to untreated cells (**g**, **h**). *Bar* = 20 μm

protein (Fig. 3g, h). PTPIP51 changed its subcellular distribution to a highly granulated form. The same applied to 14-3-3β protein. Three out of five cells in the Fig. 3g, h revealed limited or even nonexistent of PTPIP51 and 14-3-3β. As shown in the merge (Fig. 3i) the remaining proteins are partial colocalized. The nuclei of the Gefitinib treated cells reveal signs of fragmentation as indication for apoptosis (Fig. 3i).

Quantitative mRNA of PTPIP51 and 14-3-3 under Cetuximab treatment

Submitting U87 cells to increasing concentrations of Cetuximab (2.5, 5, 10 μg/ml) for 24 h did neither change PTPIP51 expression nor 14-3-3 expression (Fig. 4a) compared to the expression of the expression seen for controls (Fig. 4a). Prolongation of the incubation time to 48, 72 or 96 h had no effect on the mRNA expression (Fig. 4a) of PTIP51 and 14-3-3 protein. As seen in cells treated for 24 h increasing Cetuximab concentrations from 2.5 to 5 μg/ml or 10 μg/ml also did not influence the mRNA levels of PTPIP51 and 14-3-3 protein (Fig. 4a).

Quantitative mRNA of PTPIP51 and 14-3-3 under Gefitinib treatment

Submitting U87 cells to increasing concentrations of Gefitinib (0.1, 1 and 5 μM) for 24 h had no significant effect on PTPIP51 and 14-3-3 expression compared to the expression of PTPIP51 and 14-3-3β in control cells (Fig. 4b). Application of 0.1, 1 and 5 μM Gefitinib for 48 h to U87 cells had no significant effect on the expression of PTPIP51 and 14-3-3 mRNA levels in comparison to the mRNA levels seen in controls. Even after 72 and 96 h there were

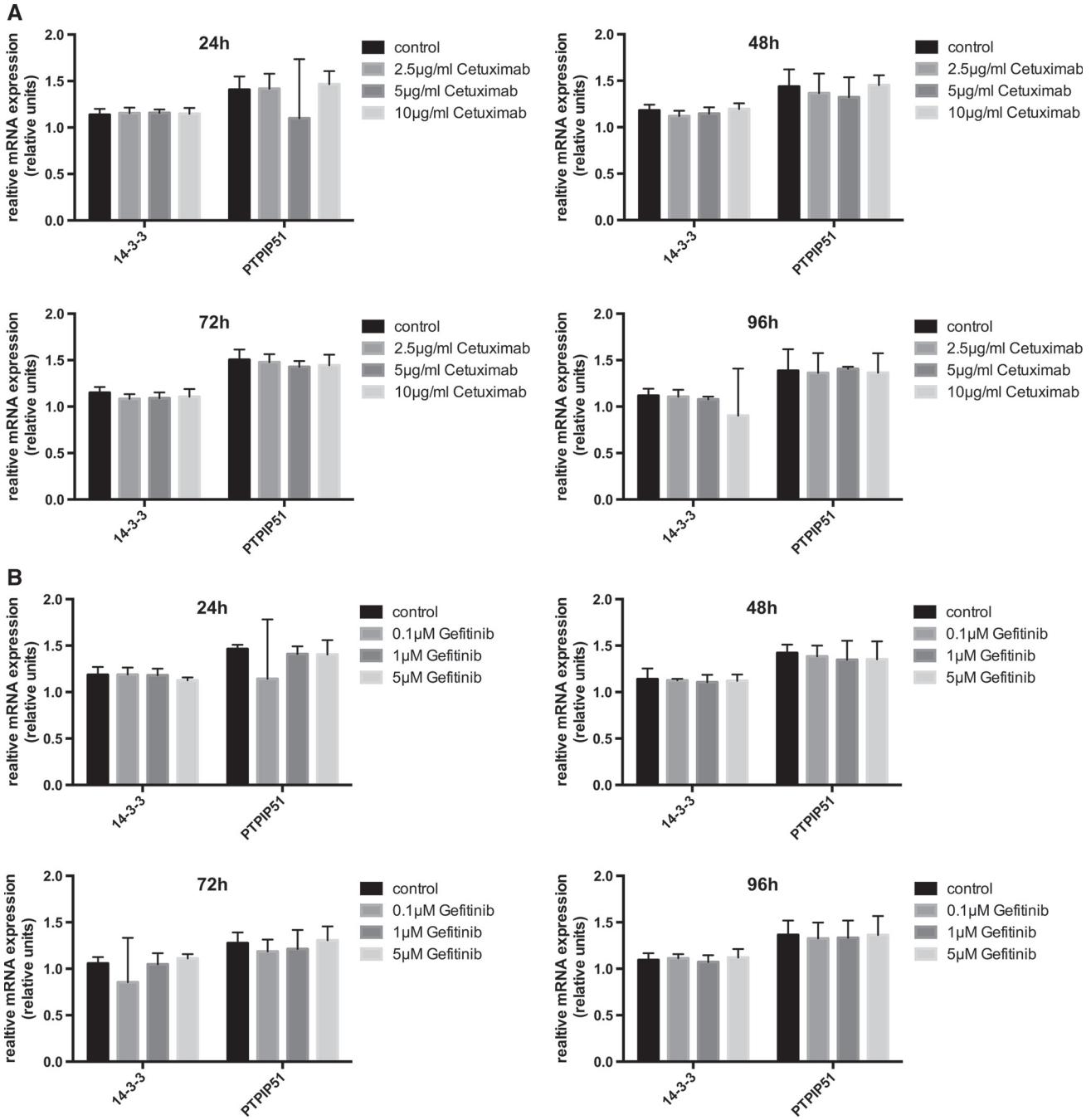

Fig. 4 Quantitative RT PCR of PTPIP51 and 14-3-3 mRNA. **a** Quantitative PCR of Cetuximab treated U87 cells: No significant differences in PTPIP51 and 14-3-3 mRNA were seen after 24 h (*upper left panel*) of treatment with 2.5, 5 and 10 µg/ml Cetuximab compared to controls. Likewise no significant differences in both proteins mRNA were detected after incubation periods of 48 h (*upper right panel*), 72 h (*lower left panel*) and 96 h (*lower right panel*). **b** Quantitative PCR of Gefitinib treated U87 cells: No significant differences in PTPIP51 and 14-3-3 mRNA were seen after 24 h (*upper left panel*) of treatment with 0.1, 1 and 5 µM Gefitinib compared to controls. Likewise no significant differences in both proteins mRNA were detected after incubation periods of 48 h (*upper right panel*), 72 h (*lower left panel*) and 96 h (*lower right panel*). Values were analyzed by using the Dunnett's multiple comparison test

no significant differences in mRNA expression levels of (Fig. 4b). Likewise, there were no significant differences of the mRNS expression levels of PTPIP51 and 14-3-3 protein compared to the values seen in controls in the primary cell cultures (Supplement A4).

Interaction profile of PTPIP51 under Gefitinib treatment

The interaction profile of PTPIP51 with selected partners was assessed by the Duolink proximity ligation assay.

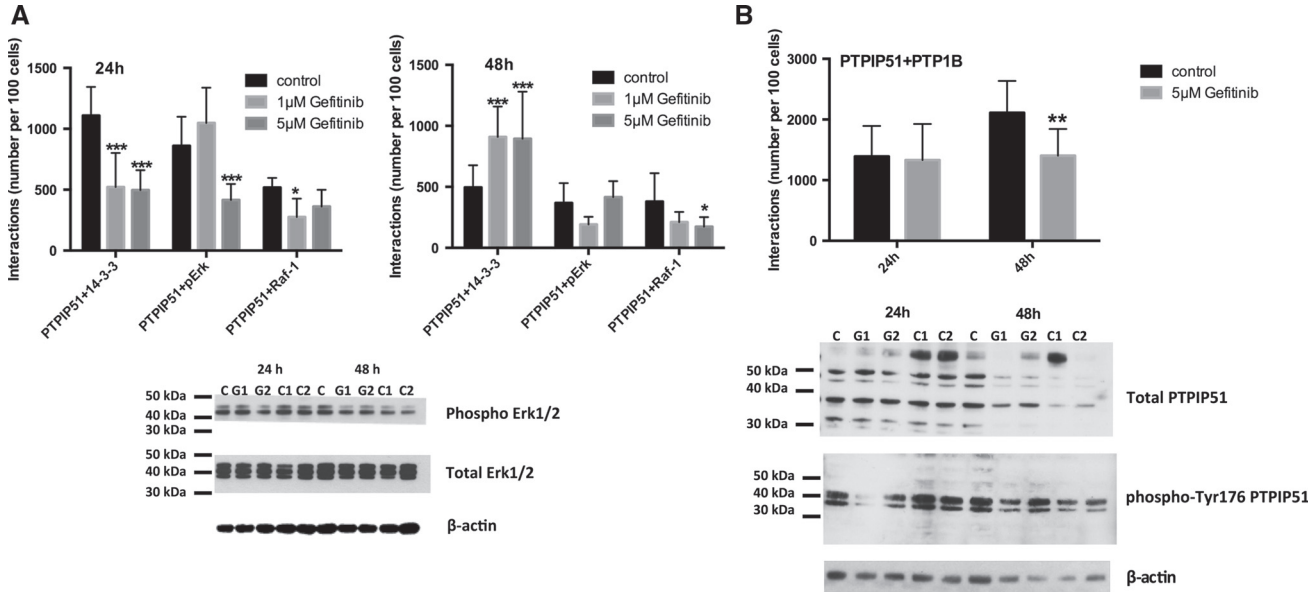

Fig. 5 Interaction profile and downstream effects. **a** Interaction profile of PTPIP51 with 14-3-3β, pErk and Raf1 in 1 and 5 μM Gefitinib treated U87 cells after 24 and 48 h of incubation. After 24 h treatment the interactions of PTPIP51 with 14-3-3β were markedly reduced in both Gefitinib concentrations (1 and 5 μM) to the same extent. After 48 h both concentrations of Gefitinib (1 and 5 μM) treatment led to an increased number of interactions of PTPIP51 with 14-3-3β compared to control. After 24 h treatment the interactions of PTPIP51 with pErk were only reduced by 5 μM Gefitinib. After 48 h only 1 μM Gefitinib negatively affected the number of interactions. After 24 h treatment the interactions of PTPIP51 with Raf1 were reduced in both Gefitinib concentrations (1 and 5 μM). After 48 h both concentrations of Gefitinib (1 and 5 μM) treatment led to a decreased number of interactions of PTPIP51 with Raf1. Immunoblot analyses of phopsphorylated Erk1/2 and total Erk1/2 in control cells (**C**) and cells treated with 1 μM Gefitinib (G1), 5 μM Gefitinib (G2), 5 μg/ml Cetuximab (C1) or 10 μg/ml Cetuximab (C2) are shown either for 24 or 48 h. The downstream effect of EGFR inhibition by 1 (G1) and 5 μM Gefitinib (G2) resulted in reduced phosphorylated Erk1/2 after 24 h as well as after 48 h. The total Erk1/2 displayed any difference in Gefitinib treated compared to the control. β-actin was used for standardization. **b** Interaction profile of PTPIP51 with PTP1B in 5 μM Gefitinib treated U87 cells after 24 and 48 h of incubation. There were no differences in the number of interactions per 100 cells between control and Gefitinib treated cells after 24 h. 48 h of Gefitinib treatment markedly reduced the interactions of PTPIP51 and PTP1B compared to control. Values were analyzed by using the Dunnett's multiple comparison test. *$p < 0.05$, **$p < 0.01$ and ***$p < 0.001$. *Upper panel*: Immunoblot analyses of total PTPIP51 in control cells (C) and in cells treated with 1 μM Gefitinib (G1), 5 μM Gefitinib (G2), 5 μg/ml Cetuximab (C1) or 10 μg/ml Cetuximab (C2) either for 24 h or 48 h. Lower panel: Immunoblot analyses of tyrosine 176 phosphorylated PTPIP51 in control cells (C) and in cells treated with 1 μM Gefitinib (G1), 5 μM Gefitinib (G2), 5 μg/ml Cetuximab (C1) or 10 μg/ml Cetuximab (C2) either for 24 or 48 h. β-actin was used for standardization

Treating U87 cells with 1 and 5 μM Gefitinib for 24 h significantly reduced the interaction with 14-3-3β protein. The number of interactions was reduced by about 50 % under either concentration (Fig. 5a). Treating U87 cells with 1 μM and 5 μM Gefitinib for 48 h significantly increased the number of interactions with 14-3-3β protein by about 87 and 84 % respectively (Fig. 5a).

The interaction with Raf1 was affected in a comparable way. One μM Gefitinib reduced the interactions by 50 % whereas 5 mM Gefitinib reduced the number of interactions by about 40 % after 24 h of incubation. After 48 h the number of interactions with Raf1 was reduced by 50 and 58 %, respectively (Fig. 5a).

The interaction of PTPIP51 with pERK slightly increased under the influence of 1 μM Gefitinib (+17 %), whereas 5 μM Gefitinib resulted in a significant reduction in the number of interactions (about 50 %) after 24 h of treatment. After 48 h of incubation the number of interactions of PTPIP51 with pERK in U87 cells decreased by the application of 1 μM Gefitinib. Treating the cells with 5 μM Gefitinib for 48 h slightly increased the number of interactions by about 6 %. Under these conditions the number of interactions of PTPIP51 with PTP1B was reduced by 44 %. (Figure 5a).

After 24 h of 5 μM Gefitinib exposure the interaction profile of PTPIP51 with PTP1B revealed any differences compared to the number of interactions in control group. The number of interactions between PTPIP51 and PTP1B decreased significantly after 48 h of incubation by 5 μM Gefitinib (Fig. 5b).

Immunoblot

Cells treated either with 1 and 5 μM of Gefitinib for 24 h displayed tendending reduced PTPIP51 protein as displayed in the immune blot (Fig. 5b). An incubation period

of 48 h led to a further reduction in the PTPIP51 protein. Both concentrations of Gefitinib lowered the fraction of tyrosine 176 phosphorylated PTPIP51 independent of the incubation time.

The downstream effect of EGFR inhibition by 1 and 5 μM Gefitinib resulted in reduced phosphorylated Erk1/2 after 24 h as well as after 48 h. The total Erk1/2 displayed any difference in Gefitinib treated compared to the control (Fig. 5a).

EGF receptor profile

U87 cell line as well as the primary cell cultures used for this study displayed the full length transcript for Wildtype EGFR from exon 1 to 8. Additional analysis of possible mutations in the exons 18-21 displayed no cell culture with a mutated EGFR.

Erlotinib

Additionally, we investigated Erlotinib incubation of U87 cell by in increasing concentrations (1 and 20 μM) for increasing times (24, 96 h) by immnostaining as shown in supplements. Like Gefitinib, Erlotinib targets the EGFR tyrosine kinase by reversible binding to the ATP binding site of the receptor. The application of 1 μM Erlotinib for 24 h resulted in dispersed granular cytoplasmic distribution of PTPIP51. After 96 h treatment with 1 μM Erlotinib a more attenuated granular pattern of the reduced PTPIP51 protein (A3B) was seen. The application of 20 μM Erlotinib resulted in a distinct subcellular localization of PTPIP51 with highest concentrations in the perinuclear region (A3 C and F). With increasing incubation time (96 h) 20 μM Erlotinib treatment resulted in a further redistribution of PTPIP51 to a dispersed granular pattern (A3 D).

Discussion

The epidermal growth factor receptor pathway is probably the most significant signalling pathway in glioma, which successfully can be exploited clinically [21, 22]. About 30 % of GBM reveal this specific EGFR mutation. This mutation leads to the loss of exons 2–7 coding for part of the extracellular domain and a constitutively enhanced EGF signalling promoting tumour growth [23]. As shown, the primary glioblastoma cells as well as the U87 cell line displayed wt alleles of *EGFR*. Nevertheless, these cells displayed aggressive growth behaviour accompanied by enhanced EGFR signalling. The EGFR is linked to a variety of downstream signalling molecules, such as the Ras/Raf/MEK/Erk cascade [24]. This MAPK pathway is essential for proliferation and cell division, all hallmarks of the malignant nature of glioma cells [3, 4]. The MAPK pathway activity is tightly regulated by subsequent serine phosphorylation of the signalling molecules [24]. In addition, several modulating molecules bind to specific targets of the MAPK pathway, for example the Raf1 kinase inhibitor protein (RKIP), which in turn binds to Raf1 to inhibit the MAPK pathway at the Raf1 level [25]. Here, RKIP tightly regulates Raf1 during mitosis, which titrates the signal of the MAPK pathway ensuring normal cell division, essential for tumour cell growth. A recent study identified RKIP to inhibit cell growth in glioma cells [25].

Of note, PTPIP51 acts also on Raf1 level as an activator of the MAPK pathway. Furthermore, PTPIP51 interacts with the main receptor tyrosine kinase of the MAPK pathway, namely the EGFR. PTPIP51 interactions are regulated by its tyrosine phosphorylation status [17]. The phosphorylation status affects the Raf1 binding ability as well as the interaction of PTPIP51 with its linker protein 14-3-3. The active EGFR is capable to phosphorylate PTPIP51 at tyrosine 176 residue and therefore preventing the Raf1 activation induced by PTPIP51. Treating a human keratinocyte cell line (HaCaT) with Gefitinib resulted in an increase of the PTPIP51/Raf-1 and PTPIP51/14-3-3 interactions [17]. Administrating the epidermal growth factor (EGF) to the cell line resulted in a sharp drop of both interactions. Interestingly, long-time exposition of HaCaT cells to EGF induced a decrease in the overall mRNA level of PTPIP51 [15].

Treating glioma cells with Gefitinib the tyrosine 176 phosphorylation of PTPIP51 was slightly reduced after 24 and 48 h. In contrast to results obtained in the HaCaT cell line the interaction of PTPIP51/14-3-3 and PTPIP51/Raf1 was reduced in GBM cells. The lowered activation of Erk1/2 reflects the decreased interaction of PTPIP51 with Raf1. Notably, there was still a basal level of MAPK activation of Gefitinib exposed cells as seen by immunoblotting. These observations may be explained by increased activity of Src kinase family members linked to alterations of glioblastoma cells [26, 27]. As reported by Du and coworkers, Src is frequently activated in human GBM lines and primary tumours [27]. The c-Src activation of EGFR results in the basal MAPK pathway activity and the basal level of tyrosine 176 phosphorylation of PTPI51. Interstingly, after 24 h Gefitinib incubation there was no counter-regulation of this tyrosine 176 phosphorylation by PTP1B. Moreover, c-Src is also capable of phosphorylating tyrosine 176 residue of PTPIP51 and preventing Raf1 activation [16]. After 48 h of Gefitinib incubation the PTPIP51/PTP1B interaction was additionally decreased. Interestingly, the PTPIP51/14-3-3 was increased analogue to the effect in the HaCaT cell line as a compensatory mechanism, whereas the Raf1 interaction level remained low [28]. These observations also resemble the known high

activity of c-Src and the accompanying low PTP1B interaction inhibiting PTPIP51 to interact with Raf1 [26].

Higher levels of the phosphorylated Erk1/2 in glioblastoma activate MAPK [29]. This leads to a variety of transcription factor activations in the nucleus, such as c-myc activated by Erk1/2. Interestingly, there is an inherent c-myc binding site in the PTPI51 promoter as annotated in the USCS genome browser (http://genome-euro.ucsc.edu/cgi-bin/hgc?hgsid=201968018_OSKna1QFaHG9YIz0kDpv5QtlJoF1&c=chr15&o=41047249&t=41047699&g=wgEncodeRegTfbsClusteredV3&i=MYC). Therefore, the elevated Erk1/2 probably inhibits a sharp decrease in PTPIP51 mRNA. The long-time adaptation of PTPIP51 protein expression does not work in contrast to the observations made on the HaCaT cell line [14, 25]. Additionally similar results were proved in a phase II trial of Gefitinib in glioblastoma hinting to a regulation of downstream signal transducers in the EGFR pathway probably dominated by regulatory circuits independent of EGFR phosphorylation [8, 10]. This argues for the development of resistance against Gefitinib therapy, which has already been observed in lung cancer [30].

To investigate another inhibitory mechanism a monoclocal antibody to EGFR (Cetuximab) was used. The monoclonal antibody Cetuximab neither effected tumour cell proliferation nor PTPIP51 and 14-3-3β mRNA and protein expression. Comparable failure of action was seen in clinical trials with GBM patients [27, 31, 32], despite successful clinical use in patients suffering from lung, colorectal and head and neck cancers [5, 33, 34]. The lack of response to Cetuximab treatment may be due to heterodimerization of the EGFR with Her2 (Erb2), to c-Met/HGF or activation IGF-1R activation [35]. A study by Clark et al. revealed the circumvention of EGFR inhibition by turning on two other EGFR family receptors (ERBB2 and ERBB3) in cancer stem cells, which continued to grow [11]. Activation of ERBB2 signalling in cell lines, either through ERBB2 amplification or through heregulin up-regulation leads to a permanent ERK1/2 signalling essentially resulting in resistance to Cetuximab-mediated inhibition of the EGFR [23]. In addition, glioblastomas expressing wt EGFR –as in the employed cell lines of this work- are less sensitive to treatments in combination with Cetuximab [36].

To conclude, PTPIP51 was identified to be involved in the EGFR/MAPK pathway in glioblastoma cells. This indicates a possible therapeutic target to resistance mechansims in anti-EGFR therapy by Gefitinib. Further studies are needed to investigate the potential of interference in the EGFR phosphorylation independent regulatory circuits, in order to make the MAPkinase pathway sensitive for the knock down of PTPIP51.

Acknowledgments We are grateful to Martin Bodenbenner and Claudia Tag (Institute of Anatomy and Cell Biology, Giessen) for their excellent technical assistance, to Mrs. A. Erkel and Mrs. B. Fröhlich (Department of Urology and Pediatric Urology, Giessen), Mrs. M. Hof and Mrs. G. Kierok (Neurosurgical Neurooncologic Laboratory, Justus-Liebig-University, Cell Culture Lab, Giessen).

Conflict of interest The authors declare that they have no conflict of interest.

Ethical standards The authors declare that all experiments were done according to ethical standards and comply with the current laws of Germany.

References

1. Gao Q, Lei T, Ye F (2013) Therapeutic targeting of EGFR-activated metabolic pathways in glioblastoma. Expert Opin Investig Drugs 22(8):1023–1040
2. Petri MK, Koch P, Stenzinger A, Kuchelmeister K, Nestler U, Paradowska A, Steger K, Brobeil A, Viard M, Wimmer M (2011) PTPIP51, a positive modulator of the MAPK/Erk pathway, is upregulated in glioblastoma and interacts with 14-3-3β and PTP1B in situ. Histol Histopathol 26:1531–1543
3. Karpel-Massler G, Schmidt U, Unterberg A, Halatsch ME (2009) Therapeutic inhibition of the epidermal growth factor receptor in high-grade gliomas: where do we stand? Mol Cancer Res 7:1000–1012
4. Loew S, Schmidt U, Unterberg A, Halatsch ME (2009) The epidermal growth factor receptor as a therapeutic target in glioblastoma multiforme and other malignant neoplasms. Anticancer Agents Med Chem 6:703–715
5. Galizia G, Lieto E, De Vita F, Orditura M, Castellano P, Troiani T, Imperatore V, Ciardiello F (2007) Cetuximab, a chimeric human mouse anti-epidermal growth factor receptor monoclonal antibody, in the treatment of human colorectal cancer. Oncogene 26:3654–3660
6. Gridelli C, De Marinis F, Di Maio M, Cortinovis D, Cappuzzo F, Mok T (2011) Gefitinib as first-line treatment for patients with advanced non-small-cell lung cancer with activating epidermal growth factor receptor mutation: review oft he evidence. Lung Cancer 71(3):249–257
7. Chakravarti A, Wang M, Robins HI, Lautenschlaeger T, Curran WJ, Brachman DG, Schultz CJ, Choucair A, Dolled-Filhart M, Christiansen J, Gustavson M, Molinaro A, Mischel P, Dicker AP, Bredel M, Mehta M (2013) RTOG 0211: a phase 1/2 study of radiation therapy with concurrent gefitinib for newly diagnosed glioblastoma patients. Int J Radiat Oncol Biol Phys 85:1206–1211
8. Uhm JH, Ballman KV, Wu W, Giannini C, Krauss JC, Buckner JC, James CD, Scheithauer BW, Behrens RJ, Flynn PJ, Schaefer PL, Dakhill SR, Jaeckle KA (2011) Phase II evaluation of gefitinib in patients with newly diagnosed Grade 4 astrocytoma: Mayo/North Central Cancer Treatment Group Study N0074. Int J Radiat Oncol Biol Phys 80:347–353
9. Prados MD, Yung WK, Wen PY, Junck L, Cloughesy T, Fink K, Chang S, Robins HI, Dancey J, Kuhn J (2008) Phase-1 trial of gefitinib and temozolomide in patients with malignant glioma: a North American brain tumour consortium study. Cancer Chemother Pharmacol 61:1059–1067
10. Hegi ME, Diserens AC, Bady P, Kamoshima Y, Kouwenhoven MC, Delorenzi M, Lambiv WL, Hamou MF, Matter MS, Koch A,

Heppner FL, Yonekawa Y, Merlo A, Frei K, Mariani L, Hofer S (2011) Pathway analysis of glioblastoma tissue after preoperative treatment with the EGFR tyrosine kinase inhibitor gefitinib—a phase II trial. Mol Cancer Ther 10(6):1102–1112
11. Clark PA, Lida M, Treisman DM, Kalluri H, Ezhilan S, Zomiak M, Wheeler DL, Kuo JS (2012) Activation of multiple ERBB family receptor mediates glioblastoma cancer stem-like cell resistance to EGFR-targeted inhibition. Neoplasia 14(5):420–428
12. Yu C, Han W, Shi T, Lv B, He Q, Zhang Y, Li T, Zhang Y, Song Q, Wang L, Ma D (2008) PTPIP51, a novel 14-3-3 binding protein, regulates cell morphology and motility via Raf-ERK pathway. Cell Signal 20:2208–2220
13. Ewing RM, Chu P, Elisma F, Li H, Taylor P, Climie S, McBroom-Cerajewski L, Robinson MD, O'Connor L, Li M, Taylor R, Dharsee M, Ho Y, Heilbut A, Moore L, Zhang S, Ornatsky O, Bukhman YV, Ethier M, Sheng Y, Vasilescu J, Abu-Farha M, Lambert JP, Duewel HS, Stewart II, Kuehl B, Hogue K, Colwill K, Gladwish K, Muskat B, Kinach R, Adams SL, Moran MF, Morin GB, Topaloglou T, Figeys D (2007) Large-scale mapping of human protein-protein interactions by mass spectrometry. Mol Syst Biol 3:89
14. Yang X, Cao W, Lin H, Zhang W, Lin W, Cao L, Zhen H, Huo J, Zhang X (2009) Isoform-specific expression of 14-3-3 proteins in human astrocytoma. J Neurol Sci 276:54–598
15. Yu C, Han W, Shi T, Lv B, He Q, Zhang Y, Li T, Zhang Y, Song Q, Wang L, Ma D (2008) PTPIP51, a novel 14-3-3 binding protein, regulates cell morphology and motility via Raf-ERK pathway. Cell Signal 20:2208–2220
16. Stenzinger A, Schreiner D, Koch P, Hofer HW, Wimmer M (2009) Cell- and molecular biology oft he novel protein tyrosine phosphatase interacting protein 51. Int Rev Cell Mol Biol 275:183–246
17. Brobeil A, Bobrich M, Tag C, Wimmer M (2012) PTPIP51 in protein interactions: regulation and in situ interacting partners. Cell Biochem Biophys 63:211–222
18. Bobrich MA, Schwabe SA, Brobeil A, Viard M, Kamm M, Mooren FC, Krüger K, Tag C, Wimmer M (2013) PTPIP51: a new interaction partner of the insulin receptor and PKA in adipose tissue. J Obes 2013:476240
19. Hamid R, Rotshteyn Y, Rabadi L, Parikh R, Bullock P (2004) Comparison of alamar blue and MTT assays for high through-put screening. Toxicol In Vitro 18(5):703–710
20. Towbin H, Staehelin T, Gordon J (1979) Electrophoretic transfer of proteins from polyacrylamide gels to nitrocellulose sheets: procedure and some applications. Proc Natl Acad Sci USA 76:4350–4354
21. Paul I, Bhattacharya S, Chatterjee A, Ghosh MK (2013) Current understanding on EGFR and Wnt/β-catenin signalling in glioma and their possible crosstalk. Gene Cancer 4:427–446
22. Hu Y, Gao H, Vo C, Ke C, Pan F, Yu L, Siegel E, Hess KR, Linskey ME, Zhou YH (2014) Anti-EGFR function of EFEMP1 in glioma cells and patient prognosis. Oncoscience 1:205–215
23. Gan HK, Cvrljevic AN, Johns TG (2013) The epidermal growth factor receptor variant III (EGFRvIII): where wild things are altered. FEBS J 280:5350–5370
24. Chen RE, Thorner J (2007) Function and regulation in MAPK signaling pathways lessons learned from the yeast saccharomyces cerevisiae. Biochim Biophys Acta 1773(8):1311–1340
25. Chen Zigui, Cheng Quan, Ma Zhiming, Xi Haipeng, Peng Renjun, Jiang Bing (2013) Overexpression of RKIP inhibits cell invasion in glioma cell lines through upregulation of miR-98. Biomed Res Int. 2013:695179
26. Huveldt D, Lewis-Tuffin LJ, Carlson BL, Schroeder MA, Rodriguez F, Giannini C, Galanis E, Sarkaria JN, Anastasiadis PZ (2013) Targeting Src family kinases inhibits bevacizumab-induced glioma cell invasion. PLoS ONE 8:e56505
27. Du J, Bernasconi P, Clauser KR, Mani DR, Finn SP et al (2009) Bead-based profiling of tyrosine kinase phosphorylation identifies SRC as a potential target for glioblastoma therapy. Nat Biotechnol 27:77–83
28. Brobeil A, Koch P, Eiber M, Tag C, Wimmer M (2014) The known interactome of PTPIP51 in HaCaT cells: inhibition of kinases and receptors. Int J Biochem Cell Biol 46:19–31
29. Bhaskara VK, Panigrahi M, Challa S, Babu PP (2005) Comparative status of activated ERK1/2 and PARP cleavage in human gliomas. Neuropathology 25:48–53
30. Ochi N, Takigawa N, Harada D, Yasugi M, Ichihara E, Hotta K, Tabata M, Tanimoto M (2014) Kiura K (2014) Src mediates ERK reactivation in gefitinib resistance in non-small cell lung cancer. Exp Cell Res 322(1):168–177
31. Brand TM, Lida M, Wheeler DL (2011) Molecular mechanisms of resistance tot he EGFR monoclonal antibody cetuximab. Cancer Biol Ther 11(9):777–792
32. Hasselbalch B, Lassen U, Hansen S, Holmberg M, Sørensen M, Kosteljanetz M, Broholm H, Stockhausen MT, Poulsen HS (2010) Cetuximab, bevacizumab, and irinotecan for patients with primary glioblastoma and progression after radiation therapy and temozolomide: a phase II trial. Neuro Oncol 12:508–516
33. Pirker R (2014) Novel drugs against non-small-cell lung cancer. Curr Opin Oncol 26:145–151
34. Péron J, Polivka V, Chabaud S, Poupart M, Ceruse P, Ramade A, Girodet D, Zrounba P, Fayette J (2014) An effective and well-tolerated strategy in recurrent and/or metastatic head and neck cancer: successive lines of active chemotherapeutic agents. BMC Cancer 14:504
35. Carrasco-García E, Saceda M, Martínez-Lacaci I (2014) Role of receptor tyrosine kinases and their ligands in glioblastoma. Cells 3:199–235
36. Yonesaka K, Zejnullahu K, Okamoto I, Satoh T, Cappuzzo F, Souglakos J, Ercan D, Rogers A, Roncalli M, Takeda M, Fujisaka Y, Philips J, Shimizu T, Maenishi O, Cho Y, Sun J, Destro A, Taira K, Takeda K, Okabe T, Swanson J, Itoh H, Takada M, Lifshits E, Okuno K., Engelman JA, Shivdasani RA, Nishio K, Fukuoka M, Varella-Garcia M, Kazuhiko Nakagawa, Pasi A (2011) Activation of ERBB2 signalling causes resistance to the EGFR-directed therapeutic antibody cetuximab. Sci Transl Med 7. 3, (99), p. 99ra86

édition scientifique
VVB LAUFERSWEILER VERLAG

VVB LAUFERSWEILER VERLAG
STAUFENBERGRING 15
D-35396 GIESSEN

Tel: 0641-5599888 Fax: -5599890
redaktion@doktorverlag.de
www.doktorverlag.de

ISBN: 978-3-8359-6545-4